

**Phytochemical and Biological Investigation of some Endemic  
Plants of Egypt with Development of a New HPTLC- $\beta$ -  
Glucuronidase Inhibition Assay**

Dissertation

zur Erlangung des Doktorgrades

der Naturwissenschaften (Dr. rer. nat.)

dem

Fachbereich Pharmazie der Philipps-Universität Marburg

vorgelegt von

**M.Sc. Ehab Ghareeb Mohammed Mahran**

Aus Kairo, Ägypten

Marburg/Lahn 2019

Erstgutachter: Prof. Dr. Michael Keusgen

Zweitgutachter: Prof. Dr. Gertrud Morlock

Eingereicht am 03.09.2019

Tag der mündlichen Prüfung am 15.10.2019

Hochschulkennziffer: 1180

## **Acknowledgements**

It is my great pleasure to thank all those who have contributed to the completion of this thesis.

First, I would like to express my deepest appreciation to my supervisor Prof. Dr. Michael Keusgen, who in the first place gave me the opportunity to join his research group and to conduct my PhD study. Throughout my research, he offered the honest guidance, support and advice. His valuable instructions and discussions have considerably improved my scientific experience, and helped me to bring the thesis into the form presented today.

Also, I would like to thank and pay tribute to Prof. Dr. Gertrud Morlock for her continuous support and encouragement. She thankfully accepted me at her lab and trustfully transferred many of her wealthy scientific experiences to me. Her comments, suggestions, and instructions have greatly improved my scientific knowledge.

I also would like to thank Prof. Dr. Shu-Ming Li and Prof. Dr. Moritz Bünemann, for their acceptance to be part of my examination committee and for the time and effort they gave to judge my thesis.

My sincere gratitude to Yousef Jameel Fund Program for the financial support during the whole period of study, including stipend, chemicals, and conferences participation. My deepest appreciation is also extended to DAAD for the financial support to attend an international conference.

I am really indebted to my colleagues in the working groups of Prof. Keusgen and Prof. Morlock for their help and support. Many thanks specially given to Nina Zitzer, Mariam Jamshidi-Aidji, Ebrahim Azadniya, and Daniel Meyer.

The last and not the least thanks should go to all my family. I do thank my wife for her patience and the high enthusiasm she was always giving to me.

# Table of contents

<b>Acknowledgments</b> .....	I
<b>List of tables</b> .....	IV
<b>List of figures</b> .....	V
<b>List of abbreviations</b> .....	VII
<b>Abstract</b> .....	1
<b>Zusammenfassung</b> .....	2
<b>1. Introduction</b> .....	3
1.1. General .....	3
1.2. Plants as a source of natural drugs .....	5
1.3. Plant secondary metabolites.....	6
1.4. Flora of Egypt as a source of Medicinal plants .....	9
1.4.1. Genus <i>Primula</i> .....	10
1.4.1.1. Taxonomic classification .....	10
1.4.1.2. General morphological characters and geographical distribution .....	11
1.4.1.3. Biological activities of genus <i>Primula</i> .....	11
1.4.1.4. Chemical constituents of genus <i>Primula</i> .....	12
1.4.2. Genus <i>Anarrhinum</i> .....	14
1.4.2.1. Taxonomic classification .....	15
1.4.2.2. General morphological characters and geographical distribution .....	15
1.4.2.3. Biological activities of genus <i>Anarrhinum</i> .....	15
1.4.2.4. Chemical constituents of genus <i>Anarrhinum</i> .....	16
1.5. Phytochemical and biological analysis of plants .....	18
1.5.1. HPTLC .....	18
1.5.1.1. (HP)TLC-based hyphenated techniques .....	19
1.5.2. HPLC-MS .....	21
1.6. HPTLC-GUS .....	24
1.6.1. Glucuronidation and deglucuronidation .....	24
1.6.2. GUS inhibition .....	25
1.6.3. GUS inhibition assay .....	25
<b>2. Aims and objectives</b> .....	27
<b>3. Material and methods</b> .....	29
3.1. Material .....	29
3.2. Instruments .....	31
3.3. Biological evaluation and active metabolites identification in <i>P. boveana</i> & <i>P. veris</i> .....	32
3.3.1. HPTLC development .....	32
3.3.2. HPTLC-antibacterial bioassay .....	33
3.3.3. HPTLC-AChE/BChE inhibition assay .....	34
3.3.4. Active metabolites identification .....	34
3.3.5. AChE inhibition equivalency calculation of <b>Pb1</b> .....	35
3.4. Biological evaluation and active metabolites identification in <i>A. pubescens</i> .....	36
3.4.1. HPTLC development .....	36
3.4.2. HPTLC-AChE inhibition assay .....	36
3.4.3. Active metabolites identification .....	36
3.4.4. AChE inhibition equivalency calculation of compounds ( <b>A1-A3</b> ) .....	37
3.5. HPTLC-GUS hyphenation .....	37
3.5.1. Method development .....	37
3.5.2. Optimization and validation of the method .....	37



3.5.3.	Statistical analysis .....	38
3.5.4.	Verification of the method .....	38
3.5.5.	Active metabolites identification .....	39
3.6.	HPLC-HRMS followed by EPI scanning for flavonoids profiling of <i>P. boveana</i> .....	41
<b>4.</b>	<b>Results</b> .....	<b>42</b>
4.1.	Biological evaluation and active metabolites identification of <i>P. boveana</i> (leaf) and <i>P. veris</i> (flower) .....	42
4.1.1.	HPTLC-antibacterial bioassay .....	42
4.1.2.	HPTLC-AChE/BChE inhibition assay .....	43
4.1.3.	Active metabolites identification .....	44
4.1.4.	AChE inhibition equivalency calculation of <b>Pb1</b> .....	47
4.2.	Biological evaluation and active metabolites identification of <i>A. pubescens</i> .....	49
4.2.1.	HPTLC-AChE inhibition assay .....	49
4.2.2.	Active metabolites identification .....	49
4.2.3.	AChE inhibition equivalency calculation of compounds ( <b>A1-A3</b> ) .....	53
4.3.	HPTLC-GUS inhibition assay hyphenation .....	55
4.3.1.	Optimization of the method parameters .....	55
4.3.2.	Method validation .....	57
4.3.3.	Method verification .....	57
4.4.	HPLC-HRMS and EPI analysis for identification of flavonoid constituents in <i>P. boveana</i> leaves .....	61
<b>5.</b>	<b>Discussion</b> .....	<b>66</b>
5.1.	Biological evaluation and active metabolites identification in <i>P. veris</i> flowers and <i>P. boveana</i> leaves .....	66
5.2.	Biological evaluation and active metabolites identification in <i>A. pubescens</i> .....	72
5.3.	HPTLC-GUS inhibition assay hyphenation .....	74
5.4.	HPLC-HRMS and EPI analysis for identification of flavonoids constitutes in <i>P. boveana</i> leaves .....	80
	<b>Summary</b> .....	<b>83</b>
	<b>Deliverables</b> .....	<b>86</b>
	<b>References</b> .....	<b>87</b>
	<b>Appendix</b> .....	<b>97</b>

## List of tables

Table No.	Title	Page
Table 1	Selected medicinal drugs from natural sources.....	4
Table 2	Flavonoids aglycones identified in genus <i>Primula</i> .....	13
Table 3	<sup>1</sup> H and <sup>13</sup> C NMR data of the compounds <b>A1</b> and <b>A3</b> .....	50
Table 4	Flavonoids identified in the hydro alcoholic extract of <i>P. boveana</i> using HPLC-HRMS and EPI analysis.....	63

## List of figures

Figure No.	Caption	Page
<b>Fig. 1</b>	Line graph shows the Pubmed database analysis using "plant natural product" as a hit .....	5
<b>Fig. 2</b>	Representatives of phenolic SMs .....	7
<b>Fig. 3</b>	Basic structure of flavonoids .....	7
<b>Fig. 4</b>	Chemical structure of artemisinin and vincristine .....	9
<b>Fig. 5</b>	Photographs of wild <i>P. boveana</i> .....	10
<b>Fig. 6</b>	Photographs of wild <i>A. pubescens</i> .....	14
<b>Fig. 7</b>	Iridoids isolated from genus <i>Anarrhinum</i> .....	17
<b>Fig. 8</b>	Schematic representation of (HP)TLC-based (bio)analytical hyphenations ....	20
<b>Fig. 9</b>	Possible scan modes of tandem mass analysis .....	23
<b>Fig. 10</b>	Experimental workflow of HPTLC-EDA pursued in the study .....	33
<b>Fig. 11</b>	HPTLC-MS interface (elution-head based) with representative diagram showing the mechanism by which compounds are eluted for MS analysis .....	35
<b>Fig. 12</b>	Schematic representation of the verification study showing the optimized HPTLC-GUS inhibition assay hyphenation as applied to <i>P. boveana</i> and SFLG extracts .....	40
<b>Fig. 13</b>	Chromatograms of <i>P. veris</i> flower extract ( <b>A</b> ) and <i>P. boveana</i> leaf extract ( <b>B</b> ) at UV 254 and 366 nm (1 and 2), after <i>p</i> -anisaldehyde derivatisation at white light illumination and UV 366 nm (3 and 4) and respective <i>A. fischeri</i> , <i>B. subtilis</i> , acetyl and butyryl cholinesterase autograms (5 - 8) .....	43
<b>Fig. 14</b>	Negative ion HPTLC-ESI-HRMS spectra obtained for compounds <b>Pv1</b> and <b>Pv2</b> and their structures .....	44
<b>Fig. 15</b>	Positive ion HPTLC-ESI-HRMS spectra obtained for compounds <b>Pb1-Pb4</b> .	45
<b>Fig. 16</b>	<sup>1</sup> H NMR spectra and structures of compounds <b>Pb1-Pb4</b> .....	47
<b>Fig. 17</b>	AChE inhibition equivalency experiment: AChE autogram of <i>P. boveana</i> extract (1 g/10 mL, 0.5 and 0.1 µL applied, three replicates of 50 and 10 µg/band) with standard Riv applied as track pattern after development (1 mg/mL, 1-10 µL applied, 1 - 10 µg/band) and respective densitogram (absorbance measurement) at 500 nm obtained by inverse scanning .....	48
<b>Fig. 18</b>	Chemical structure of Riv .....	48
<b>Fig. 19</b>	HPTLC chromatograms of the <i>A. pubescens</i> extract at UV 254 ( <b>A</b> ), UV 366 nm ( <b>B</b> ), white light ( <b>C</b> ) and UV 366 nm after <i>p</i> -anisaldehyde derivatization ( <b>D</b> ) as well as HPTLC autogram after the acetylcholinesterase assay ( <b>E</b> ) and the determined structures of the isolated bioactive metabolites <b>A1-A3</b> .....	49
<b>Fig. 20</b>	Key <sup>1</sup> H- <sup>13</sup> C HMBC correlations of compounds <b>A1</b> and <b>A3</b> .....	50
<b>Fig. 21</b>	HRMS/MS spectrum of compound <b>A2</b> ( <b>A</b> ) and detailed structural fragmentation pathway ( <b>B</b> ) (foliamenthic acid, FA; cinnamic acid, CA; glucose, Glc) .....	52
<b>Fig. 22</b>	HPTLC autogram after AChE assay ( <b>A</b> ) and densitometric fluorescence measurement at 500 nm ( <b>B</b> ) of compounds <b>A1-A3</b> (20 µg/band, <i>n</i> = 3) as well as rivastigmine tartrate (0.5 - 14 µg/band, <i>n</i> = 3) applied as track pattern	54
<b>Fig. 23</b>	UV/Vis spectrum (200 - 800 nm) of the autogram background: the white inhibition zone of SL served as a reference .....	55
<b>Fig. 24</b>	Effect of GUS concentration, incubation time, and fluorescent indicator on peak areas of the standard inhibitor, SL (1 mg/mL, applied as 1 µg/band, <i>n</i>	

	= 3). Areas were recorded on TLC scanner in fluorescens mode ( $\lambda$ 612 nm) .	56
<b>Fig. 25</b>	<b>Left:</b> Densitometric analysis of SL (0.75 - 2000 ng/band) applied as band pattern showing that 62 ng/band is the lowest concentration used in this experiment and could be detected visually (Also, proof of the calculated $S/N \geq 3$ ). <b>Left:</b> the standard calibration curve for SL over the range (62 - 1000 ng/band) fits best to second order polynomial regression line .....	57
<b>Fig. 26</b>	<b>A)</b> HPTLC-GUS hyphenation for detection of the enzyme inhibitors in <i>P. boveana</i> extract applied as 0.5 $\mu$ L. Chromatogram under UV 254 nm (1); UV 366nm (2); after NP/PEG derivatization at 366 nm (3); after assay application at 366 nm (4) and under white light (5). <b>B)</b> Confirmation of the active inhibitors by co-chromatographic elution of the <i>P. boveana</i> extract with reference compounds in 1 $\mu$ L/band each, detected under UV 254 and 366 nm light .....	58
<b>Fig. 27</b>	HPTLC-GUS hyphenation for detection of the enzyme inhibitors in SFLG extract applied as 1.0 $\mu$ L using two different developing systems, MP1 ( <b>A</b> ) and MP2 ( <b>B</b> ), as well as mass analysis, HRMS ( <b>C</b> ) & HRMS/MS at collision energy of 20 V ( <b>D</b> ) of the active inhibitor, <b>SFLG1.1</b> , Chromatogram at UV 254 nm; 2, at UV 366 nm; 3, after NP/PEG derivatization at 366 nm; 4, fluorometric detection after assay application (with neutralization); 5, colorimetric detection (with neutralization); 6, colorimetric detection (without neutralization) .....	59
<b>Fig. 28</b>	HPLC chromatogram of <i>P. boveana</i> hydro-alcoholic extract at UV 254 nm ..	61
<b>Fig. 29</b>	HRESIMS spectra of compound <b>9</b> ( <b>A</b> ), <b>11</b> ( <b>B</b> ) and <b>12</b> ( <b>C</b> ) ( <b>left</b> ); the corresponding EPI spectra of each molecular ion peak ( <b>right</b> ) .....	64
<b>Fig. 30</b>	Reduction of MTT into purple formazan by <i>B. subtilis</i> bacteria .....	67
<b>Fig. 31</b>	Enzymatic reaction of AChE and BChE on the corresponding substrate with formation of azo dye .....	69
<b>Fig. 32</b>	GUS enzymatic reaction using X-Gluc as a substrate .....	75

## List of abbreviations

Acet	Acetone
AChE	Acetylcholinesterase
AD	Alzheimer's Disease
<i>A. fischeri</i>	<i>Aliivibrio fischeri</i>
ATS-4	Automatic TLC Sampler
<i>B. subtilis</i>	<i>Bacillus subtilis</i>
BSA	Bovine Serum Albumin
CE	Collision Energy
CF	Chloroform
ChE	Cholinesterase
COSY	Correlation Spectroscopy
EDA	Effect-Directed Analysis
EPI	Enhanced Product Ion
ESI	Electrospray Ionization
EtOAc	Ethyl acetate
FA	Formic Acid
FDA	Food and Drug Administration
FLD	Fluorescence Detection
GUS	$\beta$ -Glucuronidase from <i>Escherichia coli</i> Type VII-A
HMBC	Heteronuclear Multiple Bond Correlation
HPLC	High Performance Liquid Chromatography
HPTLC	High Performance Thin Layer Chromatography
HRMS	High Resolution Mass Spectrometry
HSQC	Heteronuclear Single Quantum Correlation
IUCN	International Union for Conservation of Nature
LOD	Limit Of Detection
MeOH	Methanol
MP	Mobile Phase
MS	Mass Spectrometry
MTT	Tetrazolium Salt (3-(4,5-Dimethylthiazol-2-yl)-2,5-diphenyl-tetrazolium bromide
NOESY	Nuclear Overhauser Effect Spectroscopy

NP	Natural Product Reagent
NMR	Nuclear Magnetic Resonance
PEG	Polyethylene Glycol
PUFAs	Poly unsaturated fatty acids
Riv	Rivastigmine Tartrate
S/N	Signal to Noise Ratio
SFLG	Silymarin Flavonolignans
SL	D-saccharic acid 1,4-lactone monohydrate (Saccharolactone)
SMs	Secondary Metabolites
St. Catherine	Saint Catherine
UV	Ultraviolet
Vis	Visible
X-Gluc	5-Bromo-4-chloro-3-indolyl $\beta$ -D-glucuronide sodium salt

## Abstract

St. Catherine region is located in Sinai Peninsula of Egypt, where two continents, Asia and Africa, are geographically connected. The area has a characteristic floristic diversity, within which a number of endemic plant species grow. So far, the biological and/or chemical analysis of many of these endemic species has not thoroughly reported. Accordingly, this study aimed at biological and chemical investigation of two plant species, *P. boveana* and *A. pubescens*, growing endemically in St. Catherine.

The bacterial/ChE inhibition activities of *P. boveana* (leaf) and *P. veris* (flower) extracts were evaluated via HPTLC-EDA hyphenation. Identification of the active metabolites was based on the HPTLC-MS and NMR analysis. The active metabolites were identified as linoleic and linolenic acids (in *P. veris*) and unsubstituted flavone, 2'-methoxy-, 2'-hydroxy-, and 5,6,2',6'-tetramethoxyflavone (in *P. boveana*).

In *A. pubescens*, the HPTLC-AChE inhibition activity screening of the 80% alcoholic extract of the plant led to determination of three active metabolites. Their characterization was based on the analysis of the collected mass and NMR data. Two of these metabolites were defined as newly isolated natural compounds; were elucidated to be 6-*O*-, 6'-*O*-di-*trans*-cinnamoyl-antirrhinoside and 5-*O*-, 6-*O*-difoliamenthoyl-antirrhinoside, while the previously known compound was determined as 6-*O*-foliamenthoyl-(6'-*O*-cinnamoyl)-antirrhinoside.

In the third part of the study, a new HPTLC- $\beta$ -glucuronidase inhibition assay was developed. The method was optimized and also verified using two botanical materials. The new hyphenation allowed, for the first time, the direct determination of the  $\beta$ -glucuronidase inhibitors present in complex mixtures.

The fourth part of the study reported the HPLC-HRMS (/MS) analysis of the 80% alcoholic extract of *P. boveana*. A total of 25 metabolites have been tentatively identified as flavonoid compounds. The metabolites included, glycoconjugated flavonoids and flavonoid aglycones.

Overall conclusion, the study supported the herbal-evidenced based medicine through establishment of important bioactivities to some plant species. It also confirmed the potential of chromatography/biological activity/chemical analysis hyphenation in evaluation of biological samples present in few amounts.

## Zusammenfassung

Die Region St. Katharina liegt auf der ägyptischen Sinai-Halbinsel, wo zwei Kontinente, Asien und Afrika, geographisch miteinander verbunden sind. Das Gebiet besitzt eine charakteristische floristische Vielfalt, in der eine Reihe von endemischen Pflanzenarten wachsen. Bisher wurde nur wenig über die biologische und/oder chemische Analyse vieler dieser Arten berichtet. Die vorhandene Studie zielt auf die biologische und chemische Untersuchung von zwei Pflanzenarten, die endemisch in der Region St. Katharina wachsen, *P. boveana* und *A. pubescens*.

Die antibakterielle Aktivität sowie die Inhibierung der ChE von Extrakten der *P. boveana* (Blatt) sowie *P. veris* (Blüte) wurde durch HPTLC-EDA Kupplung ausgewertet. Die Identifizierung der aktiven Metaboliten basierte auf Untersuchungsmethoden wie HPTLC-MS und NMR-Analyse. Die aktiven Metaboliten wurden als Linol- und Linolensäure (in *P. veris*) sowie nicht substituiertes Flavon, 2'-Methoxy-, 2'-Hydroxy- und 5,6,2',6'-Tetramethoxyflavon (in *P. boveana*) identifiziert. Das HPTLC-AChE Assay (Enzyminhibierung) des 80%igen alkoholischen Extrakts der Pflanze *A. pubescens* führte zur Bestimmung von drei aktiven Metaboliten. Ihre Charakterisierung basiert auf der Analyse der gesammelten Massen- und NMR-Daten. Zwei dieser Metaboliten wurden als neu isolierte Naturstoffe definiert. Sie wurden mit 6-*O*-, 6'-*O*-Di-trans-Cinnamoyl-antirrhinosid und 5-*O*-, 6-*O*-Difoliamenthoyl-antirrhinosid identifiziert, während die zuvor bekannte Verbindung als 6-*O*-Foliamenthoyl-(6'-*O*-cinnamoyl)-antirrhinosid bestimmt wurde. Im dritten Teil der Studie wurde ein neuartiger HPTLC- $\beta$ -Glucuronidase-Inhibitor-Assay entwickelt. Die Methode wurde optimiert und mit zwei Materialien botanischer Art verifiziert. Die neu etablierte Trennung ermöglichte erstmals die direkte Bestimmung der in komplexen Gemischen vorhandenen  $\beta$ -Glucuronidase-Inhibitoren. Der vierte Teil der Studie befasst sich mit der HPLC-HRMS(/MS) Analyse des 80%igen alkoholischen Extrakts von *P. boveana*. Insgesamt 25 Metaboliten wurden vorläufig als Flavonoidverbindungen identifiziert. Zu den Metaboliten gehören glykokonjugierte Flavonoide und Flavonoid-Aglykone.

Zusammenfassend die hier vorgestellten Methoden leisten einen wichtigen Beitrag zur Phytomedizin, da in den untersuchten Pflanzen neue Bioaktivitäten beschrieben werden konnten. An mehreren Beispielen konnte gezeigt werden, dass eine Kombination aus Chromatographie und Aktivitätstestung dazu geeignet ist, biologische Materialien, die nur in geringen Mengen verfügbar sind, aussagekräftig zu untersuchen.



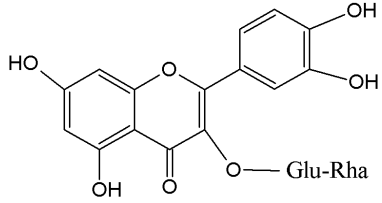
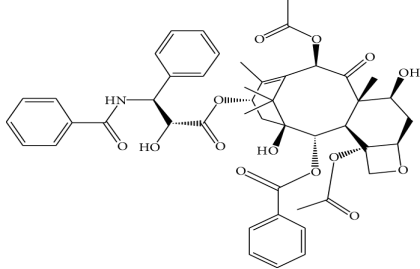
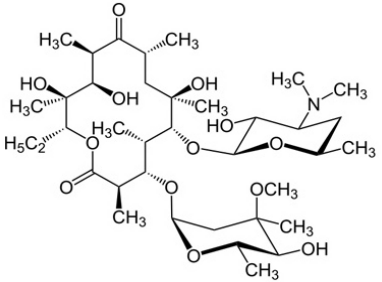
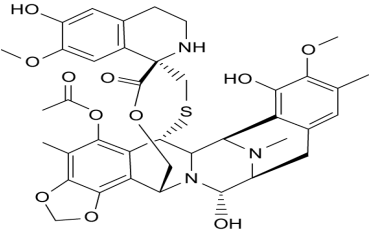
# 1. Introduction

## 1.1. General

Nature is a major source of numerous valuable ingredients. A broad range of biological systems including plants, microbes, and marine organisms, have supplied humans with many important drugs. Even though some modern means of drug discovery have been well-developed, *e.g.* chemical synthesis and computer-based molecular modeling, still multiple aspects are remained questionable. For examples, the encountered undesirable side actions of the synthetic molecules, the complexity and cost effectiveness of the production process, and the affordability to the world population (Tyler 1999; Rates 2001; Veeresham 2012). Together, these challenges have reignited the interest of many researchers to reconsider the nature as a comparably safe, easy to access, and sustainable source of drugs. Over the time frame 1981-2010, approximately 48.6% of the approved drugs by FDA or similar organizations were natural products or derivatives of natural products; the anti-infective area was found

mainly dependent on natural products (Newman and Cragg 2012, 2016). Representative examples of naturally occurring compounds with approved medicinal uses are presented in Table 1.

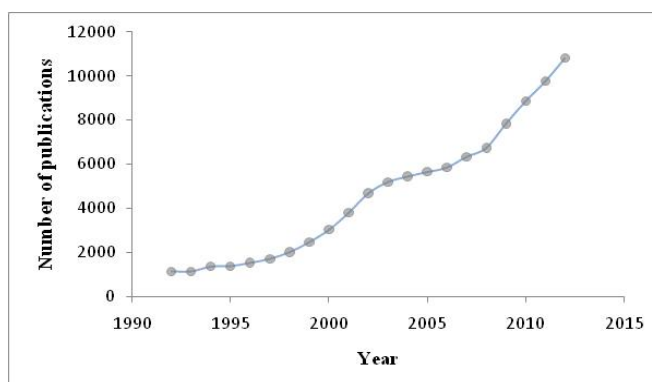
**Table 1:** Selected medicinal drugs from natural sources (Guerram et al. 2012; Martins et al. 2014; Ganeshpurkar and Saluja 2017).

Name	Source	Pharmacological activities	Chemical structure
Rutin	Plants	<ul style="list-style-type: none"> <li>• Antioxidant</li> <li>• Capillary fragility</li> <li>• Antiinflammatory</li> </ul>	
Paclitaxol	Plants	<ul style="list-style-type: none"> <li>• Anticancer</li> <li>• Antiviral</li> </ul>	
Erythromycin	Terrestrial microbes	<ul style="list-style-type: none"> <li>• Antibiotic</li> </ul>	
Trabectedin	Marine organisms	<ul style="list-style-type: none"> <li>• Anticancer</li> </ul>	

## 1.2. Plants as a source of drugs

Plants represent an important source of bioactive agents. Reliance on plants as a primary health caretaker dates back to ancient generations. Past civilizations developed several curatives from botanical sources; many of them are still in use until now. Prominent examples are the ancient Egyptians (2900 BC), who used plants as remedies and their preserved records is “Ebers Papyrus” from about 1550 BC. Also, the traditional Chinese medicine has historical applications with first report dates back to 1100 BC and the Indian Ayurvedic system dates from before 1000 BC (Cragg and Newman 2013). Approximately, 320000 plant species in our planet (Sneader 2005). It was only at the beginning of the 19<sup>th</sup> century until the notion of metabolites isolation has been evolved, which initially presented by the German apothecary assistant Friedrich Sertürner who succeeded to isolate the first natural compound, morphine, from opium (Atanasov et al. 2015). Sequentially in the following decades, a progress in the purification of plant-based natural products has been significantly rocketed, which led to the use of the concentrated effective fractions/substances instead of the whole herbal products that could contain many irrelevant constituents. Currently, the ethnopharmacological information for many plants is better available, facilitating the process of targeted drug discovery. About 80% of the 122 plant-derived drugs that reported for use globally were from plants having ethnomedical use of similar or closely related indications as the respective isolated candidates are prescribed (Atanasov et al. 2015). A trend analysis on the Pubmed database (**Fig. 1**) showed a significant increase in the number of researches concerned with plant natural products as indicated by the number of publications during the period 1992-2012. Analysis was generated (March 2019) using the webtool MEDSUM (<http://webtools.mf.uni-lj.si/public/medsum.html>).

**Fig. 1.** Line graph shows the Pubmed database analysis using "plant natural product" as a hit. Webtool used is (<http://webtools.mf.uni-lj.si/public/medsum.html>).



### 1.3. Plant secondary metabolites

Plants are splendid machines, capable of synthesizing many secondary metabolites with varied chemical structures. Full understanding of the beneficial roles of the SMs in plants is always an active area of research. However, several reports have evidenced the functions of SMs as mainly related to their defense actions toward the adverse effects of biotic and/or abiotic stresses (Zaynab et al. 2018; Takshak and Agrawal 2019). Furthermore, these compounds possess a physiological importance, like attracting pollinators (Stevenson et al. 2017; Wink 2018) and supplying key components of plant tissue structure (Liu 2018).

Chemotaxonomic classification of SMs relies primarily on their chemical structures. Three major categories (phenolics, terpenoids, and nitrogen-containing compounds) have been recognized mostly in the scientific reports; these categories cover almost all of these chemicals (Kabera et al. 2014).

**Phenolic compounds** comprise a large group of SMs occurring abundantly in many plants. Their structures widely differ from considerably simple molecules containing only one benzene ring to quite large polymerized compounds (Lin et al. 2016). Due to this broad structures variation, plant phenolics are usually undergo further classification into several divisions (Tsimogiannis and Oreopoulou 2019). Phenolic metabolites include, benzoic acid derivatives, phenylpropanoids, lignans and lignins, coumarins, aromatic polyketides, flavonoids, and stilbens. Representative examples of the major phenolic classes are shown in **Fig. 2**.

Typically, phenolics like flavonoids are biosynthesized in plants *via* shikimate pathway; this pathway is also shared by other SMs, *e.g.* alkaloids. The biosynthetic pathway depends on two other proceeding pathways, glycolytic and pentose phosphate pathways, which provide phosphoenol pyruvate and D-erythrose-4-phosphate, respectively. Together, these two precursors form shikimic acid. Shikimic acid is a central intermediate, serving as a branching point from which the phenolics compounds are obtained after several series of biosynthetic reactions (Dewick 2002; Lin et al. 2016).

Flavonoids constitute a large division of plant phenolics. They are ubiquitously found in many plants including dietary foods like fruits and vegetables (Yao et al. 2004; Panche et al. 2016). Being the most prevailing SMs present in almost all plants, flavonoids receive a great interest in studying their biosynthesis, biological activities, and chemical properties.

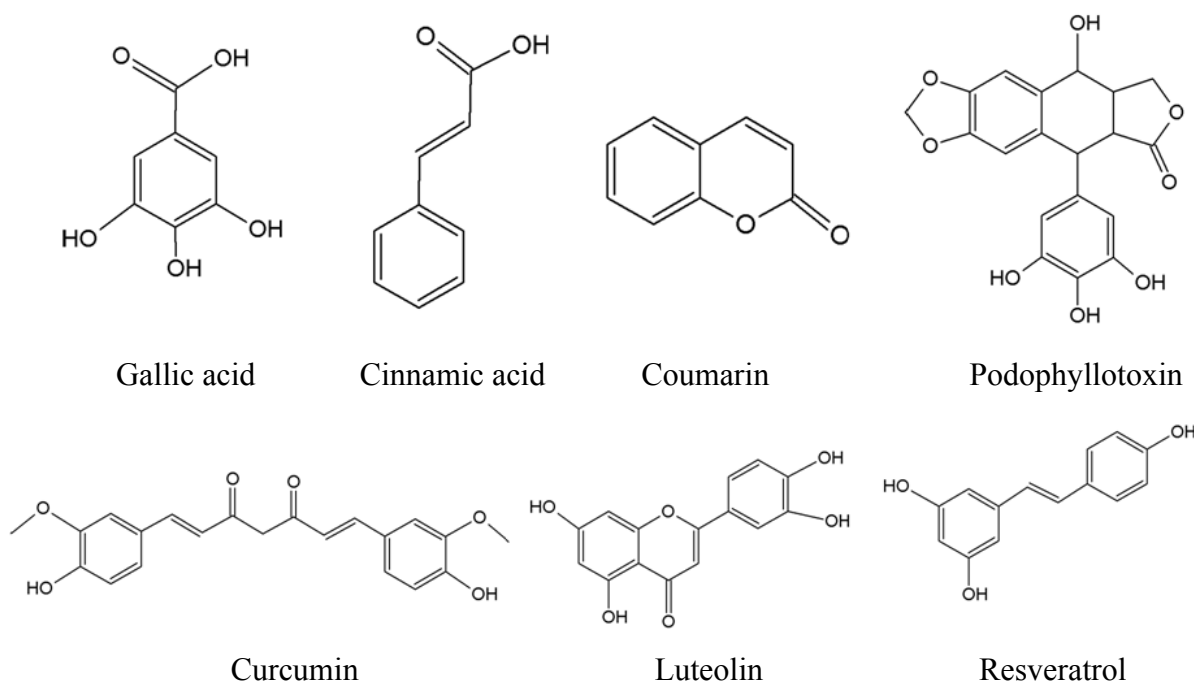


**Fig. 2.** Representatives of phenolic SMs

Their structures contain mainly two phenolic rings, A and B, linked *via* a heterocyclic pyran ring, C (**Fig. 3**) from which the major classes of flavonoids are derived as flavone, flavonone, flavonols, flavanone, flavan-3-ols, and isoflavones (Kumar and Pandey 2013). They occur either as free aglycones or as glycoconjugates. Both structural forms are then nicely decorated through different degree of hydrogenation, hydroxylation and methoxylation giving rise to a wide range of different polyphenolic compounds with various physiochemical characteristics.

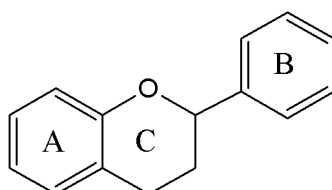


**Fig. 3.** Basic structure of flavonoids

In addition to their essential roles in plant growth and defense responses, flavonoids also possess versatile health benefits (Xiao et al. 2011). Flavonoids are potent antioxidants and chelating agents (Pietta 2000); this property was claimed to be responsible for most of the biological activities exhibited by flavonoids (Heim et al. 2002), which is obviously illustrated

through their cardiovascular protective effects evoked by inhibition of LDL oxidation. They also showed antimicrobial (Cushnie and Lamb 2005; Jucá et al. 2018), anti-inflammatory (Rathee et al. 2009; Pan et al. 2010), and anticancer (Chahar et al. 2011; Batra and Sharma 2013) potentials. Flavonoids are reported to modulate the cytochrome P450 enzyme system (Hodek et al. 2009). They have shown inhibitory activity against AChE (Roseiro et al. 2012; Xie et al. 2014; Khan et al. 2018),  $\alpha$ -glucosidase (Proença et al. 2017), and xanthine oxidase (Pirouzpanah et al. 2009). Thus, attracting an increased curiosity to their therapeutic importance in relevant diseases like AD, myasthenia gravis, glaucoma, diabetes, and gout.

**Terpenoids** are regarded as the largest and oldest class of SMs occurring in plants (Caputi and Aprea 2011). The building block of terpenoids is the isoprene, which is a five-carbon unit. The biosynthesis of terpenoids is compartmentalized, *i.e.* in cytosol, the mevalonate pathway is the source of isoprene unit, leading to the formation of sesquiterpenes and triterpenes. While in plastids, the methyl-D-erythritol-4-phosphate pathway supplies the C5 unit, from which the other terpenoids are usually derived, *e.g.* monoterpenes, diterpenes, and tetraterpenes. Terpenoids have broad applications in industry as flavors, fragrances, spices, and in perfumery and cosmetics (Caputi and Aprea 2011). In addition, terpenoids have been proven to display a potent anticancer activity (Patlolla and Rao 2012), a major example is paclitaxol (Slichenmyer and Von 1991) and anti-malarial, *e.g.* artemisinin (**Fig. 4**) (Krungkrai and Krungkrai 2016).

**Nitrogen-containing compounds**, *e.g.* alkaloids. Alkaloids are low molecular weight compounds containing one or more nitrogen atoms in their structures, which impart the basic characters to these chemicals. They are usually subdivided according to the nitrogen-containing structure (*e.g.* pyrrolidine, piperidine, quinoline, isoquinoline, indole) (Dewick 2002). Alkaloids feature the SMs of many plant families like Apocynaceae, Asteraceae, Papaveraceae, and Solanaceae. They have numerous bioactivities including, anticancer, *e.g.* vincristine (**Fig. 4**) & vinblastine, antimicrobial, antiparasitic, and estrogenic (Aniszewski 2007). Despite their vast medicinal properties, alkaloids are also known to be highly poisonous; some of them are considered as euphoric, psychomimetic and hallucinogenic agents (Aniszewski 2007).

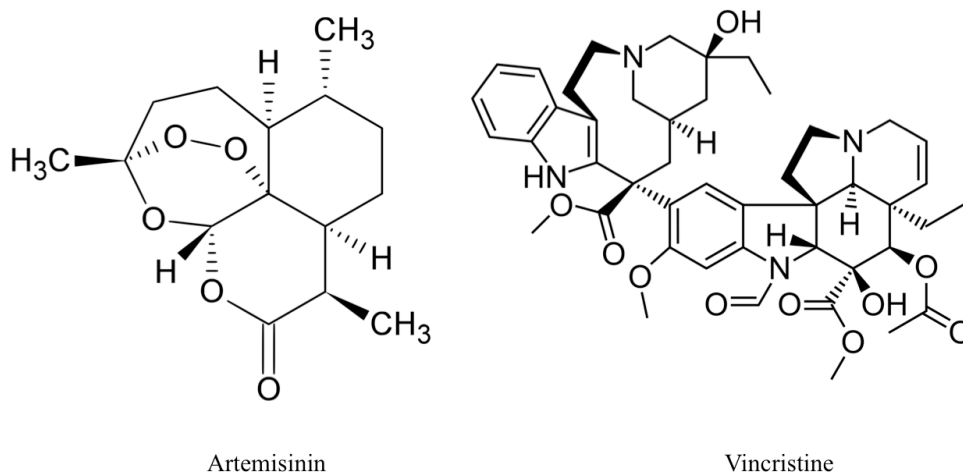


**Fig. 4.** Chemical structure of artemisinin and vincristine.

#### 1.4. Flora of Egypt as a source of medicinal plants

Egypt is located in the northeastern corner of Africa, but also linked to Asia through Sinai Peninsula. Egypt's location is unique, as it represents the point of convergence for floristic features of four phytogeographical regions (EL Hadidi and Hosni 1996). Egypt has a severe arid climate with a mean temperature exceeding 30 °C in summer and average annual rainfall of 100 mm and as little as 50 mm in the extreme deserts (Hegazy and Lovett-Doust 2016). Flora of Egypt comprises more than 2000 plant species hosting 48 endemic taxa belonging to 18 families (Abdelaal et al. 2018). Sinai Peninsula with its distinct landform and geographical position holds the high number of endemism in Egypt (approximately 26 species); most of these endemic species are concentrated in St. Catherine region (Ayyad et al. 2000). The elevated mountains impart a high floristic diversity to the area. However, stressing environmental impacts (*e.g.* climate change) and some human activities (*e.g.* urbanization and over grazing) resulted in a growth disturbance to most of the area's endemic species. Several species are currently classified by IUCN as being endangered, *e.g.* *Anarrhinum pubescens* or critically endangered species like *Primula boveana*.

Historically, Egyptian plants have served as medicines since early times. Ancient Egyptians documented their medicinal recipes on the wall of temples and some have been recorded in Ebers Papyrus. Interestingly, many of these medicinally valued herbs are still in use till current time (Saxena 2001).

Taking into account the historical standpoint of the medicinal plants of Egypt and the stressing environmental/human influences, which suggested the induction of secondary metabolites to help plants to survive, the chemical and biological evaluation of the native Egyptian species could reveal promising bioactive/lead metabolites.

#### 1.4.1. Genus *Primula*



**Fig. 5.** Photographs of wild *P. boveana*.

##### 1.4.1.1. Taxonomic classification

Kingdom	Plantae
Subkingdom	Tracheophyta
Division	Magnoliophyta
Class	Magnoliopsida
Order	Primulales
Family	Primulaceae
Genus	<i>Primula</i>
<i>Species</i>	<i>boveana</i> Decne. ex Duby



#### ***1.4.1.2. General morphological characters and geographical distribution***

*Primula* plants are perennial herbs, slightly to moderately succulent, bloom mostly in spring. **Leaves** are usually developed in single rosettes with omitted or obscured petiole. Leaves have different shapes: blade linear, broadly lanceolate, oblanceolate, oblong-obovate, rhombic, or elliptic to cuneate or spatulate. **Flowers** often heterostylous; sepals are 5, green, calyx broadly campanulate to cylindrical or urceolate, and glabrous; petals are 5, lavender, magenta, pink, rose, violet, white, or yellow (Richards 2003; Bawri et al. 2014).

*Primula* is the largest genus in the family Primulaceae; it comprises more than 400 species. They inhabit mainly the temperate regions, so, widely distributed over Asia and Europe with a major occurrence in Himalayas and the European Alps (Richards 2003; Bawri et al. 2014).

*Primula boveana* Decne. ex Duby (also known as Sinai primrose) is an endemic species to Mount St. Catherine in Sinai peninsula of Egypt. It grows wild in the high mountainous areas, particularly moist ground close to the wells in Gebel Musa, Gebel Safsaf, Gebel Serbal and Gebel Umm Shaumar. Currently, the total number of the plant's populations shows an increasing decline due to the harsh environmental such as the climate change as well as some human activities (Jiménez et al. 2014; Zaghoul et al. 2016), hence the species has been classified as a critically endangered plant (Mansour et al. 2013; IUCN 2014). Owing to the limited access to the plant, phytochemical and/or biological properties of the plant have not thoroughly studied yet.

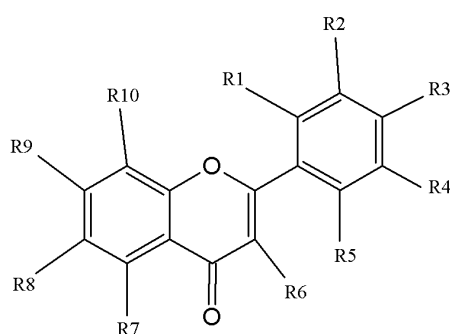
#### ***1.4.1.3. Biological activities of genus Primula***

*Primula* plants are recognized for their richness in several phyto-constituents belonging to different chemical classes, however, phenolic and saponin compounds were found as major secondary metabolites produced by these plants. These phytochemicals have imparted significant bioactivities to the plants of the genus. The most common medicinal use of the *Primula* is as antitussive. Herbal preparation from the underground organs (roots) and/or flowers of *P. veris* L. as well as *P. elatior* L. Hill are equally indicated for treatment of a range of respiratory disorders such as productive cough, bronchitis, whooping cough, and asthma; this could be traced to the secretolytic potential of the triterpenoidal saponin constituents. These medicinal indications have been also described in the European pharmacopeia (EMA 2012). Alongside, many other bioactivities have been reported to these two species as well as to other species. *Primula* sp. have demonstrated remarkable antimicrobial activities. Najmus-Saqib et al.

(2009) verified the antifungal activity of *P. macrophylla* D. Don crude extract and its prepared fractions. The methanolic extract of *P. auriculata* Lam. flowers showed antibacterial activity against nine Gram positive and Gram-negative bacterial strains (Jaberian et al. 2013). *P. veris* flower extract and *P. vulgaris* Huds. leaf extract showed significant antibacterial properties against a number of Gram-positive and Gram-negative bacteria (Başbülbul et al. 2008; Majid et al. 2014). Also, the antioxidant activity was amongst the recorded biological characteristics of the genus *Primula*, which could be due to their high contents of the phenolic compounds. Many *Primula* species demonstrated antioxidant activities (Jaberian et al. 2013; Mostafa et al. 2014). Some other bioactivities displayed by *Primula* plants include: cytotoxic, antidiabetic, and anti-inflammatory actions (Tokalov et al. 2004; Najmus-Saqib et al. 2009; Singh et al. 2014).

#### **1.4.1.4. Chemical constituents of genus *Primula***

Plants belonging to genus *Primula* accumulate excellent amount of plant phenolics and triterpenoidal saponins as their main phyto-constituents. Flavonoids are the predominant phenolic present in *Primula*; however, other phenolic classes are reported but less frequently. Studies on the phenolic contents of *Primula* dates back to the beginning of twentieth century (Colombo et al. 2017). *Primula* plants are well-known for their epicuticular flavonoids which primarily composed of flavonoids aglycones being hydroxylated and/or methoxylated at different degrees. The function of these surface-secreted metabolites is still unclear. Nevertheless, these lipophilic exudates were claimed to play crucial protection roles in plants. They protect against UV-radiation acting as natural screens, pathogens, and herbivorous attack (Cuadra and Harborne 1996). Exudate flavonoids have been also proven to possess relevant adaptation functions in freezing temperature, assisting the plant to tolerate the extremely low temperature (Isshiki et al. 2014). The chemical structures and occurrence of the major exudate flavonoids in genus *Primula* are summarized in Table 2.

**Table 2:** Flavonoids aglycones identified in genus *Primula* \*

Substituent										Species
R1	R2	R3	R4	R5	R6	R7	R8	R9	R10	
H	H	H	H	H	H	H	H	H	H	1-3, 6-10, 13-16, 18-20, 22
OH	H	H	H	H	H	H	H	H	H	1,2, 7, 9, 13-16, 18, 20
OMe	H	H	H	H	H	H	H	H	H	6, 9, 10, 15, 17-19
OH	H	H	OH	H	H	H	H	H	H	9, 15, 16
OMe	H	H	OMe	H	H	H	H	H	H	17, 18
OH	H	H	OAc	H	H	H	H	H	H	3, 6, 8-10, 19, 22
H	OMe	H	H	H	H	H	H	H	H	1, 10, 17-19
H	OH	OH	H	H	H	H	H	H	H	2, 13, 16
H	OMe	OMe	H	H	H	H	H	H	H	1,2, 17-19
H	OH	OMe	OMe	H	H	H	H	H	H	17-19
H	OMe	OMe	OMe	H	H	H	H	H	H	17-19
H	OH	H	OH	H	H	H	H	H	H	13
H	OH	OMe	OH	H	H	H	H	H	H	17
H	H	OH	H	H	H	H	H	H	H	1,2, 13, 15
H	H	H	H	H	H	OH	H	H	H	2-4, 7-9, 13-16, 19, 20, 22
OH	H	H	H	H	H	OH	H	H	H	2, 9, 13-15, 20, 22
OMe	H	H	H	H	H	OH	H	H	H	15
OMe	H	H	H	OMe	H	OMe	OMe	H	H	18
OMe	OMe	H	H	OMe	H	OMe	OMe	H	H	17
H	H	H	H	H	H	OH	H	OH	H	15
H	H	H	H	H	H	OH	H	H	OH	2, 3, 6-8, 10, 13, 15, 20
OH	H	H	H	H	H	OH	H	H	OH	9, 22
H	H	H	H	H	H	H	H	OH	OH	15
OH	H	H	H	H	H	H	H	H	OH	9, 5
OH	H	H	Benzoate	H	H	H	H	H	OH	9

\*Species names: (1: *P. albenensis*, 2: *P. auricula*, 3: *P. glaucescens*, 4: *P. glutinosa*, 5: *P. pulverulenta*, 6: *P. hirsuta*, 7: *P. marginata*, 8: *P. minima*, 9: *P. palinuri*, 10: *P. latifolia*, 11: *P. spectabilis*, 12: *P. villosa*, 13: *P. farinosa*, 14: *P. frondosa*, 15: *P. halleri*, 16: *P. nutans*, 17: *P. elatior*, 18: *P. veris*, 19: *P. vulgaris*, 20: *P. denticulata*, 21: *P. officinalis*, 22: *P. macrophylla*). References: (Wollenweber et al. 1988; Huck et al. 1999, 2000; Budzianowski et al. 2005; Bhutia and Valant-Vetschera 2012; Colombo et al. 2017).

In addition to epicuticular flavonoids, *Primulas* are also capable of producing many tissue-type flavonoids. These are mainly polar flavonoids derived from flavone or flavonol subunits that are mostly *O*-glycosylated with one or more sugar at varying positions through the molecule.

Apart from phenolic constituents, triterpenoidal saponins form another major group of metabolites that largely distribute in the roots of *Primula* plants. Generally, the identified saponins contained the triterpene aglycone, protoprimulagenin A, which gave rise to different saponins known from the genus after *O*-glycosylation with several sugars at the position C-3. Paola et al. has reviewed the saponins occurred in European *Primula* and concluded them as: primulasaponin I, primulasaponin II, priverosaponin B 22-acetate, and priverosaponin B 22-acetate (Colombo et al. 2017).

#### 1.4.2. Genus *Anarrhinum*



**Fig. 6.** Photographs of wild *A. pubescens*

#### **1.4.2.1. Taxonomic classification**

Kingdom	Plantae
Subkingdom	Tracheophyta
Division	Magnoliophyta
Class	Magnoliopsida
Order	Lamiales
Family	Plantaginaceae
Genus	<i>Anarrhinum</i>
<i>species</i>	<i>pubescens</i> Fresen.

#### **1.4.2.2. General morphological characters and geographical distribution**

*A. pubescens* Fresen. is a glandular-hairy perennial shrub, usually 30-60 cm length. Stems are erect and branched from the base. Basal leaves oblanceolate, coarsely dentate in the upper part, acute, the base attenuate into a petiole 3-8 mm. Inflorescence is raceme, corolla is white in color (Bolus 2000). Genus *Anarrhinum* is generally distributed over the Mediterranean region; represented in Egypt by *A. pubescens*, which grows on the high altitude rocky mountains of Sinai Peninsula.

#### **1.4.2.3. Biological activities of genus *Anarrhinum***

Iridoids are abundant metabolites in the genus *Anarrhinum* and the reported biological activities of the plants from the genus have been mostly done on the isolated iridoids. However, a full biological investigation of the genus is not thoroughly studied yet. So far, only two bioactivities assessed on the *Anarrhinum* plants. One was concerned with the cytotoxic activity of some iridoids isolated from *A. pubescens* against the human lung carcinoma cell line (A-549); the dimer iridoid, pubescensoside, showed a better activity compared to other iridoids reported in the study (Mahran et al. 2018). In addition, Salah El Dine et al. (2011) evaluated the hepatitis C virus protease inhibitory activity of some iridoids isolated for *A. orientale* Benth.; two of these iridoid metabolites showed a moderate inhibitory activity against the enzyme. Many studies have reported the bioactivities of iridoids as a potent biologically active class of natural compounds. Numerous pharmacological activities like antimicrobial, antidiabetic, anti-hyperlipidemic, antioxidant, hepatoprotective, and immunomodulatory activity were described for iridoid compounds obtained from plants (Tundis et al. 2008; Dinda et al.

2011). Iridoids showed also anti-inflammatory (Park et al. 2010) and anticancer potential (Dinda et al. 2011). Iridoids exhibited lipoxygenase inhibitory activity (Gousiadou et al. 2013).

#### **1.4.2.4. Chemical constituents of genus *Anarrhinum***

Iridoids were identified as the main phytochemicals occurring in plants of genus *Anarrhinum*. They are bicyclic monoterpene metabolites; mostly present as glycosides. Structurally, iridoids are considered as cyclopentane-(c)-pyran-derived compounds. Iridoid compounds originate from geraniol by a type of folding that looks different from monoterpenoids (Dewick 2002). Methylerythritol phosphate (MEP) pathway is the main biosynthetic pathway of monoterpenes and assumed to be a site-specific, *i.e.* biosynthesis of monoterpene takes place in plastids where MEP pathway is the main supplier of the isoprene units. Iridoids as a characteristic group of natural products have a significant role in chemotaxonomy of some plant families where they marked the phyto-constituents of these families (Jensen et al. 2002; Taskova et al. 2002).

Plantaginaceae family is an important source of iridoids (Fuchs and Bowers 2004; Taskova et al. 2010; Kroll-Møller et al. 2017). Aucubin, catalpol and their derivatives are the most known iridoids present in *Plantago sp.* (Taskova et al. 2002; Fuchs and Bowers 2004). Iridoids characterized in *Anarrhinum* plants were determined as derivatives of either antirrhinose or mussaenosidic acid. They were mainly esterified with foliamenthic acid and/or cinnamic acid. These characteristic structural features could be a useful chemotaxonomic marker for the genus. The structures of the iridoids isolated from *A. orientale* and *A. pubescens* are shown in **Fig. 7**.

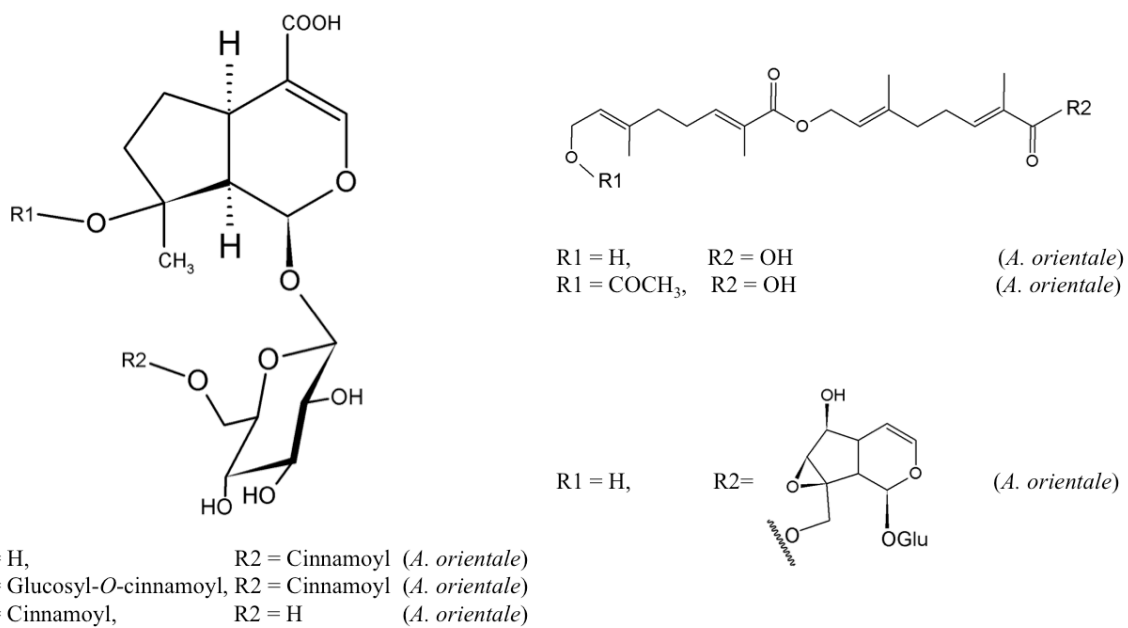
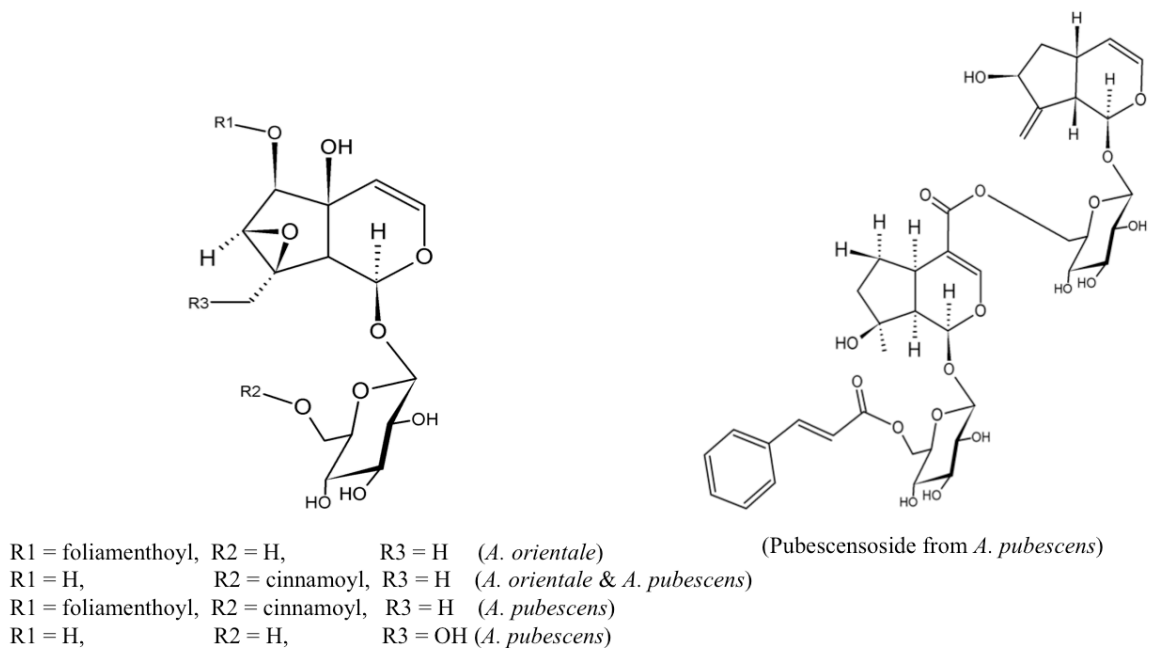


**Fig. 7.** Iridoids isolated from genus *Anarrhinum*.

## 1.5. Phytochemical and biological analysis of plants

Plants contain a huge number of metabolites distributed all over its parts. Knowledge of the plant metabolites would be of worth applications in many scientific disciplines such as phytochemistry, phytomedicine, plant physiology, taxonomy, and ecology. Nonetheless, these metabolites are belonging to broad chemical classes with different physicochemical properties. Meaning, the comprehensive chemical and/or biological investigation of these metabolites would be a challenging research. The availability of the plant material is also a crucial aspect, as analysis could be significantly hampered if the plant material is very rare or has a restricted access. Accordingly, the analytical methods intended for metabolites analysis should be thoroughly considered in terms of their separation and detection efficiency as well as the amount of sample consumption. As species selected in this study are regarded as a rare material; the access to a large amount is considerably restricted, the amount of sample consumption for analysis should be considered.

Currently, hyphenated techniques have been widely developed and multiple analytical instruments can be linked together in order to overcome the aforementioned challenging aspects. So, these hyphenated systems have a special importance in the field of discovery of lead therapeutic agents from plants (Wolfender et al. 2006; Patel et al. 2010). The most commonly used online hyphenated instruments are TLC-UV/Vis/FLD, HPLC-MS, and GC-MS. Furthermore, extension of the hyphenation to involve a streamlined biological evaluation of the studied samples has been made available and witnessing many interesting innovations, *e.g.* HPTLC-EDA. Hyphenations is beneficial in chemical and biological analysis, it generates massive information like chromatographic, spectral, and structural properties, leading to conclusive results in a relatively short time.

### 1.5.1. HPTLC

Thin layer chromatography and its optimized form, HPTLC, are the most popular categories of planar chromatography. Stationary phase of TLC has been supremely optimized in order to suit the high performance separation and that give rise to the development of HPTLC. The main characteristic feature of HPTLC is that the stationary phase is composed of small-sized silica particles, allowing higher packing density and smother surface resulting



in better compound resolution, improved detection, and faster analysis time than the classical TLC (Spangenberg et al. 2011).

HPTLC complements HPLC and despite the separation superiority of HPLC, HPTLC still offers several other crucial compensatory options making it more preferable in many cases (Morlock and Schwack 2010). HPTLC permits parallel separation of compounds mixture in one run, resulting in a high sample throughput and analysis of multiple samples under identical conditions. Also, HPTLC allows flexible use of different stationary phases where a new stationary phase should be used for each analysis, thus, avoiding cross sample contamination and the sample cleaning is not necessary prerequisite for analysis.

Another major difference lies in the detection of the separable components. In HPLC, sample detection is achieved while they are in the mobile phase leading to many unavoidable restrictions in the mobile phase composition. In contrast, (HP)TLC permits detection after complete removal of the residual mobile phase, hence, excluding any interference to the measurements (Morlock and Schwack 2010; Spangenberg et al. 2011).

#### ***1.5.1.1. (HP)TLC-based hyphenated techniques***

Considering the distinguished features of (HP)TLC, hyphenation become an increasingly adopted approach in planar chromatography. The reason is that the analytical task could be achieved for every individual component without worry of any possible mobile phase interference. Notably, automated instrumentation of (HP)TLC to involve almost all chromatographic steps has forcibly derived the hyphenation to more promising applications. The hyphenation of (HP)TLC involves coupling of the chromatograms to different spectroscopic instruments and/or bioactivity assays, giving rise to broader applications of (HP)TLC.

The spectroscopic means facilitate the structural identification of the separated substances while still residing on the plate; this considerably eliminated the need to preparative isolation of these metabolites which seems laborious, tedious and time consuming procedures. The UV, Vis, FLD, Fourier-transform infrared, MS, and HRMS are different structure elucidating means that have been successfully linked to (HP)TLC (Morlock and Schwack 2010).

Moreover, the hyphenation has been extended to include the bioactivity assays. Through this combination, the bioactivity of individual components contained in a single or multiple sample(s) could be directly evaluated on the developed plates, so-called "*Effect directed analysis*". A wide range of bioactivities is currently performed using this strategy, *e.g.* antioxidant

activity or testing the inhibitory potential against either biological enzymes or biosystems, like microbes (**Fig. 8**).

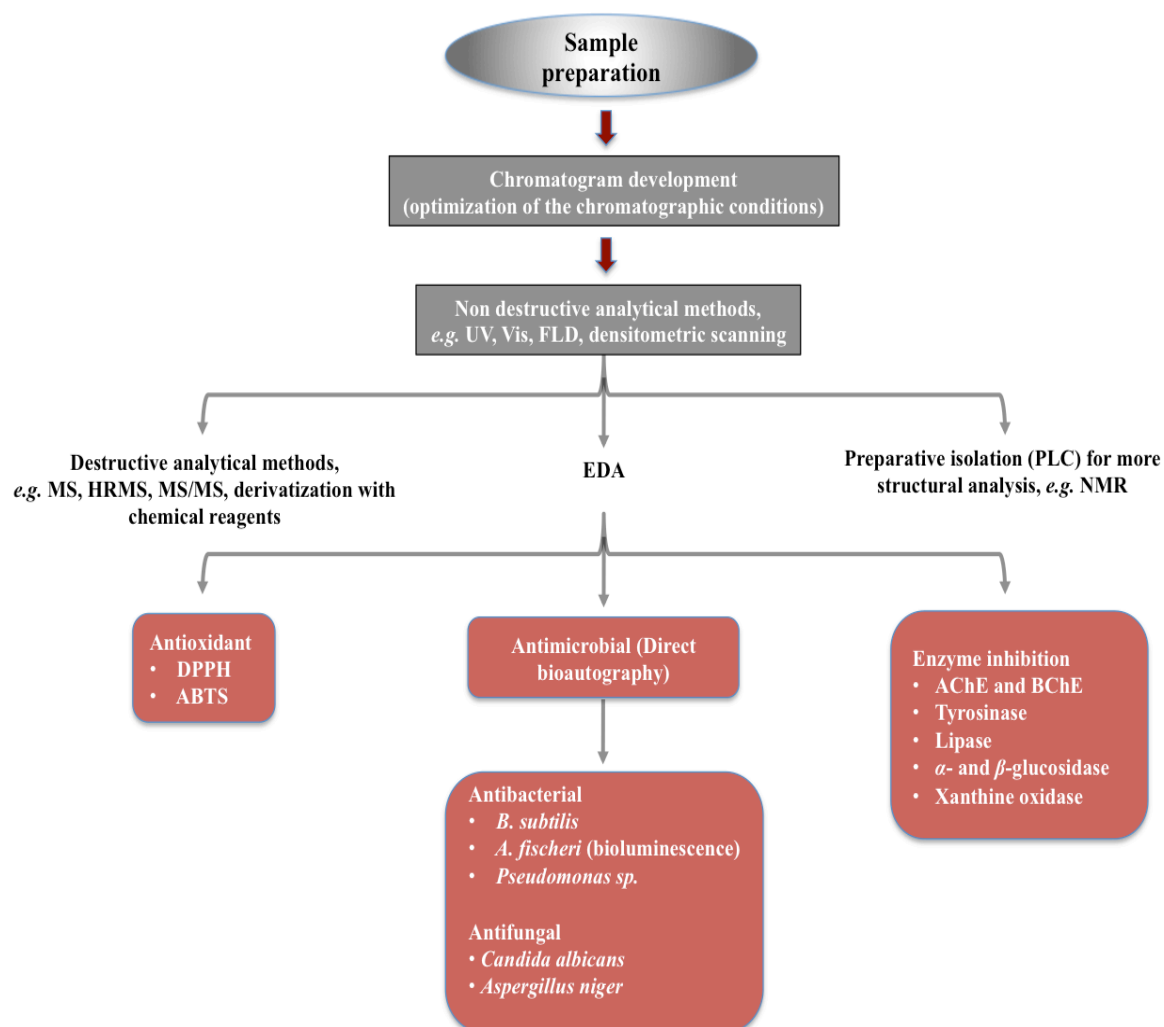


**Fig. 8.** Schematic representation of (HP)TLC-based (bio)analytical hyphenations (Morlock and Schwack 2010, Dewanjee et al. 2015).

Biodensitometric measurement after application of the (bio)assays can also be performed using the TLC scanner. It mainly gives an indication regarding the potentiality of studied inhibitors through measuring the peak area of the inhibition zones, which in most of the cases appear as white spots vs. the colored background. Noteworthy, the inhibitory impact generated by the compounds can be biologically referred to that of a known standard inhibitor. Thus, providing comprehensive biocomparison information.

In summary, linking HPTLC to the (bio)analytical methods places this technique steps ahead from many other conventional methods. It leads to high-throughput detection of poten-

tial drugs, remarkably from natural sources, like antimicrobials, antioxidants, and enzymes inhibitors in a relatively short time with minimal consumption of both samples and chemicals.

### 1.5.2. HPLC-MS

HPLC-MS is another common hyphenated system. It interfaces the chromatographic technique to various detection methods like UV and mass spectrometer, thus, allowing on-line separation and identification of compounds in a complex mixture.

Due to the diverse nature of plant metabolites, a universal method for separation, detection, and identification is practically not possible. Hence, HPLC-based hyphenation has been greatly advanced in order to suit these a broad needs. The chromatography part (HPLC) consists of five main components: solvent reservoir, pumps, sample inlet, column compartment, and detector. Based on the column dimension and working flow rate, the HPLC instruments are usually classified as preparative, analytical, micro, nano, and chip HPLC (Waksmundzka-Hajnos and Sherma 2010). The most widely used packing material for HPLC columns is silica which could be modified to work under different separation modes such as normal phase or reversed phase.

With regard to the detection methods, a purpose-based classification is reported. So, for just recording the chromatographic traces, UV, evaporative light scattering detectors or electrochemical detectors would be suitable. While, the UV-DAD (photodiode array detection) and MS detectors are considered appropriate for compounds identification objectives (Larson et al. 2000). Although considered as a relatively expensive when compared to other detectors, MS still one of the most selective and sensitive detector for analysis of natural products. The principle task of mass spectrometers is to aid in the structure elucidation of compounds from the conveyed molecular mass information. When coupled to HPLC, MS could be satisfactory for identification of the individually resolved compounds from complex matrices. Typically, all mass spectrometers constructed of three main parts *ion source*, *mass analyzer*, and *detector*.

Mass analysis starts with the most crucial step, which is the conversion of the introduced neutral molecules into a gas phase while ionizing them. Several ion sources are available differing principally in the way they transfer the molecular species into gas phase and affecting ionization. Ion sources could be either hard techniques like electron ionization or soft techniques as in case of chemical ionization, electrospray ionization, and matrix-assisted laser

desorption ionization (Bhardwaj and Hanley 2014). Electrospray ionizers are the most widely used ionization sources, even though, it poorly ionize the nonpolar compounds. The ionization occurs under the atmospheric pressure leading eventually to isolated gas-phase ions. The mechanism involves passing the liquid analyte through a capillary maintained at a high electrostatic voltage (3-5 kV). This generates a mist of micrometer-sized electrically charged droplets, which upon evaporation of the solvents would shrink and disintegrate into fine particles leading to formation of the isolated gas-phase ions (Fenn et al. 1990; Wilm 2011; Medhe 2018). The ion beam is now directed towards the mass analyzers working under high vacuum conditions. Various types of mass analyzers have been developed utilizing different modes of ion separation. Common mass analyzer devices include: Time-of-flight, Magnetic sector, Linear quadrupole, Linear quadrupole ion trap, Quadrupole ion trap, Fourier transform-ion cyclotron resonance, and the most recent Orbitrap analyzers (Pitt 2009). Till now the first two steps of mass measurement have been accomplished, *i.e.* ion generation and separation, but still the visual translation into an informative data remains as an exclusive function to the detectors. In general, ion detectors receive a lesser attention in mass reviews than ion sources and mass analyzers, although it represents an integral role in analysis output. Two common ion detectors have been discussed mostly in many reports, Faraday and electron multiplier detectors (Koppenaal et al. 2005).

The development of tandem mass analysis (MS/MS or MS<sup>n</sup>) has a spectacular impact on structural characterization of components of a complex mixture, in particular, when it is coupled to HPLC. The idea that features the MS/MS process is that two mass analyzers are connected in series (either in space or time) with a collision compartment in between (Snyder et al. 2018). Tandem mass analysis could be performed in different modes depending on the mass information needed, however, all modes could be integrated together to permit structural determination of the measured analyte. Four scan modes are widely used so far in tandem mass experiments: *product ion*, *precursor ion*, *neutral loss*, and *single reaction monitoring* (**Fig. 9**). In product ion scanning, which is frequently used, the first mass analyzer (MS1) is selected while the third mass analyzer (MS3) is scanned over a mass range and in between is the collision cell.

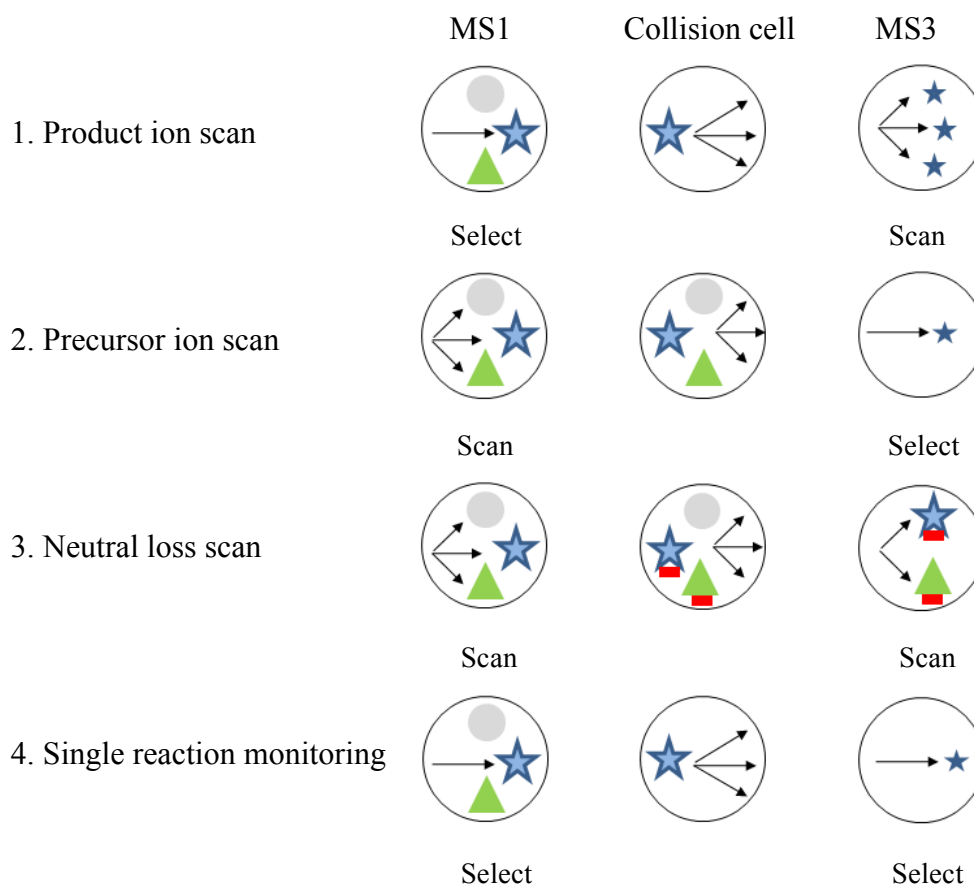


**Fig. 9.** Possible scan modes of tandem mass analysis (shapes represent different ion species).

With high selectivity and sensitivity of the different scan modes of MS/MS, a high throughput phytochemical screening of botanical extracts has been achieved (Yang et al. 2009; Stylos et al. 2017). Phenolics, with its major subdivision, flavonoids, have been extensively studied by HPLC-MS/MS means (March and Brodbelt 2008; Kachlicki et al. 2016), the reason could be their ubiquitous abundance, physiological roles in plants, and broad health benefits. Sequential mass information obtained through precursor ion fragmentation allowed complete analysis of phenolics exist in conjugated forms (Stobiecki et al. 2010; Orčić et al. 2014). Characteristic loss or cleavage of the molecule compositional unites could be easily determined from the difference between the  $m/z$  of the parent and daughter (fragment) ions. Flavonoids are mostly occur as glycoconjugates with aglycone part is being attached to sugar (mono-, di-, tri-, and tetra-) and in many cases one or more of the aglycone or sugar OHs is acylated with different aliphatic (acetyl and malonyl) or aromatic (benzyl, cinnamoyl, coumaroyl, galloyl, feruloyl, and sinapoyl) acyl groups. So, assignment of the conjugated moiety can be known from the mass of the diagnostic fragment. For examples, loss of

mass units equal to 162 indicates (hexose unit), and 146 (deoxy sugar), 152 (pentose), 86 (malonyl), 146 (coumaroyl) (Cuyckens and Claeys 2004).

## **1.6. HPTLC-GUS**

### **1.6.1. Glucuronidation and deglucuronidation**

In general, the process of xenobiotics detoxification involves two metabolic phases namely, phase I and phase II. phase I is mostly considered as a preparatory process. The reactions executed in phase I involve oxidation, epoxidation, hydroxylation, dealkylation, hydrolysis, or similar modifications that result in formation of a slight enhancement in the polarity of the metabolites. In phase II, the products of phase I and the xenobiotics themselves, if having the proper functional groups, is conjugated with an endogenous polar moiety, giving rise to highly polar metabolites that are readily excreted from the body through the bile (Hodgson 2010). Examples of the endogenous conjugating moieties are sugars, amino acids, sulfate, and acetate. Therefore, the phase II metabolism is considered as a detoxification process, such that helps the body to eliminate the administered xenobiotics like pesticides, food-borne carcinogens, and drugs.

Glucuronidation is a common phase II detoxification reaction. It is the major pathway for elimination of many xenobiotics. Compounds with functional groups like -OH, -COOH, and -NH<sub>2</sub> are possibly conjugate with the glucuronide source, uridine-5'-diphosphoglucuronic acid, employing uridine diphosphate glucuronosyl transferase as a catalytic enzyme (Baynes and Hodgson 2010). Although, glucuronidation plays an essential role in elimination of xenobiotics, the rate is suggested to be limited by the deglucuronidation process mediated by GUS. The enzyme leads to release of the glucuronide moiety through hydrolysis mechanism, yielding the original unconjugated form of the parent compounds. Therefore, increasing the possibility of their re-absorption into the circulation system and subject the body to prolonged unwanted effects of these potentially toxic compounds, resulting in dose limitation.

### 1.6.2. GUS inhibition

Potential health consequences of such hydrolytic reactivation of glucuconjugated xenobiotics or drug metabolites by GUS have been widely reported. Some examples of xenobiotics that typically eliminated by the glucuronidation route but retrieve their activity after being deglucuronidated by GUS are here given:

- 4-(methylnitrosamino)-1-(3-pyridyl)-1-butanone and 1,2-dimethylhydrazine are producers of reactive oxygen species that lead to DNA damage, mutagenesis, and carcinogenesis and reactivation of their glucuconjugated metabolites leads to intestinal injury and colon cancer (Cheng et al. 2015).
- Irinotecan (CPT-11), a potent anticancer drug and reactivation of the glucuconjugated metabolite results in a serious chemotherapy-induced diarrhea (Roberts et al. 2013).
- Nonsteroidal anti-inflammatory drug, reactivation of the glucuconjugated metabolite leads also to intestinal injury (Roberts et al. 2013).

Thus, it becomes obviously evidenced that inhibition of GUS would be of pivotal health benefits. Intriguingly, reactivation of the readily glucuconjugated metabolites is highly specific, in such a way that it takes place only by GUS of the gut bacteria, *e.g. E. coli*, rather than the human orthologs (Cheng et al. 2015). Accordingly, several lead drugs have been emerged as selective inhibitors that solely inhibit the bacterial GUS; the introduced inhibitors didn't alter the activity of the parent drug or even harm the bacteria or human cells (Wallace et al. 2010; Pellock et al. 2018).

### 1.6.3. GUS inhibition assay

As a selective marker for detection of the enteric bacteria, *e.g. E. coli* in food, water, and environmental samples, GUS assays have been adequately proposed. With growing interest in finding an appropriate substrate for the histochemical demonstration of GUS, detection assays of the enzyme have been well advanced. Two methods of detection, fluorometric and colorimetric, have been reported frequently in literature.

Fluorometric assay uses 4-methylumbelliferyl- $\beta$ -D-glucuronide as a substrate, which upon hydrolyses with GUS, releases the fluorogenic 4-methylumbellifon as an end product that could be observed at a longer UV light (366 nm) (Moberg 1985). Colorimetric assay, as referred from the name, results in a colored product typically after hydrolysis of the substrate

by GUS. A variety of chromogenic substrates have been evolved for this purposes, *e.g.* *p*-nitrophenyl- $\beta$ -D-glucuronide (Kim et al. 1999), phenolphthalein- $\beta$ -D-glucuronide (Lampe et al. 2002), naphthol derivatives (Jeffrey 1969), and indoxyl- $\beta$ -D-glucuronide (Haines et al. 1993).

One other sensitive GUS substrate is X-Gluc (Frampton et al. 1988). The substrate works efficiently for histochemical localization of GUS in plants giving a blue-colored precipitate at the presumptive sites of the enzyme activity (Jefferson 1987). It also showed a profound capacity to detect *E. coli* bacteria in clinical samples (Wu et al. 2018). The reaction mechanism of such substrate involves at first hydrolytic cleavage affording the colorless indoxyl intermediate, which undergoes further oxidation by the atmospheric oxygen and ultimately dimerization takes place to yield the end product as a blue-colored precipitate, dichlorodibromoin-digo (Jefferson 1987).



## 2. Aims and objectives

The occurrence of SMs in plants is highly influenced by several exogenous factors, among which the environmental ones are regarded as key contributors. Plants accumulate such metabolites as a part of their defense mechanisms in an effort to survive. In addition to their beneficial roles in plants, SMs display wide scope of important pharmacological activities, favoring their use as medicines in several diseases. Plants growing endemically in St. Catherine region in Egypt are exposed to many stressing impacts, which might induce some interesting chemical and/or biological properties.

To prove the relevant bioactivity of SMs present in any studied material, standardized (bio)assays are necessarily followed. The emergence of several streamlined hyphenation techniques that couple the chromatographic separation to the bioactivity testing have considerably reduced the experiment time as well as the sample consumed; made it possible to directly track the bioactive metabolites in the botanical material. With the formentioned motifs in mind, the current study was designed with the following **aims**.

1. Biologically guided isolation of the bioactive metabolites from two plant species growing natively in St. Catherine region in Egypt, namely *P. boveana* (Primulaceae) and *A. pubescens* (Plantaginaceae), along with one medicinally important plant, *P. veris* (Primulaceae).
2. Development of a new HPTLC-EDA hyphenation for the simultaneous detection of GUS inhibitors present in complex matrices with a particular focus on verification to botanical material.
3. HPLC-MS based flavonoids profiling in *P. boveana* extract.

## Objectives

1. Implementation of the HPTLC-EDA technique as a straightforward, material saving methodology for biological screening of the studied plant species. With this objective, the cutting-edge technologies in chromatography and (bio)assay application on HPTLC are intended for use.
2. The bacterial and AChE/BChE inhibitory activities were considered for biological screening of *P. boveana* and *P. veris*.
3. Investigate the *A. pubescens* extract for the presence of active AChE inhibitors. With this objective, we planned to provide wider insights with regard to the ChE inhibitory activity of iridoids occurring in the plant. The outcomes would advance and support the application of iridoids in neurodegenerative diseases like AD.
4. Structure elucidation of the bioactive metabolites detected in the studied plant extracts and, when necessary, compounds separation should be also carried out.
5. Establishment of HPTLC-GUS inhibition assay hyphenation. The developed protocol would be optimized, validated, and verified.
6. HPLC-HRMS and tandem mass analysis of *P. boveana*. Considering its critically endangered status and the lack of information regarding its chemical constituents, *P. boveana* is worth chemically investigating with the purpose of possible revealing a plant-specific chemical profile.

## 3. Material and Methods

### 3.1. Material

#### Plant material

*Primula veris* L.: dried flowers were purchased from Caesar & Loretz GmbH (Hilden, Germany).

*Primula boveana* Decne. ex Duby: leaves were collected (June, 2017) from Shag Mousa area in St. Catherine, Egypt; authenticated by Prof. Hasnaa Hosni, Professor of Flora and plant taxonomy, Cairo University Herbarium.

*A. pubescens* Fresen.: Aerial parts were collected (April, 2015) from Wadi El-Arbeen in St. Catherine, Egypt; authenticated by the taxonomy staff members of St. Catherine protectorate.

### Solvents and reagents

All solvents used for extraction and chromatographic separations in this study were high purity grade solvents and obtained from Fischer Scientific, Acros Organics, and VWR (Germany). Methanol-d<sub>4</sub> for NMR measurement (CD<sub>3</sub>OD) obtained from Euisotop (Saarbrücken, Germany).

### HPTLC plates

Silica gel 60 with glass support, F<sub>254</sub> (20 cm × 10 cm) were obtained from Merck (Darmstadt, Germany).

### Enzymes

AChE, BChE, GUS were purchased from Sigma-Aldrich (Steinheim, Germany).

### Microorganisms

*B. subtilis* spore suspension (2.0 ml ampoules) from Merck, product No. 110649 (Darmstadt, Germany), Luminescent *A. fischeri* strain (Leibniz Institute DSMZ-German Collection of Microorganisms and Cell Cultures, Berlin, Germany).

### Growth media

*B. subtilis* was cultured on Mueller-Hinton growth medium, product No. 70192 (Sigma Aldrich, Germany), optical density of the bacterial suspension was monitored using spectrophotometer (M501, SpectronicCamspec, Leeds, UK). *A. fischeri* growth medium was prepared according to DIN ENISO, Section 5 (DIN 2009) and contained in 1 L of H<sub>2</sub>O, NaCl (30 g), NaH<sub>2</sub>PO<sub>4</sub>·H<sub>2</sub>O (6.1 g), K<sub>2</sub>HPO<sub>4</sub> (2.75 g), MgSO<sub>4</sub>·7H<sub>2</sub>O (0.204 g), (NH<sub>4</sub>)<sub>2</sub>HPO<sub>4</sub> (0.5 g), glycerin (3.0 mL), peptone from casein (5 g), and yeast extract (0.5), pH adjusted to 7.0 with 20% NaOH solution or 1M HCL.

### Substrates and reagents

α-Naphthyl acetate was from BioChemica (Germany), X-Gluc (Carbosynth, Berkshire, UK), SFLG, Fast Blue B salt and Riv were from Sigma-Aldrich (Steinheim, Germany), MTT, *p*-anisaldehyde, natural product reagent, and polyethylene glycol 400 were purchased from Carl Roth (Karlsruhe, Germany), SL was obtained from Santa Cruz Biotechnology (Heidelberg, Germany).

## 3.2. Instruments

### Instruments for HPTLC application, development and documentation

All HPTLC instrumental platform was from CAMAG (Muttenz, Switzerland) and included: Automatic Thin Layer Chromatography (ATS-4), Automatic Developing Chamber (ADC2), TLC visualizer, TLC scanner 4, TLC derivatizer, BioLuminizer, TLC plate heater 3, Chromatogram immersion device III, smartCUT TLC Plate Cutter.

### Preparative HPLC and NMR

Preparative HPLC isolation was carried out on DeltaPrep chromatography system, Waters (Milford, MA, USA) controlled by MassLynx V4.1 software. The instrument is equipped with preparative LC controller, fluid handling unit, dual  $\lambda$  absorbance detector 2487, and pumps (All Waters<sup>®</sup>, USA) and solvents were degassed with Helium gas. Column was RP-column (vp 250/10/5  $\mu$ m, Nucleodur C18, Macherey-Nagel, Düren, Germany). NMR: ECX-400 (400 MHz), JEOL (Freising, Germany).

### HPLC-EPIMS, HPLC-HRMS, and HPTLC-MS

HPLC-HRMS: HPLC system was Agilent 1100 series equipped with degasser (G1322A), Bin pump, auto-sampler, column compartment and DAD detector (Agilent Technologies Deutschland GmbH). Column was EC 250/4/5 (Nucleodur C18, Macherey-Nagel, Düren, Germany). The HPLC system was coupled with the hybrid LTQ-FT Ultra mass spectrometer (Thermo Fischer Scientific, Germany) hybrid mass spectrometer having a linear ion trap and Fourier transform ion cyclotron resonance as an analyzer. The ion source was ESI.

EPIMS: EPIMS analysis was achieved on hybrid Q-Trap mass spectrometer (Applied Biosystems SCIEX 2000, Darmstadt, Germany). The instrument is equipped with ESI source. Source temperature was 200 °C and nitrogen was the nebulizer gas. Data were collected and processed using Analyst 1.1.4 software. Extract was introduced *via* the integrated syringe pump at a flow rate 10  $\mu$ L/min.

HPTLC-MS: mass analysis of eluted bands directly on chromatograms was achieved using HPTLC-MS interface (Plate Express, Advion, NY, USA) for online zone transfer

to the QExactive™ PlusHybrid Quadrupole-Orbitrap mass spectrometer (Thermo Fisher Scientific, Germany).

### **3.3. Biological evaluation and active metabolites identification in *P. boveana* & *P. veris***

#### **3.3.1. HPTLC development**

The workflow of HPTLC procedures followed in this research is illustrated in **Fig. 10**.

##### Sample preparation:

Air-dried *P. boveana* leaves and *P. veris* flowers were finely pulverized using lab mixer. One gram of each plant powder was extracted with 10 mL mixture of toluene and EtOAc (1:1, *V/V*) for 24 h under continuous stirring. Each extract was filtered through 0.45 µm membrane filters (Chromafil®, Germany) and kept at –20 °C till analysis.

##### Application, development and documentation:

Applied volumes were optimized depending on the resulting separation pattern of samples as well as the appearance of the inhibition zones, so that to avoid any overlapping of eluted bands. Bands of 8 mm wide were applied using ATS-4. Chromatogram developed with mobile phase composed of hexane : EtOAc (7:3, *V/V*) in Twin Trough Chamber (presaturated with the mobile phase for 3 min) up to 80 mm migration distance. Plates documented by the TLC Visualizer at UV 254 nm, 366 nm, and white light illumination (reflectance, transmittance, and both modes together).

##### Derivatization

*p*-Anisaldehyde/sulfuric acid reagent was prepared by adding 5.0 mL conc. sulfuric acid to a mixture of 85 mL methanol and 10 mL acetic acid. Then, 0.5 mL of *p*-anisaldehyde was added. Developed HPTLC plates were sprayed with 3.0 mL of the reagent solution followed by heating at 105 °C on the TLC plate heater for ca. 4 min. The chromatograms were documented at UV 366 nm and under white light illumination.



**Fig. 10.** Experimental workflow of HPTLC-EDA pursued in the study

### 3.3.2. HPTLC-antibacterial bioassay

#### *A. fischeri* bioassay

The bacterial suspension was prepared in the growth medium mentioned in section (3.2.1). The developed plates were immersed in the bacterial suspension (time 1 s, immersion speed 3 cm/s). The inhibitory activity displayed by the active metabolites on *A. fischeri* was documented using the BioLuminizer set to capture an image every 2 min for a total of 10 images. Bioactive zones appeared as dark zones against a bright background.

#### *B. subtilis* bioassay

The bacterial suspension was initiated in a 250 mL Erlenmeyer flask contained 50 mL of Mueller-Hinton growth medium and inoculated with 2.0 mL bacterial spore suspension. The inoculated broth was incubated at 37 °C under orbital shaking. Growth kinetics were moni-

tored by measuring the OD<sub>600</sub>. Incubation continued until  $9.0 \leq OD_{600} \leq 1.0$  was obtained. Developed plates were dipped in the bacterial suspension for 3 s with an immersion speed of 3 cm/s. Plates were incubated in a moistened, well-closed plastic box at 37 °C for 2 h, then dipped into 0.2% Phosphate-buffered saline-buffered MTT solution (time 1 s, immersion speed 3 cm/s). After incubation for an additional 0.5 h at 37 °C, inhibition zones appeared white against a purple background. The bioautograms were documented under white light illumination in the reflectance mode.

### 3.3.3. HPTLC-AChE/BChE inhibition assay

Solutions of both enzymes as well as the relevant substrates were piezoelectrically sprayed over the chromatograms using the TLC Derivatizer. Enzyme solutions were prepared as reported by Hage and Morlock (2017), and contained 666 units AChE or 334 units BChE in 100 mL 0.05 M TRIS buffer, pH 7.8 (0.1% BSA). Pre-wetting of the plates with 1.0 mL Tris buffer was done, followed by piezoelectric spraying of 3.0 mL of the enzyme solution. Excess liquid film allowed to be completely adsorbed by the plates before being incubated at 37 °C in moistened plastic containers for 30 min. After incubation, the plates were sprayed with 0.5 - 0.75 mL of the substrate mixture composed of  $\alpha$ -naphthyl acetate solution (3 mg/mL in methanol) and Fast Blue salt B dye (3 mg/mL in water). Active bands appeared as white zones against a purple background and results were documented with the TLC Visualizer at white light illumination.

### 3.3.4. Active metabolites Identification

Metabolites that showed inhibitory activities on either enzymes or microbes, as recognized from their inhibition zones, were identified by to UV, HRMS, and NMR spectroscopic methods. UV spectra of compounds were recorded on the TLC scanner set to absorbance measurement and wavelength range (190 - 700 nm). For HPTLC-HRMS analysis, active bands were marked and eluted through the elution head-based interface using methanol as an eluent at a flow rate 0.1 mL/min (**Fig. 11**). Full scan mode was selected and covered a mass range 100-1000. Analysis performed on -ve polarity for *P. veris* and +ve polarity mode for *P. boveana*. ESI voltage was 3.5 kV (– 3.0 kV), nebulizer gas was nitrogen, and source temperature was set at 250 °C. Data acquisition and processing controlled by Xcalibur 3.0.63 software (Thermo Fisher Scientific).



Bioactive compounds in *P. boveana* were further isolated using preparative HPLC. Separation was achieved using an isocratic elution with 60% methanol in water. Injection volume was 100  $\mu\text{L}$  per run and flow rate set to 3.0 mL/min. The detector was set at  $\text{UV}_{254\text{nm}}$  and collected fractions were evaporated under reduced pressure to obtain the active metabolites (**Pb1** - **Pb4**) in pure forms. Purified metabolites were dissolved in  $\text{CD}_3\text{OD}$  for  $^1\text{H}$  NMR measurements.

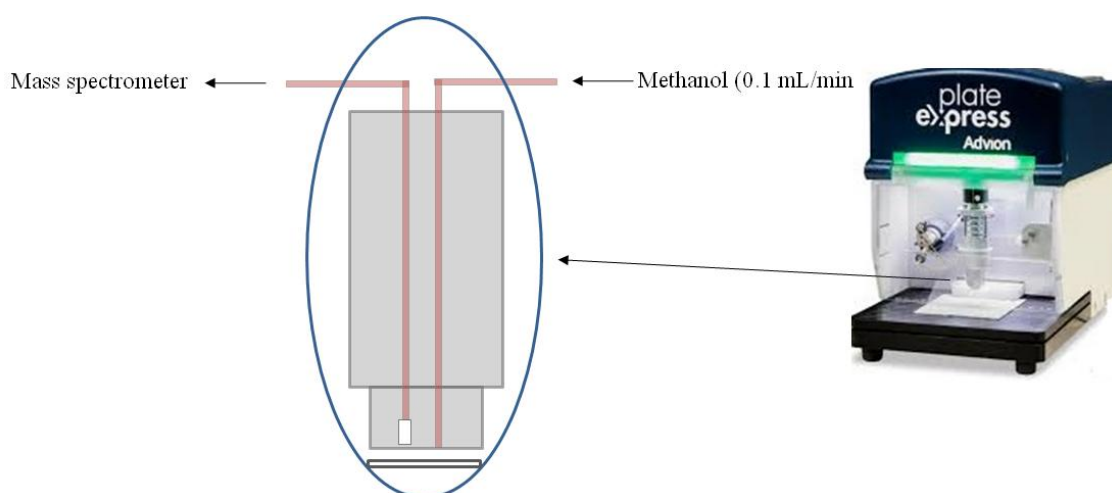


**Fig. 11.** HPTLC-MS interface (elution head-based) with representative diagram showing the mechanism by which compounds are eluted from the plate for MS analysis

### 3.3.5. AChE inhibition equivalency calculation of **Pb1**

The AChE inhibition equivalency study was performed in order to evaluate the AChE inhibitory activity exerted by the most active metabolite (**Pb1**) as equivalent to the well-known enzyme inhibitor, Riv. So, *P. boveana* extract was applied in triplicate using two different application volumes (0.5 and 0.1  $\mu\text{L}$ ) and bands were separated as described using the same mobile phase. Based on the area of the inhibition zones, the lower volume (0.1  $\mu\text{L}$ ) was used for accomplishing the equivalency calculation. Riv was applied on an edge of the chromatogram using the free mode option of the ATS-4. Five different amounts (1 - 10  $\mu\text{g}/\text{band}$ ) were applied as 8 mm-band track patterns. The HPTLC-AChE inhibition assay was performed. The standard calibration curve of the Riv was constructed and the regression equation was generated using Microsoft excel. Using this equation, direct substitution with the obtained area of inhibition of **Pb1** was done and results expressed as Riv equivalent values.

### **3.4. Biological evaluation and active metabolites identification in *A. pubescens***

#### **3.4.1. HPTLC development**

Defatted crude extract of *A. pubescens* was obtained as follow: air-dried arial parts of the plant (300 g) were finely pulverized. The plant powder was extracted with 80% methanol (1:10, *W:V*) for 24 h, and evaporated under reduced pressure. The resulting residue was defatted by liquid-liquid partitioning between 90% methanol (500 mL) and *n*-hexane (2 x 500 mL). The defatted soluble extract was completely dried by rotary evaporator. For HPTLC-EDA analysis, 20 mg of extract residue was dissolved in 1.0 mL methanol. Application volume was 2.0  $\mu$ l that applied as a band of 8 mm length. Plates were developed as described in section 3.3.1 using mobile phase composed of CF : MeOH (9:2, *V:V*) and documented by the TLC Visualizer at UV 254 nm, 366 nm, and white light illumination (reflectance, transperance, and both modes together). Also, derivatization with *p*-anisaldehyde was performed as shown in section 3.3.1 followed by image-documentation.

#### **3.4.2. HPTLC-AChE inhibition assay**

The enzyme assay to determine the active inhibitor of AChE enzyme was done as described in section 3.3.3.

#### **3.4.3. Active metabolites identification**

Defatted crude extract (1 g) was chromatographed on an open flash silica gel (230-400 mesh) column eluted with dichloromethane : MeOH (90:10, *V:V*) yielding three fractions (F1-F3). Isolation of active metabolites was achieved by the preparative HPLC. Aliquots of 100  $\mu$ L injection volumes were used and the detector set at 210 nm. Isocratic elution with different methanol/water proportions allowed separation of three metabolites in pure form. Compound **A1** (6 mg) & **A2** (2 mg) were separated from F2 using 75% methanol in H<sub>2</sub>O as mobile phase. While subfraction F3, afforded compound **A3** (5 mg) after elution with 55% methanol in H<sub>2</sub>O. Compounds (**A1** & **A3**) were dissolved in 600  $\mu$ L metahnol-d<sub>4</sub> for NMR (1D & 2D) measurements. Compound **A2** was identified based on the HRMS and HRMS/MS

spectrometric data. Analysis of the ion fragments obtained through collision-induced dissociation permitted identification of **A2**.

#### **3.4.4. AChE inhibition equivalency calculation of compound A1-A3**

Using the free mode option of ATS-4, the isolated metabolites (**A1-A3**) were applied in triplicate, 20 µg/band each while, the standard reference, Riv, was applied at different concentration (0.5 - 14 µg/band). Then, the standardized AChE inhibition assay was followed as described. Densitometric analysis of the chromatograms was done using the TLC scanner set to fluorescence mode at 500 nm without optical filter. The calibration curve obtained from plotting Riv concentrations vs. peak areas and the regression equation was then generated. The results of AChE inhibition activity were expressed as bioactivity equivalent to Riv.

### **3.5. HPTLC-GUS hyphenation**

#### **3.5.1. Method development**

A method for rapid screening and determination of GUS inhibitors present as either pure forms or a part of complex mixtures was developed. The method based on the potential of GUS to hydrolyse X-Gluc substrate into 5-bromo-4-chloro-3-indol (fluorescent, colorless) and  $\beta$ -glucuronide units. The former unit undergoes further oxidation (fluorescent, colorless) with atmospheric oxygen followed by dimerization into the end products (non fluorescent, blue colored).

#### **3.5.2. Optimization and validation of the method**

Optimization of the method involved optimizing the detection wavelength, GUS concentration, reaction time, and the impact of using plates with or without fluorescent indicator. Also, the method was validated in terms of LOD, linearity, and specificity. The current method used the up-to-date technology of TLC derivatization, *i.e.* piezoelectric spraying, achieved by TLC derivatizer. For determination of the optimal absorbance wavelength of the background, the plate was scanned using the TLC scanner in absorbance mode (200 - 800 nm) while the white inhibition zone of the standard inhibitor, SL (1 µg/band),

served as a reference. The optimum detection wavelength obtained was used afterwards as a criterion for further optimization and validation studies, in which the plates were densitometrically scanned in fluorescens mode.

With regard to the GUS optimal concentration, enzyme solution (3.0 mL) at seven different concentration levels (2 - 33 U/mL, *i.e.* 0.03 - 0.5 U/cm<sup>2</sup> in phosphate buffer 0.1 M, pH 7.0) with a fixed volume (1.5 mL) of X-Gluc (prepared as 2 mg/mL in deionized H<sub>2</sub>O) was used. Optimization of the reaction time involved incubation of the chromatogram at 37 °C in a humid atmosphere ensured by placing the HPTLC plates in a wet well-closed plastic box for periods of 20, 40, and 60 min. Then, the plates were densitometrically scanned at the optimal wavelength in a fluorescens mode and peak areas of the inhibition zones of SL (1.0 µL, *n* = 3) were determined to obtain the optimal incubation time. The influence of using HPTLC plates with and without fluorescent on colorimetric detection was investigated.

The LOD of GUS was determined using serial dilutions of the standard inhibitor SL (0.75 - 2000 ng/band). LOD determined at a signal to noise (S/N) ratio of  $\geq 3$ . Also, the linearity was examined by plotting the different SL concentrations *vs.* the peak areas of inhibition and the linear correlation equation was determined from the resulting curve. The specificity was studied by using a different substrate (2-naphthyl- $\beta$ -D-glucopyranoside).

### 3.5.3. Statistical analysis

Statistical analyses were accomplished using Minitab 17<sup>®</sup> software. Collected data were subjected to analysis of variance (ANOVA) and means were compared through Fisher Pairwise Comparison ( $p \leq 0.05$ ).

### 3.5.4. Verification of the method

To verify the new method, two samples of botanical material were screened using the optimized workflow. The studied samples were *P. boveana* extract (as prepared in section 3.3.1) and SFLG. The SFLG sample was prepared by dissolving 250 mg of the flavonolignans powder in methanol (1:10, *W:V*), sonicated for 10 min, diluted with methanol (1:100, *V/V*), then filtered through a syringe filter (0.45µm). The resulting filtrate was used as a final working solution.

The optimized protocol for screening of GUS inhibitors in both test samples was applied as shown in **Fig. 12**. Both samples were known for their phyto-constituents with varied chemical properties, which demanded the use of different developing systems with variable eluting powers to separate their individual components. Hence, offered a good option to examine the influence of different mobile phase compositions on the behavior of the method.

### **3.5.5. Active metabolites identification**

The active GUS inhibitors were determined under UV 254 and 366 light. For visualization of the possibly non-UV absorbing inhibitors, plates were derivatized with NP/PEG and documented under 366 UV light. For *P. boveana*, active inhibitors were characterized by comparison with reference compounds previously isolated in section 3.3.4. While in SFLG, the active GUS inhibitors were identified by extensive HRMS and HRMS/MS analysis. In order to prevent the strong background signals and ion suppression from the formed inorganic salts (salt clusters) due to acidic mobile phase, pretreatment of the plates was carried out as described by Glavnik et al. (2017). The plates pretreatment step involved two pre-developments of the plates, firstly with MeOH : FA (10:1, *V/V*) and secondly with acetonitrile : MeOH (2:1, *V/V*) with 20 min drying at 100 °C after each development. Mass data was collected after elution of the targeted bands with HPTLC-MS interface. Acquisition was performed in -ve mode polarity. Eluting solvent, mass range, capillary voltages, and source temperature criteria were the same as in section 3.3.4. HR-MS/MS analysis was achieved with HR-MS<sup>2</sup> scan mode acquisition. Collision energy was varied 10 - 50 V but finally 20 V was found the optimum for affecting a proper fragmentation of the precursor ions.

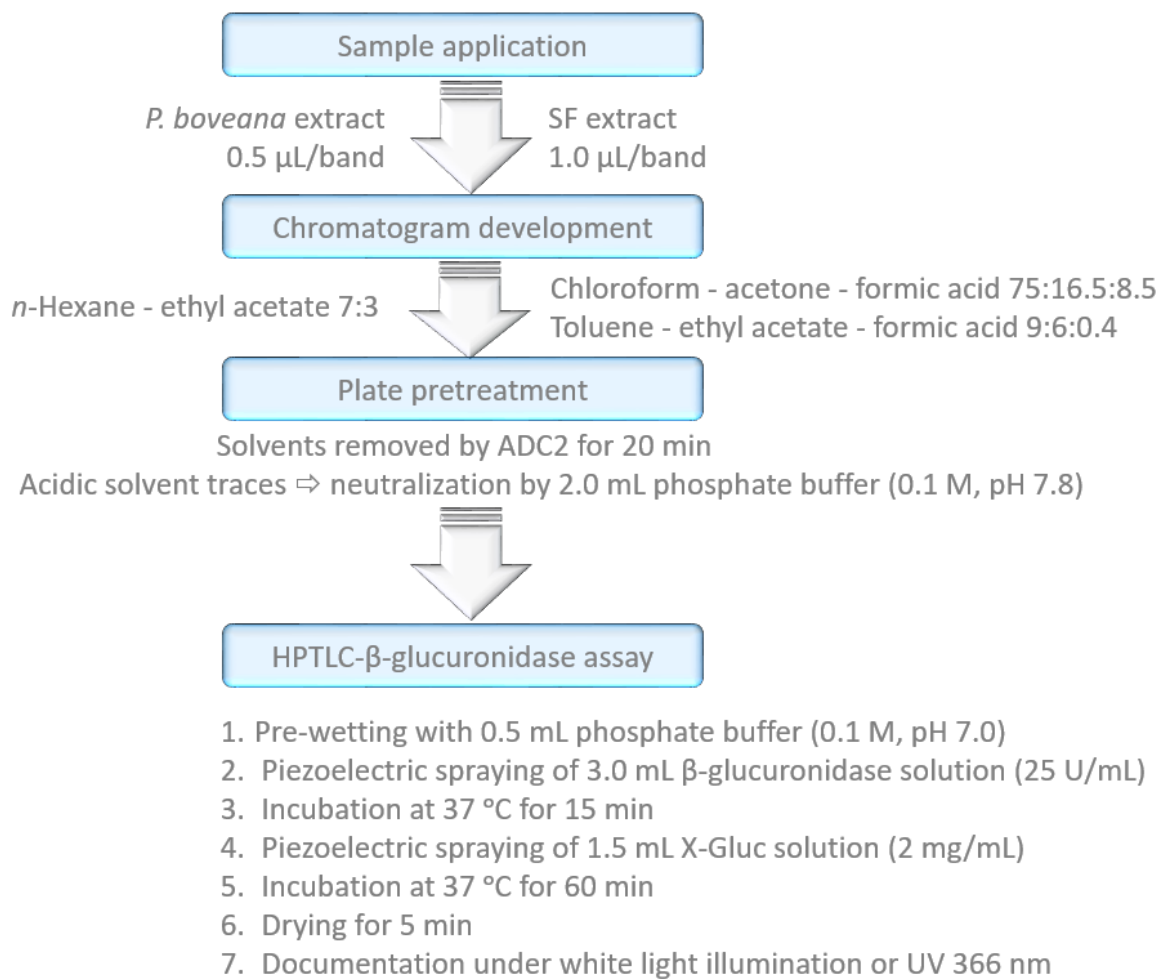


**Fig. 12.** Schematic representation of the verification study showing the optimized HPTLC-GUS inhibition assay hyphenation as applied to *P. boveana* and SFLG extracts.

### **3.6. HPLC-HRMS followed by EPI scanning for flavonoids profiling of *P. boveana***

The experimental protocol for analysis of flavonoids content in *P. boveana* depended on LC-HRMS followed by tandem mass analysis of the glycoconjugated flavonoids through EPI scanning. The mobile phase used for HPLC separation was composed of acetonitrile as solvent A and H<sub>2</sub>O (0.1% TFA) as solvent B. Flow rate was set to 0.25 mL/min and gradient elution was programmed as follow: 0 min (5% A), 5 min (5% A), 60 min (95% A), and 65 min (95% A) with an injection volume of 15 µL. PDA detector was set at  $\lambda$  254 nm. The mass data collected in a full scan mode and the spectrometer parameters included: ESI as an ion source in set to positive ion polarity, capillary voltage (3.8 kV), sheath gas (3.0 mL/min) and source temperature (310 °C).

For better understanding of the detailed structures of the flavonoids, the molecular mass of eluted metabolites was subjected to tandem mass analysis through the EPI scanning. The triple quadrupole mass spectrometer affected parent ion fragmentation through collision-induced dissociation in the second RF-only quadrupole. The Q-TRAP spectrometer set to EPI scan mode and targeted molecular ion of metabolites were entered. ESI is the source of ionization in positive ion polarity. Nebulization gas (nitrogen) pressure 40 psi, drying gas (N<sub>2</sub>) flow 9 L/min and source temperature 350 °C, capillary voltage at 4 kV. Flavonoid compounds were tentatively identified based on analysis of their accurate molecular masses and the collected MS/MS data.

## 4. Results

### 4.1. Biological evaluation and active metabolites identification of *P. boveana* (leaf) and *P. veris* (flower)

#### 4.1.1. HPTLC-antibacterial bioassay

The antibacterial activity of middle polar extracts of *P. boveana* leaves and *P. veris* flowers was evaluated by means of HPTLC-EDA approach. Two bacterial strains were used in this study, *A. fischeri* and *B. subtilis*. In *A. fischeri* bioassay, the bacterial inhibition was indicated by the loss of the bacteria's endogenous luminescence, which could be easily spotted by observing the dark inhibition zones against the luminescent background. Detection of inhibitory activity against *B. subtilis* detected as white zones against a purple background.

For *P. veris*, the extract was applied in 2.0  $\mu\text{L}$  & 1.0  $\mu\text{L}$  for *A. fischeri* and *B. subtilis*, respectively. Two metabolites (**Pv1** & **Pv2**) displayed inhibitory activity against both bacterial

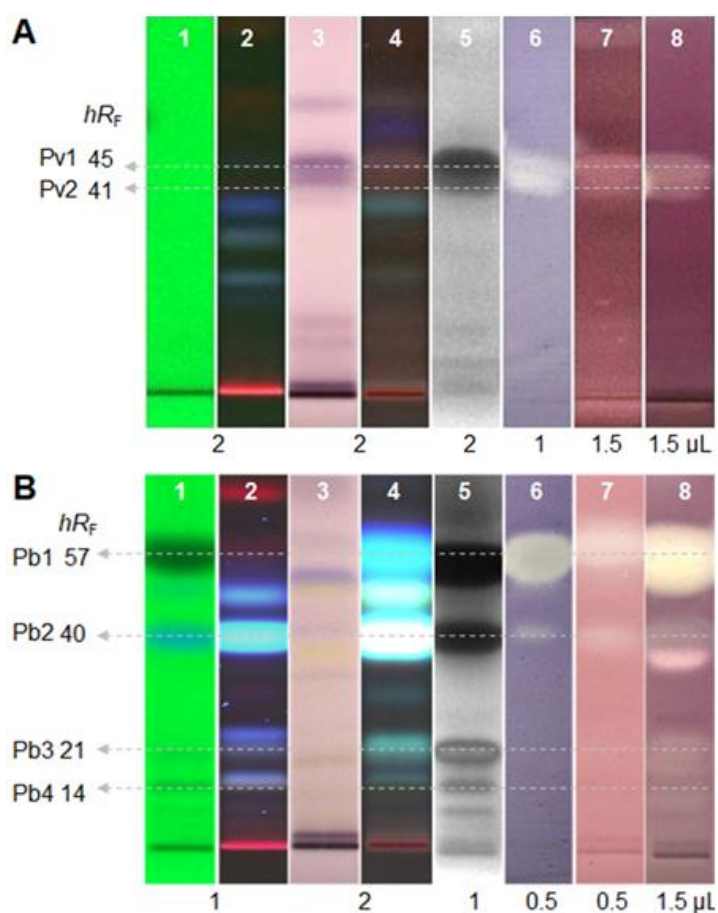


strains (**Fig. 13A**). In *P. boveana*, the extract was applied as 1.0  $\mu\text{l}$  (for *A. fischeri*) and 0.5  $\mu\text{L}$  (for *B. subtilis*). The results (**Fig. 13B**) revealed that four metabolites (**Pb1 - Pb4**) were the most active against *A. fischeri*; only two (**Pb1 & Pb2**) were found active against *B. subtilis*.

#### 4.1.2. HPTLC-AChE/BChE inhibition assay

The possible inhibitory activity of both extracts towards the ChE enzymes family was also investigated. Two enzymes, AChE and BChE were used; zones of inhibition manifested by their white bands against the purple background of the formed formazan. The results of the assay were found very comparable to those obtained for the antibacterial investigation. Compounds (**Pv1 & Pv2**) in *P. veris* extract inhibited both enzymes (**Fig. 13A**). In *P. boveana*, compounds (**Pb1 - Pb4**) inhibited BChE, while AChE has been inhibited only by **Pb1 & Pb2** (**Fig. 13B**).

**Fig. 13.** Chromatograms of *P. veris* flower extract (**A**) and *P. boveana* leaf extract (**B**) at UV 254 and 366 nm (1 and 2), after *p*-anisaldehyde derivatisation at white light illumination and UV 366 nm (3 and 4) and respective *A. fischeri*, *B. subtilis*, acetyl and butyryl cholinesterase autograms (5 - 8).



### 4.1.3. Active metabolites identification

#### HRMS analysis

Identification of the bioactive metabolites in both extracts was achieved by first collecting their HRMS data; this allowed for a tentative structural determination of the active compounds. Acquisition in -ve ESI mode was found optimum for *P. veris* compounds, where the deprotonated  $[M-H]^-$  ion peaks were predominant. In contrast, +ve ESI was better for *P. boveana* compounds, such that the sodium adducts  $[M+Na]^+$  were obtained.

The MS data suggested the molecular formula of **Pv1** as  $C_{18}H_{32}O_2$  and that of **Pv2** as  $C_{18}H_{30}O_2$ , as revealed from their molecular ion peaks at  $m/z$  279.2329 (calculated 279.2329 for  $[M-H]^-$ ) and  $m/z$  277.2174 (calculated 277.2173 for  $[M-H]^-$ ), respectively (**Fig. 14**). These mass values as well as the chromatographic characteristics on the HPTLC plate after derivatization were consistent with those of linoleic and linolenic acids (Kurata et al. 2005; Krüzselyi et al. 2016). Thus, the structure of **Pv1** was determined as linoleic acid ( $C_{18:2}$ ) and **Pv2** as linolenic acid ( $C_{18:3}$ ).

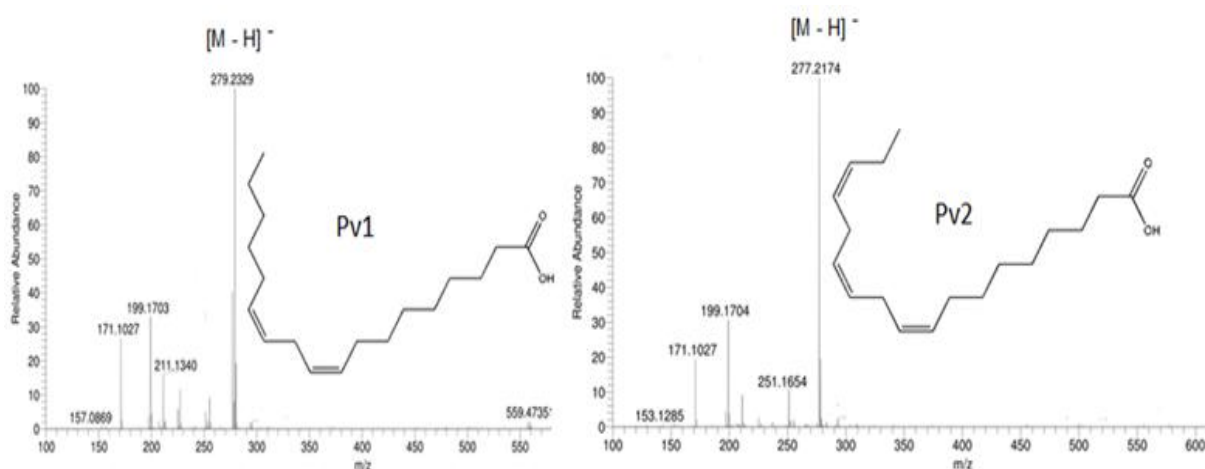


**Fig. 14.** Negative ion HPTLC-ESI-HRMS spectra obtained for compounds **Pv1** and **Pv2** and their structures

Compounds (**Pb1-Pb4**) were also assigned based on their HRMS measurements. The compounds showed base peaks corresponding to  $[M+Na]^+$  and  $[2M+Na]^+$  (**Fig. 15**), thus, affording a high formula prediction information. The molecular ion peak of **Pb1** at  $m/z$  245.0570 suggested the molecular formula as  $C_{15}H_{10}O_2$  (calculated 245.0573 for  $[M+Na]^+$ ). This mass information is consistent with the prevailing lipophilic flavonoid exists in most of the *Primula* plants, which is unsubstituted flavone (Colombo et al. 2017). So, the structure of **Pb1** was tentatively assigned as an unsubstituted flavone. Hereafter, identification of the subsequent

metabolites was based on deduction of their mass differences from **Pb1**. For the **Pb2** zone, the sodium adduct of the ion peak at  $m/z$  275.0675  $[M+Na]^+$  (calculated 275.0679), which is 30 Da higher than **Pb1**, suggested  $C_{16}H_{12}O_3$  as the molecular formula of **Pb2** and thus its structure as methoxyflavone. Similarly, **Pb3** showed an ion peak at  $m/z$  261.0520, 16 Da more than **Pb1**, indicated its molecular formula as  $C_{15}H_{10}O_3$  (calculated  $m/z$  261.0522 for  $[M+Na]^+$ ), hence, **Pb3** was deduced to be hydroxyflavone. Compound **Pb4** gave an ion peak at  $m/z$  365.0990 corresponding to a molecular formula  $C_{19}H_{18}O_6$  (calculated  $m/z$  365.0996 for  $[M + Na]^+$ ). So, **Pb4** was identified as a tetramethoxyflavone.

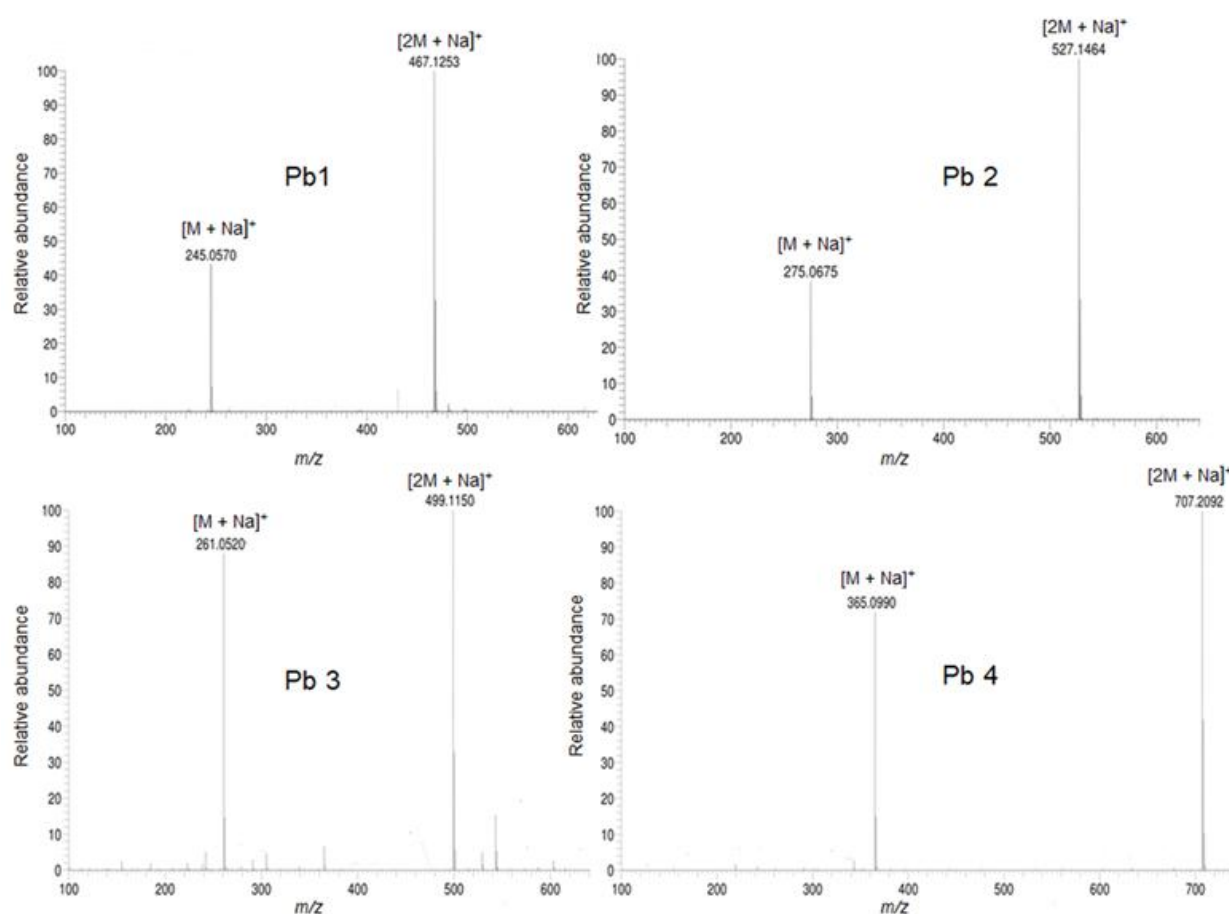


**Fig. 15.** Positive ion HPTLC-ESI-HRMS spectra obtained for compounds **Pb1** - **Pb4**.

#### NMR measurements of (**P1-Pb4**)

Despite the partial assignment of the active metabolites in *P. boveana* extract (**Pb1-Pb4**), their full structure elucidation of **Pb1-Pb4** is not completely resolved since the exact positions of the substituents (OH or OMe) have not concluded yet. Therefore, preparative isola-

tion of these active compounds was done for further NMR analysis. Successfully, the four metabolites were obtained in pure forms by chromatographic resolution of the total extract by means of the preparative HPLC over RP-column with an isocratic elution with 60% methanol in water. All compounds, **Pb1** (3.9 mg), **Pb2** (2.6 mg), **Pb3** (1.5 mg), and **Pb4** (2.1 mg) were separately subjected to  $^1\text{H}$  NMR analysis; spectra are shown in **Fig. 16**.

Compound **Pb1**: UV (max: 251 nm) in the  $^1\text{H}$  NMR spectrum, the characteristic H-3 of flavone was observed at  $\delta_H$  6.80 as singlet. Signals typical for unsubstituted ring A of flavone were assigned at  $\delta_H$  8.11 (ddd,  $J = 0.4, 1.6, 8.0$ , H-5);  $\delta_H$  7.40 (ddd,  $J = 1.1, 7.1, 8.0$ , H-6);  $\delta_H$  7.70 (ddd,  $J = 1.6, 7.1, 8.5$ , H-7);  $\delta_H$  7.60 (ddd,  $J = 0.4, 1.1, 8.5$ , H-8). Also, two peaks integrating for two protons each at  $\delta_H$  8.02 (dd,  $J = 1.5, 7.7$ , H-2' & H-6') and  $\delta_H$  7.51 (m, H-3' & H-5') together with the presence of a multiplet proton resonates at  $\delta_H$  7.54 (H-4') were detected. These findings along with the collected HRMS data and literature values' comparison (Budzianowski et al. 2005) confirmed the structure of **Pb1** as unsubstituted flavone.

Compound **Pb2** UV (max: 253 nm) & **Pb3** UV (max: 251 nm):  $^1\text{H}$  NMR spectra of both compounds have unambiguously confirmed that ring A remained unsubstituted in both structures. However, the spectrum showed a quite different pattern of ring B signals, implying that a substitution is present. In  $^1\text{H}$  NMR spectrum of **Pb2**, four aromatic protons were observed at  $\delta_H$  7.21 (dd,  $J = 1.0, 8.4$ ),  $\delta_H$  7.50 (ddd,  $J = 1.7, 7.4, 8.4$ ), 7.13 (ddd,  $J = 1.0, 7.4, 7.8$ ), and 7.95 (dd,  $J = 1.7, 7.8$ ) ascribable to H-3', H-4', H-5', and H-6', respectively. Also, in  $^1\text{H}$  NMR spectrum of **Pb3**, the four aromatic protons of ring B were observed at  $\delta_H$  7.0 (dd,  $J = 1.1, 7.1$ ),  $\delta_H$  7.30 (ddd,  $J = 1.7, 7.1, 8.3$ ), 6.90 (ddd,  $J = 1.1, 8.0, 8.3$ ), and 7.95 (dd,  $J = 1.7, 8.0$ ) ascribable to H-3', H-4', H-5', and H-6', respectively. These NMR findings were found consistent with those reported in literature for the same metabolites (Blaskó et al. 1988; Moon et al. 1982), pointing out that compound **Pb2** is a 2'-methoxyflavone and **Pb3** is a 2'-hydroxyflavone.

Compound **Pb4**: UV (max: 325, 266, 233 nm) the spin-spin multiplicity of protons of compound **Pb4** were found rather simple. The  $^1\text{H}$  NMR spectrum showed two sets of *ortho*-coupled protons at  $\delta_H$  7.52 (d,  $J = 9.3$ , H-7) &  $\delta_H$  7.31 (d,  $J = 9.3$ , H-8). It also revealed the presence of a signal at  $\delta_H$  6.70 (d,  $J = 8.5$ ) integrates for two protons H-3' & H-5' with *ortho* coupling as well as another

signal at  $\delta_H$  7.44 (t,  $J = 8.5$ ) due to H-4'. These spectral observations revealed that the four methoxy groups at  $\delta_H$  3.92 (3H, s),  $\delta_H$  3.87 (3H, s), and  $\delta_H$  3.79 (6H, s) were positioned at C-5, C-6, C-2' and C-6', respectively. From these spectroscopic views, Compound **Pb4** has been assigned as 5,6,2',6'-tetramethoxyflavone or as it is commonly known, zapotin, which previously has been found in *P. veris* (Budzianowski et al. 2005).

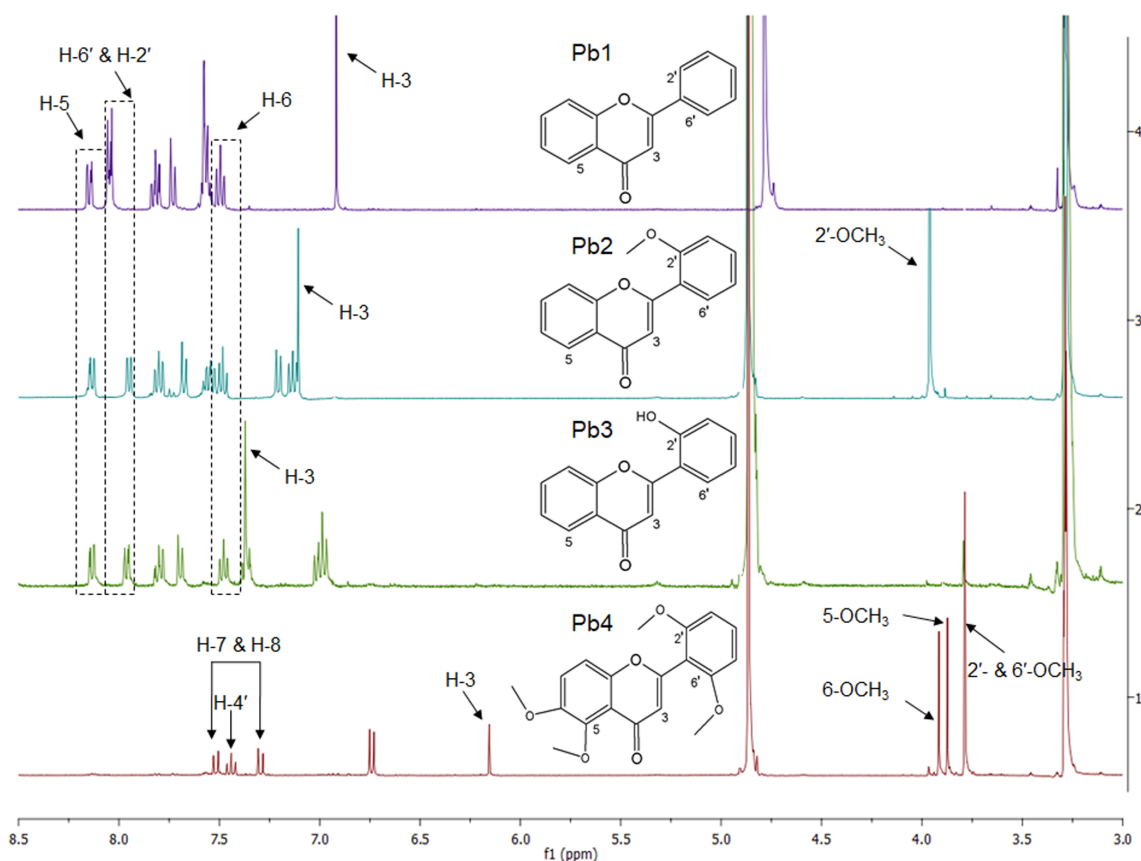


**Fig. 16.**  $^1\text{H}$  NMR spectra and structures of compounds **Pb1-Pb4**.

#### 4.1.4. AChE inhibition equivalency calculation of **Pb1**

AChE inhibition equivalency calculation of compound **Pb1** in the crude extract of *P. boveana* was performed using the HPTLC-densitometric analysis as described in section (3.3.5). The inhibitory activity of the studied metabolite was compared to the activity exhibited by a reference standard inhibitor, Riv (**Fig. 18**). The peak areas obtained by densitometric analysis of the inhibition zones of the serially diluted Riv (1 - 10  $\mu\text{g}/\text{band}$ ) (**Fig. 17**) were used to construct the calibration curve.

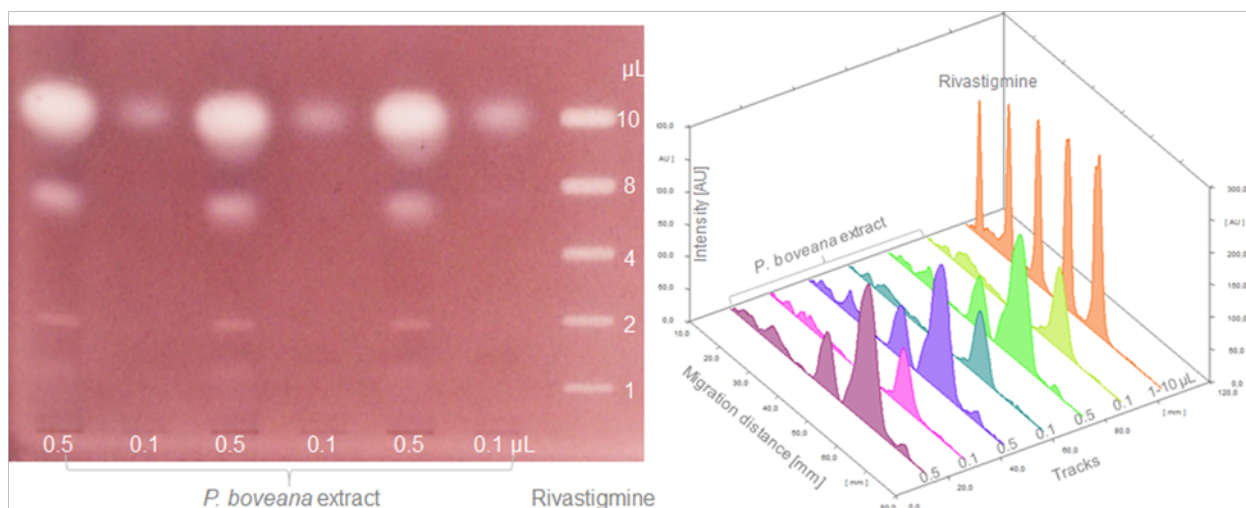


**Fig. 17.** AChE inhibition equivalency experiment: AChE autogram of *P. boveana* extract (1 g/10 mL, 0.5 and 0.1  $\mu$ L applied, three replicates of 50 and 10  $\mu$ g/band) with standard Riv applied as track pattern after development (1 mg/mL, 1-10  $\mu$ L applied, 1-10  $\mu$ g/band) and respective densitogram (absorbance measurement) at 500 nm obtained by inverse scanning.

The obtained curve showed a linear correlation within the applied range of Riv. The linear equation was generated and determined as  $y = 621.6x + 2721$ , where  $y$  is the peak area and  $x$  is the concentration of Riv in  $\mu$ g/band (**Appendix 1**). The results showed that the AChE inhibitory activity of **Pb1** contained in the applied amount of the extract (0.1 $\mu$ L extract); in other words, in 10  $\mu$ g leaf powder was biologically equivalent to a calculated amount of 4.5  $\mu$ g Riv. Meaning, the unsubstituted flavone contained in *P. boveana* leaf extract powder turned out to be half as strong as the well-known AChE inhibitor, Riv.

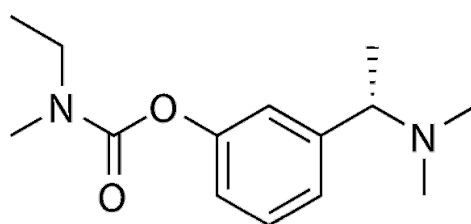


**Fig. 18.** Chemical structure of Riv

## 4.2. Biological evaluation and active metabolites identification of *A. pubescens*

### 4.2.1. HPTLC-AChE inhibition assay

With the aim of studying the AChE inhibitory activity of the iridoids constituents of *A. pubescens*, the defatted crude extract was analyzed using the HPTLC-EDA method. The results revealed the presence of three active inhibition zones corresponding to three separately eluted bands (A1 - A3) (Fig. 19).

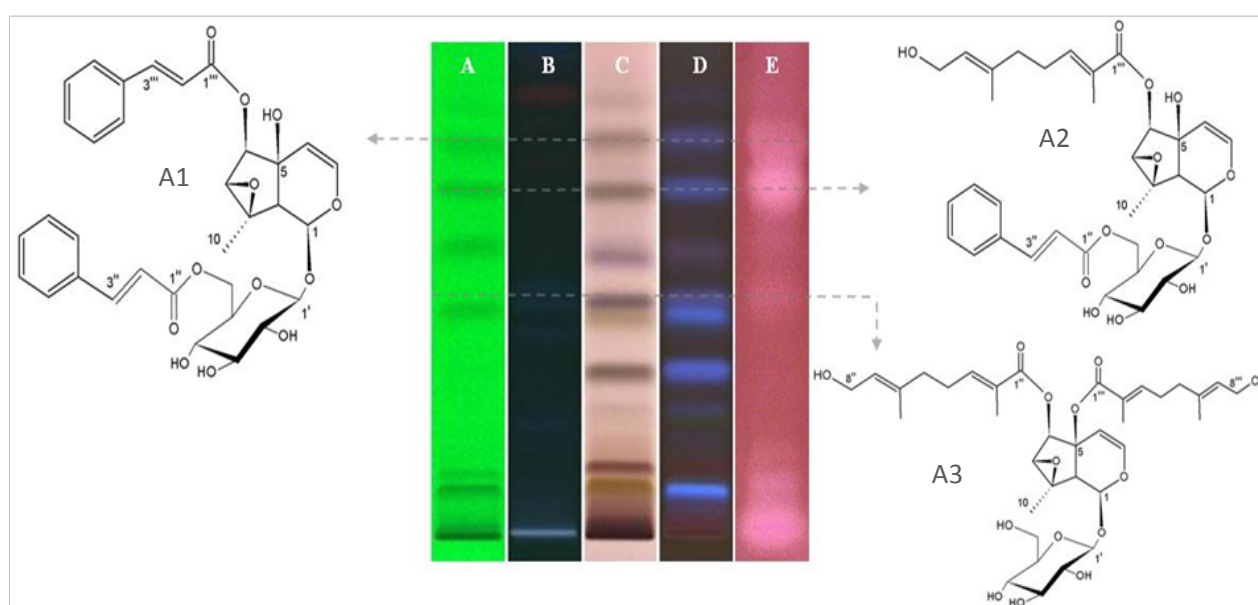


**Fig. 19.** HPTLC chromatograms of the *A. pubescens* extract at UV 254 (A), UV 366 nm (B), white light (C) and UV 366 nm after p-anisaldehyde derivatization (D) as well as HPTLC autogram after the acetylcholinesterase assay (E) and the determined structures of the isolated bioactive metabolites A1 - A3.

### 4.2.2. Active metabolites identification

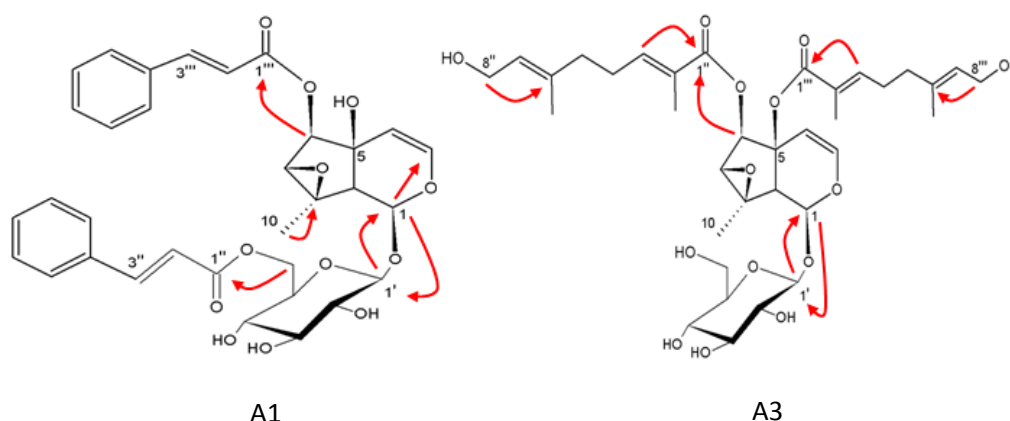
Structural elucidation of the active metabolites was also achieved. Compounds (A1 & A3) were separated through successive preparative HPLC separations and identified based on their HRMS and 1D & 2D NMR spectroscopic data while, A2 was structurally identified based on the collected HRMS and HRMS/MS data.



**Table 3:**  $^1\text{H}$  and  $^{13}\text{C}$  NMR data of the compounds **A1** and **A3**

Compound (A1)						Compound (A3)					
Position	$\delta_{\text{H}}^{\text{multi}}$ ( $J$ in Hz)	$\delta_{\text{C}}$	Position	$\delta_{\text{H}}^{\text{multi}}$ ( $J$ in Hz)	$^{13}\text{C}$	Position	$\delta_{\text{H}}^{\text{multi}}$ ( $J$ in Hz)	$\delta_{\text{C}}$	Position	$\delta_{\text{H}}^{\text{multi}}$ ( $J$ in Hz)	$^{13}\text{C}$
<b>1</b>	5.3 d (7.1)	94.0	<b>6'-O-Cinnamoyl</b>			<b>1</b>	5.7 d (2.5)	92.6	<b>6-O-foliamenthoyl</b>		
<b>3</b>	6.3 d (6.3)	141.8	<b>1''</b>	-	167.0	<b>3</b>	6.5 d (6.5)	144.7	<b>1''</b>	-	166.9
<b>4</b>	4.9 d (6.3)	106.3	<b>2''</b>	6.6 d (16.0)	117.4	<b>4</b>	5.4 d (6.5)	101.5	<b>2''</b>	-	127.4
<b>5</b>	-	73.3	<b>3''</b>	7.7 d (16.0)	145.6	<b>5</b>	-	79.5	<b>3''</b>	6.6 td (7.3, 1.4)	142.1
<b>6</b>	5.0 d (1.8)	78.4	<b>4''</b>	-	134.2	<b>6</b>	5.1 d (2.8)	75.3	<b>4''</b>	2.2 m	27.01
<b>7</b>	3.5 d (1.8)	62.7	<b>5'' &amp; 9''</b>	7.5 m	128.1	<b>7</b>	3.5 d (2.8)	63.5	<b>5''</b>	2.1 m	30.36
<b>8</b>	-	62.9	<b>6'' &amp; 8''</b>	7.3 m	128.6	<b>8</b>	-	63.5	<b>6''</b>	-	137.1
<b>9</b>	2.4 d (7.1)	52.2	<b>7''</b>	7.3 m	130.3	<b>9</b>	2.8 brs	49.2	<b>7''</b>	5.3 dd (6.8, 1.4)	125.32
<b>10</b>	1.4 s	16.2	<b>6-O-Cinnamoyl</b>			<b>10</b>	1.4 s	15.2	<b>8''</b>	4.03 d (6.8)	57.8
<b>Glucose</b>			<b>1'''</b>	-	166.5	<b>Glucose</b>			<b>9''</b>	1.7 *	11.0
<b>1'</b>	4.7 d (8.0)	98.4	<b>2'''</b>	6.6 d (16.0)	117.0	<b>1'</b>	4.6 d (7.8)	99.5	<b>10''</b>	1.7 *	22.31
<b>2'</b>	3.2 m	73.0	<b>3'''</b>	7.7 d (16.0)	145.3	<b>2'</b>	3.18 dd (9.1, 7.8)	73.6	<b>5-O-foliamenthoyl</b>		
<b>3'</b>	3.4 m	76.0	<b>4'''</b>	-	134.4	<b>3'</b>	3.3 m	76.9	<b>1'''</b>	-	166.6
<b>4'</b>	3.3 m	70.0	<b>5''' &amp; 9'''</b>	7.5 m	128.1	<b>4'</b>	3.2 m	70.2	<b>2'''</b>	-	128.1
<b>5'</b>	3.5 m	74.0	<b>6''' &amp; 8'''</b>	7.3 m	128.6	<b>5'</b>	3.3 m	77.1	<b>3'''</b>	6.7 td (7.3, 1.4)	142.3
<b>6'a</b>	4.5 dd (12.0, 2.5)	63.07	<b>7'''</b>	7.3 m	130.3	<b>6'a</b>	3.6 dd (12.0, 6.3)	61.5	<b>4'''</b>	2.2 m	27.07
<b>6'b</b>	4.4 dd (12.0, 6.0)					<b>6'b</b>	3.9 dd (12.0, 2.1)		<b>5'''</b>	2.1 m	30.38
									<b>6'''</b>	-	137.3
									<b>7'''</b>	5.4 dd (6.8, 1.4)	125.34
									<b>8'''</b>	4.06 d (6.8)	57.9
									<b>9'''</b>	1.7 *	11.2
									<b>10'''</b>	1.7 *	22.33

\* Overlapped

**Fig. 20.** Key  $^1\text{H}$ - $^{13}\text{C}$  HMBC correlations of compounds **A1** and **A3**.

**Compound A1** (6 mg) was isolated from the subfraction F2 after isocratic elution with 75 % MeOH in  $\text{H}_2\text{O}$  as yellowish powder. The molecular formula of **A1** was deduced as  $\text{C}_{33}\text{H}_{34}\text{O}_{12}$  from the observed HRESIMS molecular ion peak at  $m/z$  645.1952  $[\text{M}+\text{Na}]^+$  (Calculated 645.1942 for  $\text{C}_{33}\text{H}_{34}\text{O}_{12}\text{Na}^+$ ) (**Appendix 2**).  $^1\text{H}$  and  $^{13}\text{C}$  NMR spectral data of **A1** (Table 3, **Appendix 3 & 4**) suggested the structure of **A1** as antirrhinoside-based iridoids. This was attributed to the assignment of the acetalic methine at  $\delta_{\text{H}}$  5.3 (d,  $J = 7.1$  Hz, H-1)/ $\delta_{\text{C}}$  93.8 as well as the two doublet vinylic protons at  $\delta_{\text{H}}$  6.3 (d,  $J = 6.3$  Hz, H-3) and  $\delta_{\text{H}}$  4.9 (d,  $J = 6.3$  Hz, H-4) with their corresponding carbons at  $\delta_{\text{C}}$  141.8 &  $\delta_{\text{C}}$  106.3, respectively. Also, the



presence of aliphatic methine at  $\delta_H$  3.5 (d,  $J = 1.8$  Hz, H-7)/ $\delta_C$  62.7 (C-7) as well as quaternary carbon at  $\delta_C$  62.9 (C-8), which are indicative to the 7, 8-epoxy linkage in the cyclopentane ring of the antirrhinoside. As antirrhinoside iridoids are naturally having the sugar unit positioned at C-1, this was unambiguously observed by allocating the cross correlation between the anomeric proton of the  $\beta$ -glucopyranoside at  $\delta_H$  4.7 (d,  $J = 8.0$  Hz, H-1') and C-1 ( $\delta_C$  93.8). The  $^1\text{H}$ - $^1\text{H}$  COSY (**Appendix 5**) has also supported these assumptions, where couplings between H-3/H-4; H-6/H-7; H-1/H-9 have been observed. The NMR spectral data have also showed signals characteristic to two cinnamoyl units. The two carbonyl esters of the acyl groups were observed at ( $\delta_C$  167.0, C-1" &  $\delta_C$  166.5, C-1'''). Furthermore, the *trans* configuration of the olefinic protons was confirmed by inspecting their spin-spin coupling constants ( $\delta_H$  6.6, d,  $J = 16.0$  Hz, H-2" & H-2''' and  $\delta_H$  7.7, d,  $J = 16.0$  Hz, H-3" & H-3'''). Thus, the structure of **A1** has been partially determined to possess two cinnamoyl moieties attached to the basic antirrhinoside structure. The positions of these two acyl groups was confirmed by assigning the HMBC correlations (**Fig. 20, Appendix 7**) and were found that one cinnamoyl is attached to C-6 and the second to C-6''. Naturally occurring antirrhinosides have their H-1, H-6, H-7, and 3H-10 protons in  $\alpha$ -orientation. This also implied to **A1** in which the coupling constants  $J_{\text{H-1, H-9}} = 7.1$  Hz and  $J_{\text{H-6, H-7}} = 1.8$  Hz are in agreement with those reported for antirrhinoside (Handjieva et al. 1993; Beninger et al. 2007). Based on this analysis, the structure of **A1** was identified as 6-*O*, 6'-*O* di-*trans*-cinnamoyl-antirrhinoside (**Fig. 19**). To our knowledge, compound **A1** is herein described for the first time.

**Compound A2:** was isolated from the subfraction F2 after isocratic elution with 75 % MeOH in H<sub>2</sub>O as a yellowish brown oil. The molecular formula of **A2** was deduced as C<sub>34</sub>H<sub>42</sub>O<sub>13</sub> from the observed HRMS molecular ion peak at  $m/z$  681.2518 [M+Na]<sup>+</sup> (Calculated 681.2517 for C<sub>33</sub>H<sub>34</sub>O<sub>12</sub>Na<sup>+</sup>). Initial MS data analysis suggested the structure of **A2** as 6-*O*-foliamenthoyl-(6'-*O*-cinnamoyl)-antirrhinoside, an iridoid glucoside which previously isolated from the same plant (Mahran et al. 2018). Further confirmation of the structure was carried out through extensive analysis of the tandem mass spectrum (**Fig. 21**). The obtained fragment ions indicated successive loss/cleavage of the attached acyl and glucosyl moieties. Mass errors were up to only 1.1 ppm, proofing our interpretation for the fragments' structure. Hence, the structure of **A2** was described as 6-*O*-foliamenthoyl-(6'-*O*-cinnamoyl)-antirrhinoside (**Fig. 19**).

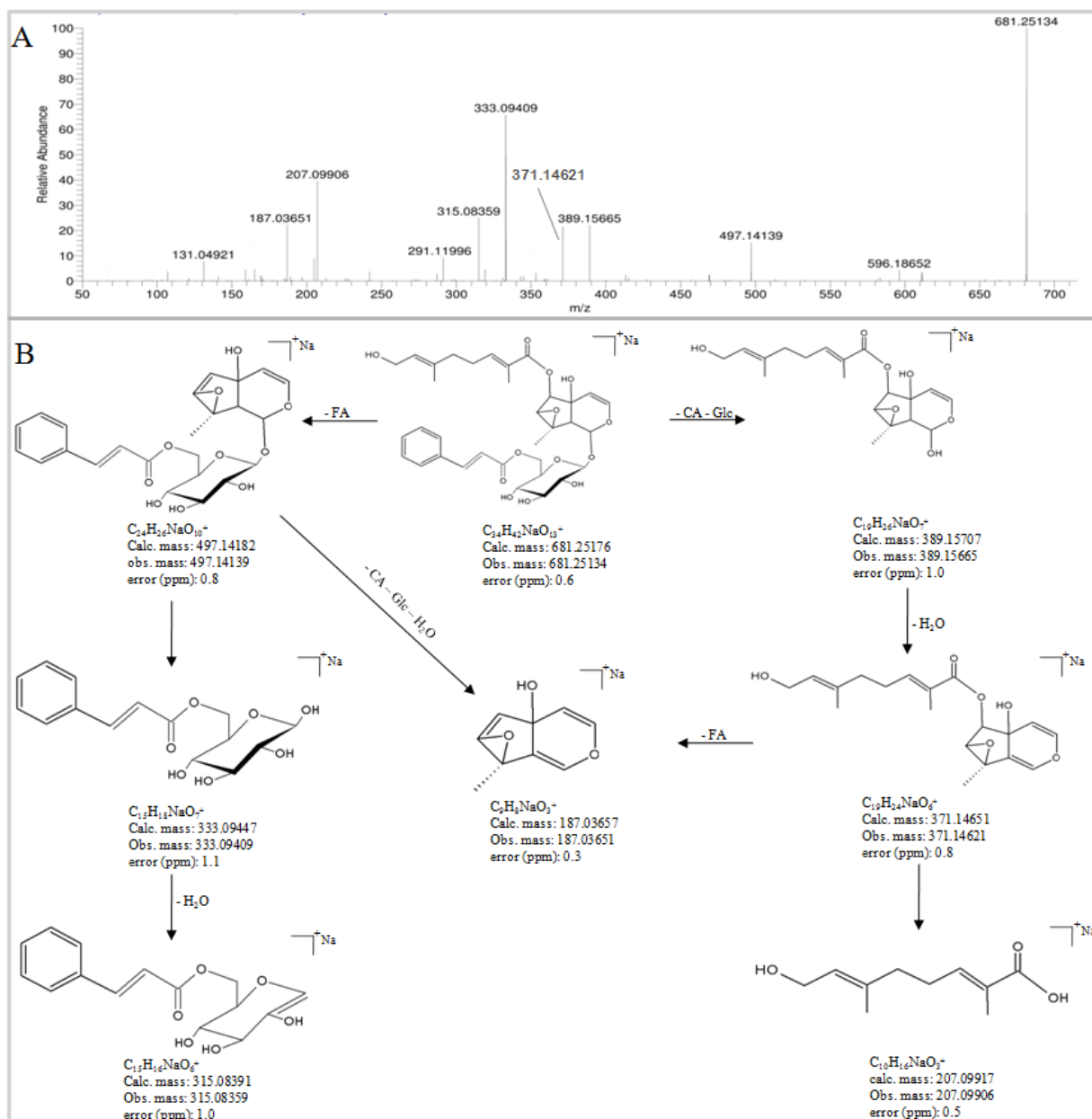


**Fig. 21.** HRMS/MS spectrum of compound **A2** (A) and detailed structural fragmentation pathway (B) (foliamenthoic acid, FA; cinnamic acid, CA; glucose, Glc)

**Compound 3:** was isolated from subfraction F3 after isocratic elution with 55 % MeOH in H<sub>2</sub>O as a faint yellowish powder. The molecular formula of **A3** was deduced as C<sub>35</sub>H<sub>50</sub>O<sub>14</sub> from the observed HRESIMS molecular ion peak at  $m/z$  717.3094 [M+Na]<sup>+</sup> (Calculated 717.3093 for C<sub>33</sub>H<sub>34</sub>O<sub>12</sub>Na<sup>+</sup>) (**Appendix 8**). <sup>1</sup>H, <sup>13</sup>C, and HSQC NMR spectra of **A3** (Table 3 & **Appendix 9, 10, 12**) showed signals referred that the antirrhinoside nucleus is also embed-

ded within the structure. The resonances corresponding to the acetalic methine  $\delta_H$  5.7 (d,  $J = 2.5$  Hz, H-1)/ $\delta_C$  92.6; vinylic methines at  $\delta_H$  6.5 (d,  $J = 6.5$  Hz, H-3)/  $\delta_C$  144.7 and  $\delta_H$  5.4 (d,  $J = 6.5$  Hz, H-4)/ $\delta_C$  101.5 were clearly assigned. When compared to iridoids previously reported for the genus, spectral values of **A3** demonstrated a close resemblance to those of 6-*O*-foliamenthoyl-antirrhinoside (Dawidar et al. 1989). The characteristic differences were that **A3** displayed signals due to additional 10 carbon atoms along with a downfield shift of C-5. Meaning, **A3** should include a second monoterpene unit in its structure, which was proved by observing a second set of protons and carbons of additional foliamenthoyl unit. With the help of the HMBC data (**Fig. 20, Appendix 13**), the position of the first foliamenthoyl unit was defined at C-6 whereas, the second was determined to be attached to C-5 as indicated from the remarkable downfield shift of C-5 ( $\delta_C$  79.5, normally  $\approx 73.3$ ). As in **A1**, the sugar occupied the C-1 position with  $\beta$ -orientation. Also,  $J_{H-6, H-7} = 2.8$  Hz confirmed their  $\alpha$ -orientation which further established through the NOESY analysis (**Appendix 14**). NOESY cross peaks between H-6/H-7; H-1/H-10; H-7/H-10 proved their  $\alpha$ -configuration. Thus, compound **A3** was structurally identified as 5-*O*, 6-*O* difoliamenthoyl-antirrhinoside (**Fig. 19**), and this is also reported here as a new isolated natural compound.

#### 4.2.3. AChE inhibition equivalency calculation of compounds (A1 - A3)

The equivalency experiment was performed using the free mode application of 20  $\mu\text{g}/\text{band}$  of each compound as well as serial dilutions (0.5 - 14  $\mu\text{g}/\text{band}$ ) of the standard enzyme inhibitor, Riv. The inhibitory zones were densitometrically measured (**Fig. 22 A and B**). The curve showed a linear range within the range of 1 - 8  $\mu\text{g}/\text{band}$  of Riv. The regression equation obtained from plotting the Riv concentration vs. the peak area was  $y = 404.7x + 2180$ , where  $y$  is the peak area of the inhibition zone and  $x$  is the amount of Riv. Compound **A1** showed inhibitory activity that turned out to be equivalent to 1.5  $\mu\text{g}$  of Riv. Compound **A2** showed inhibitory activity equivalent to 5.9  $\mu\text{g}$  Riv. On the other hand, the applied amount of Compound **A3** was found to be below the limit of quantitation of the given equation. Noteworthy, Riv as 200 ng/band is still detectable following the described HPTLC-AChE workflow, meaning, the LOD is below this level (Azadniya and Morlock).

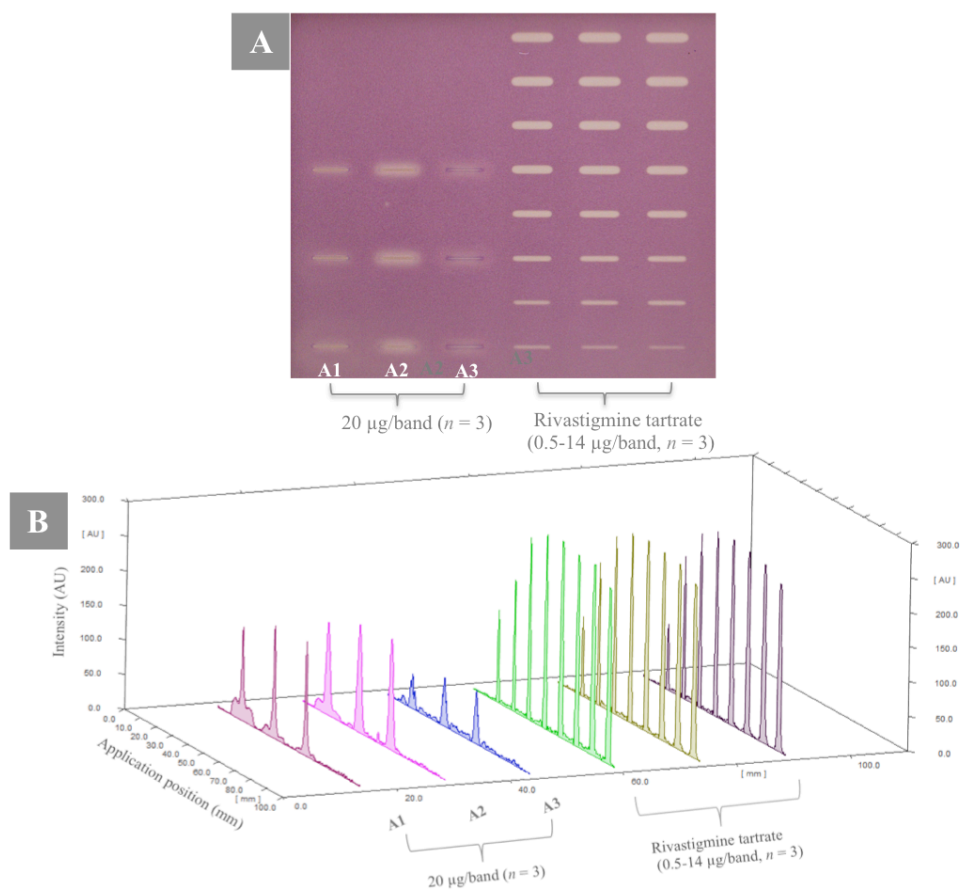


**Fig. 22.** HPTLC autogram after AChE assay (A) and densitometric fluorescence measurement at 500 nm (B) of compounds **A1** - **A3** (20 µg/band,  $n = 3$ ) as well as rivastigmine tartrate (0.5 - 14 µg/band,  $n = 3$ ) applied as track pattern.

### 4.3. HPTLC-GUS inhibition assay hyphenation

The aim of this experiment was to transfer the GUS inhibition assay to HPTLC. Therefore, the individual inhibition activity of each component exist in a mixture could be directly evaluated after their HPTLC chromatographic separation. The method made use of the potential of GUS to hydrolyze X-Gluc into a colored end product and hence, inhibitors could be easily detected as a white zones.

#### 4.3.1. Optimization of the method parameters

##### Wavelength:

The background was scanned within the range of 200 - 800 nm in order to obtain the optimum absorption wavelength. The white inhibition zone of SL served as a reference. The obtained spectrum showed that the background exhibits several absorption maxima at 259, 306, and 353. Also, it showed absorption ranging from 610 - 650 nm (**Fig. 23**). Statistical analysis showed no significant difference between peak areas of inhibition zones ( $n = 3$ ) collected at 612 and 650 nm. So, any of these wavelengths could be used as a colorimetric detection wavelength in densitometric analysis.

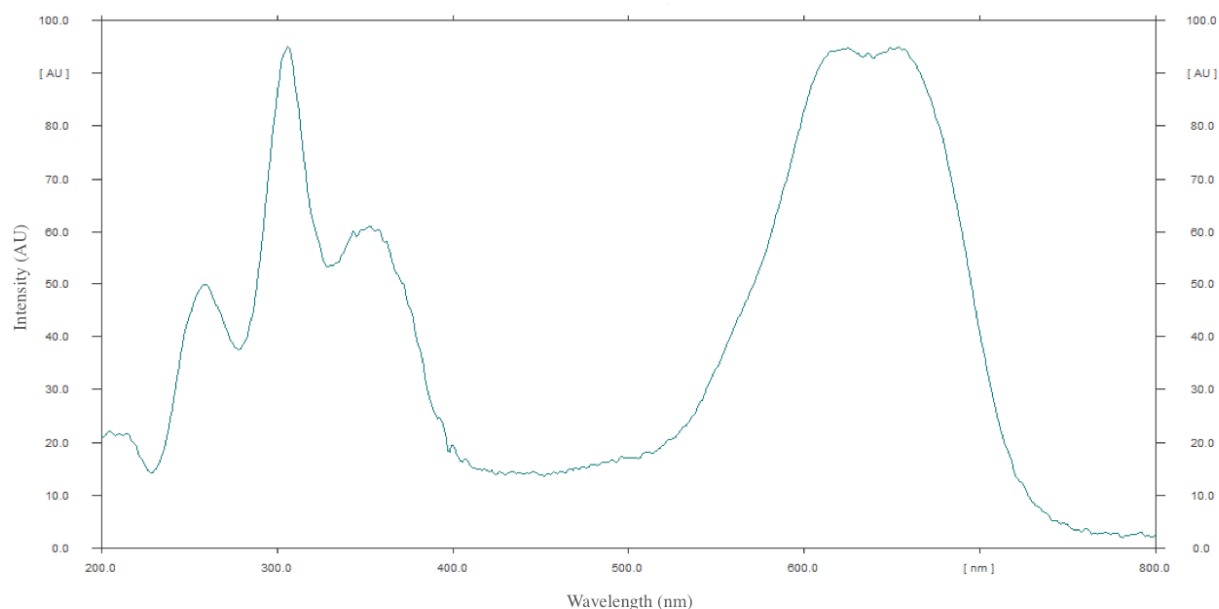


**Fig. 23.** UV/Vis spectrum (200 - 800 nm) of the autogram background: the white inhibition zone of SL served as a reference.

##### GUS concentration, reaction time, and effect of fluorescent indicator

Seven different concentrations of the GUS solution (2 - 33 U/mL, *i.e.* 0.03 - 0.5 U/cm<sup>2</sup>) were applied with 1.5 mL X-Gluc solution (2 mg/mL, *i.e.* 22.5 μM/cm<sup>2</sup>). The autograms, after assay application, were densitometrically scanned at λ 612 nm (**Fig. 24A**). The statistical analysis showed that GUS applied as 3.0 mL of 25 U/mL (*i.e.* 0.375 U/cm<sup>2</sup>) was the optimum GUS concentration. The optimum reaction time has been inspected initially over a three time levels (20, 40, and 60 min) (**Fig. 24B**) employing the optimum GUS concentration (3.0 mL of 25 U/mL solution). The peak areas of the SL inhibitory zones were collected at 612 nm (*n* = 3). Sixty minutes reaction time afforded the highest peak areas. However, shorter reaction times still useable for visual detection but the background/spot contrast would be weaker. Another attempt was done to examine a longer duration time (120 min) was performed. Although a longer reaction time of, *i.e.* 120 min was statistically (*p* ≤ 0.05) still more significant, it was decided against, for the sake of a shorter workflow and 60 min was found as a reasonable time. The impact of using HPTLC plates with or without fluorescent indicator on the colorimetric detection has been also investigated. Plates with fluorescent indicator afforded higher peak areas (**Fig. 24C**), indicating that in this assay, plates with fluorescent indicator are preferable.

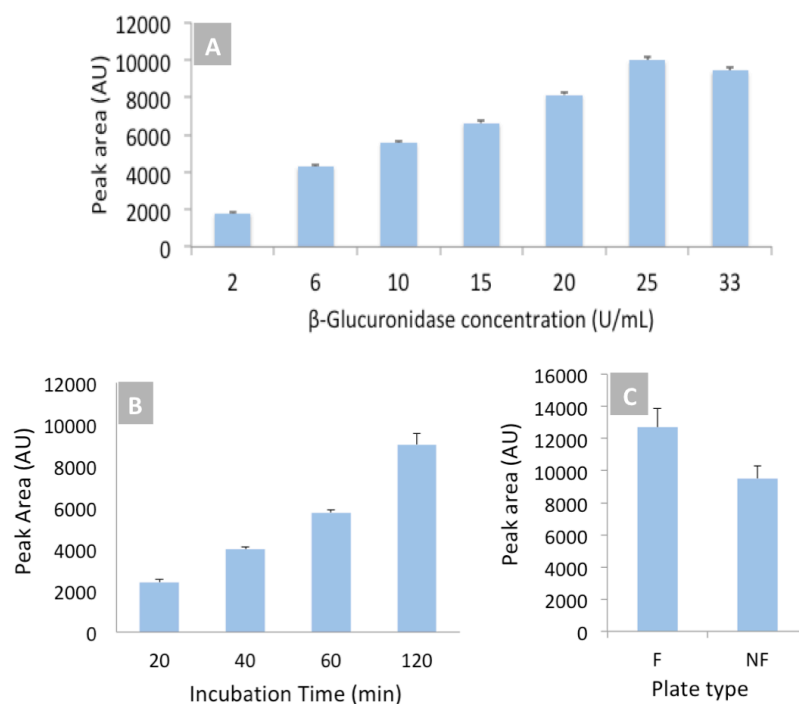


**Fig. 24.** Effect of GUS concentration (**A**), incubation time (**B**), and fluorescent indicator (**C**) on peak areas of the standard inhibitor, SL (1 mg/mL, applied as 1 μg/band, *n* = 3). Areas were recorded on TLC scanner in fluorescens mode (612 nm).

### 4.3.2. Method validation

The developed method has been validated in terms of the lowest concentration of SL the produce  $S/N \geq 3$ , linearity, and specificity. Serial dilutions of the SL solution (0.75 - 2000 ng/band,  $n = 3$ ) were applied (**Fig. 25, left**), the peak areas were measured at 612 nm. The lowest concentration applied in this study and found to give  $S/N$  value  $\geq 3$  was corresponding to 62 ng/band ( $S/N = 4$ ). Regression line was established within the range (62 - 1000 ng/band) where the results fit well to the second order polynomial function (**Fig. 25, right**),  $y = -0.004x^2 + 8.400x + 22.69$  with  $R^2$  of 0.993. Furthermore, a specificity experiment was done in order to confirm the specific affinity of GUS to the used substrate. In this experiment a different substrate was used that has another sugar ( $\beta$ -glucose); the results revealed that the background showed no color (**Appendix 15**).

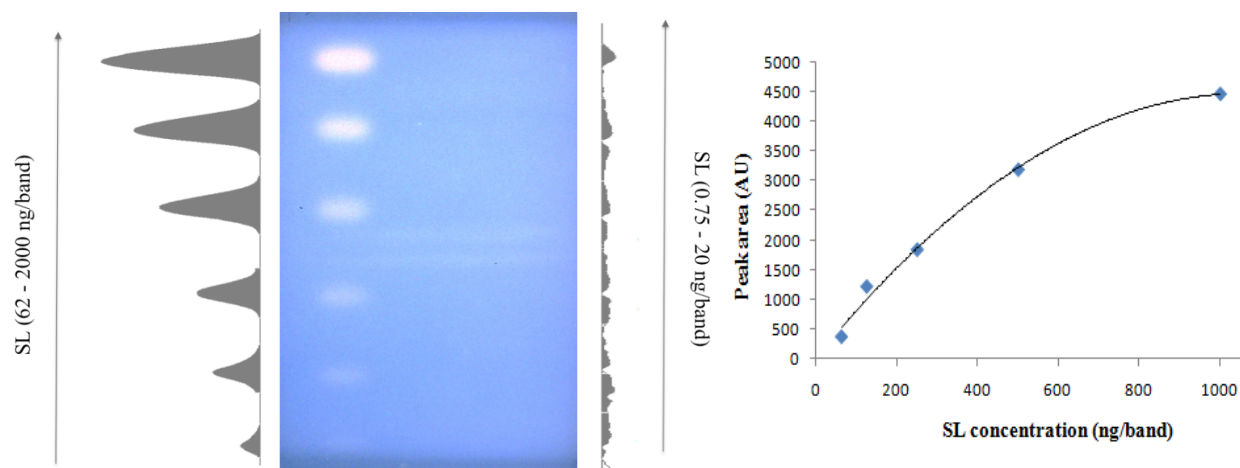


**Fig. 25. Left:** Densitometric analysis of SL (0.75 - 2000 ng/band) applied as band pattern showing that 62 ng/band is the lowest concentration used in this experiment and could be detected visually (Also, proves the calculated  $S/N \geq 3$ ). **Right:** the standard calibration curve for SL over the range (62 - 1000 ng/band).

### 4.3.3. Method verification

In order to verify the developed method, the optimized assay was performed on two different botanical samples, *P. boveana* leaves extract & SFLG extract. The assay was carried out as illustrated in **Fig. 12**.

### HPTLC-GUS-HRMS analysis of *P. boveana*

Two active inhibitors, **Pb1** & **Pb2**, (**Fig. 26**) were detected in *P. boveana* extract. Active metabolites were detected both fluorometrically (under UV 366 nm) as well as colorimetrically (under white light), proving the dual readout detection of the developed hyphenation. These active metabolites were previously elucidated as unsubstituted flavone and 2'-methoxy flavone (section 4.1.3).

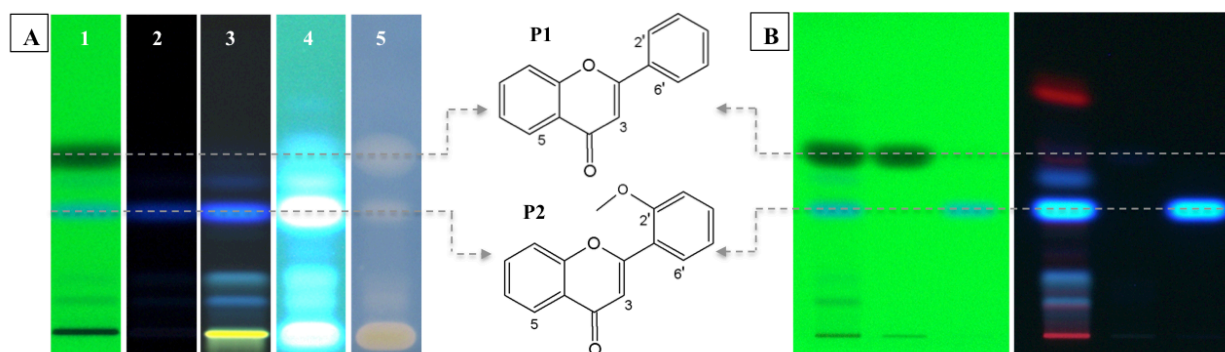


**Fig. 26.** **A)** HPTLC-GUS hyphenation for detection of the enzyme inhibitors in *P. boveana* extract applied as 0.5  $\mu$ L. Chromatogram under UV 254 nm (1); UV 366nm (2); after NP/PEG derivatization at 366 nm (3); after assay application at 366 nm (4) and under white light (5). **B)** Confirmation of the active inhibitors by co-chromatographic elution of the *P. boveana* extract with reference compounds in 1  $\mu$ L/band each, detected under UV 254 and 366 nm light.

### HPTLC-GUS-HRESIMS/MS analysis of SFLG

The flavonolignan constituents of silymarin were separated using two MP (**Fig. 27 A and B**), MP1 (CF : Acet : FA, 75:16.5:8.5, *V/V/V*) & MP2 (Toluene : EtOAc : FA, 9:6:0.4, *V/V/V*). Both systems contained FA but in different proportions, which also permitted monitoring the assay results under other variable chromatographic conditions than those mentioned with *P. boveana* in the later experiment. Apparently, one major band (**SFLG1**) has demonstrated a remarkable inhibition to GUS. With the use of MP1, the assay was impaired in non-neutralized plates, but worked well when the plates subjected to neutralization with phosphate buffer at pH 7.8. So, the neutralization step seems essential when FA intended to be used at a higher concentration. By using MP2 as a mobile phase, the assay (in plates with and without pre-neutralization) was still able to provide detection information, indicating that



the assay could the FA addition until its concentration in the mobile phase increases to a limit that eventually leads to inhibition of the enzymatic assay.

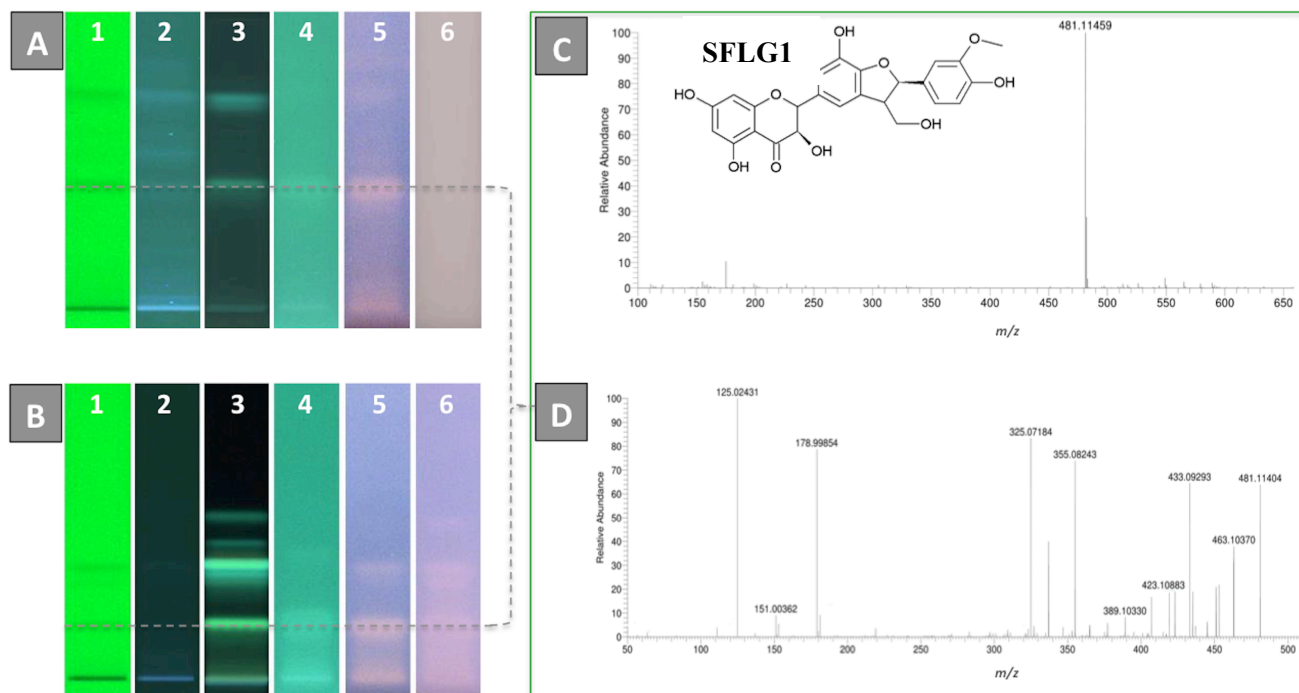


**Fig. 27.** HPTLC-GUS hyphenation for detection of the enzyme inhibitors in SFLG extract applied as 1.0  $\mu$ L using two different developing systems, MP1 (**A**) and MP2 (**B**), as well as mass analysis, HRMS (**C**) and HRMS/MS at collision energy of 20 V (**D**) of the active inhibitor, **SFLG1.1**, Chromatogram at UV 254 nm; **2**, at UV 366 nm; **3**, after NP/PEG derivatization at 366 nm; **4**, fluorometric detection after assay application (with neutralization); **5**, colorimetric detection (with neutralization); **6**, colorimetric detection (without neutralization).

Characterization of the active metabolites was based on HRMS/MS analysis. The molecular formula of **SFLG1** was deduced as  $C_{25}H_{22}O_{10}$  as revealed from the observed ion peak at  $m/z$  481.11459 (calculated 481.11402 for  $[M-H]^-$ ) (**Fig. 27C**). Distinguishing the individual flavonolignans mixture of silymarin through MS analysis is always a challenge analysis as they share the same molecular masses of 482 Da and almost comparable fragmentation behavior. Recent studies have focused on MS/MS-based characterization of major components in SFLG and set some criteria in order to facilitate their rapid identification. These criteria depended mainly on the presence of some diagnostic peaks as well as their relative abundance at a defined CE (Kuki et al. 2012a, 2012b; Brinda et al. 2012). The  $MS^2$  scan of **SFLG1** acquired at six different levels of CE (10, 20, 25, 30, 40, and 50 V) is displayed in **Appendix 16**. As the fragmentation is energy-dependent, meaning, **SFLG1** showed more

fragment ions as the energy increases, until CE of 20 V is attained, at which the optimum fragmentation pattern with multiple ion peaks is obtained. At higher energies 25-50 V, only stable ions are visible. In MS<sup>2</sup> spectrum of **SFLG1** collected at CE of 20 V (**Fig. 27 D**), the base peak at *m/z* 125 followed by an ion at *m/z* 179 are the most intense peaks; the ratio of 463/453 ions intensities is more than 1; fragment ion at *m/z* 301 is almost 1 or less; the presence of fragment ions at *m/z* 355 & 433, are all hallmarks of silychristin flavonolignan. Hence, the active GUS inhibitor, **SFLG1** has been identified as silychristin.

#### 4.4. HPLC-HRMS and EPI analysis for identification of flavonoid constituents in *P. boveana* leaves

In this experiment, the HPLC coupled to HRMS followed by MS/MS (represented by EPI scan type) analysis were pursued in order to tentatively characterize the flavonoid constituents of *P. boveana*. The accurate molecular masses obtained from the HRMS analysis (**Appendix 17**) were used as entry points for collecting the CID MS/MS data (**Appendix 18**). A total of 25 compounds (Table 4, **Fig. 28**) were characterized.

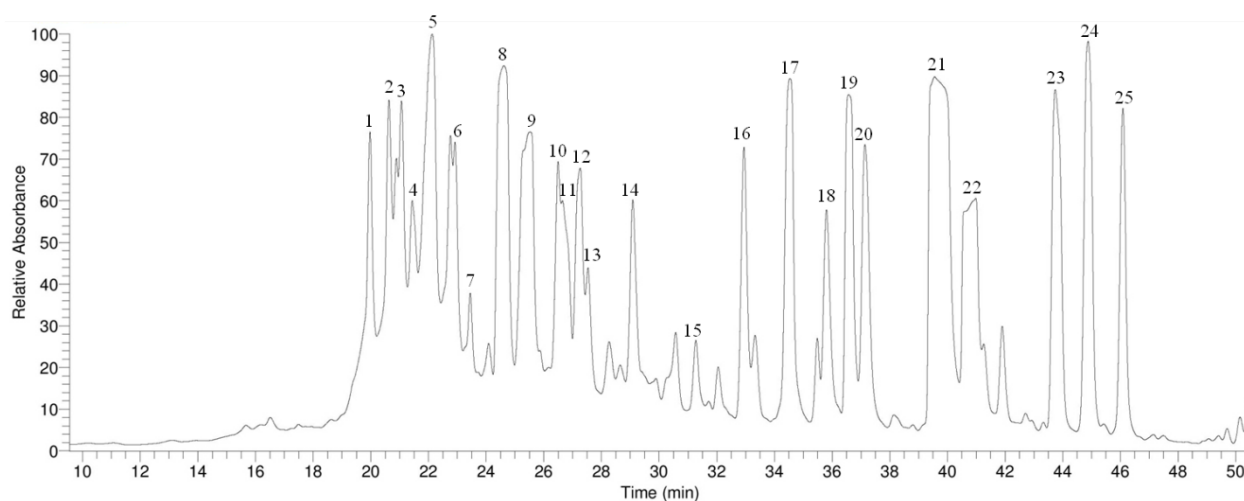


**Fig. 28.** HPLC chromatogram of *P. boveana* hydro-alcoholic extract at UV 254 nm

The recognized compounds covered a wide range of flavonoids metabolites; in harmony with many previously studied *Primula sp.*, *P. boveana* has demonstrated a considerable number of polar as well as nonpolar flavonoids. Initial determination of the elemental composition of each eluted peak depended on the LC-HRMS data with a maximum mass error of 0.7 ppm. Then, the low-energy CID mediated through EPI scan analysis of  $[M+H]^+$  ions has afforded a comprehensive fragmentation pattern through which the characterization of the molecular subunits of the flavonoids glycoconjugates was accomplished.

##### Glycoconjugated flavonoids

Thirteen compounds (**1 - 13**) in the extract were determined as glycoconjugated flavonoids. These compounds represented several aglycone structures that are linked to varying sugar compositions (mono-, di-, and tri-saccharides); three out of these thirteen compounds have showed a conjugation with the organic acid, malonate. The aglycone part of these me-

tabolites has also showed different degree of hydroxylation (mono-, di-, tri-, tetra-, and penta-hydroxylated flavone). Glycoconjugates of kaempferol and quercetin were the most recognized flavonoid glycosides present in *Primula* plants (Colombo et al. 2017; Apel et al. 2017). Henceforth, the compounds in the extract that have been assigned to contain aglycones with four or five OH groups were defined here as kaempferol and quercetin derivatives, respectively. Diagnostic ion peaks corresponding to sequential loss of one or more glycosyl and/or malonate moieties made it plausible to determine the size of the glycone as well as the aglycone parts. However, the compound profiling based solely on MS analysis sometimes encounter difficulties in assigning the conjugation sites between the aglycones and glycones units, hence, a tentative assignment of the compounds is proposed. The common mass losses detected in this study with their corresponding identity were as follow: loss of 162, 146, 308, and 84 Da, indicated the presence of hexose, deoxyhexose (rhamnose), hexose-deoxyhexose, and malonyl moieties, respectively (Cuyckens and Claeys 2004). Compounds (**9**, **11** - **13**) demonstrated spectacular mass features that are distinct from those previously known for the *Primula* are herein described in details.

Compound **9** showed a molecular ion peak in **Fig. 29A (left)** at  $m/z$  401.1233 corresponding to the molecular formula of  $C_{21}H_{20}O_8$  (calculated 401.1230 for  $[M+H]^+$ ). Flavonoid with such molecular mass has not been previously described in genus *Primula*. The structure of **9** showed a simple fragmentation pattern as shown in **Fig. 29A (right)**. The EPI spectrum showed a single product ion (due to loss of 162 Da) at  $m/z$  239  $[M\text{-hexoside}+H]^+$ , indicating the structure of the aglycone part as monohydroxyflavone. So, compound **9** has been tentatively identified as monohydroxyflavone hexoside.

The malonylated flavonoid glycosides were identified as: dihydroxyflavone-malonylhexoside (**11**), monohydroxyflavone-malonylhexoside (**12**), and dihydroxyflavone-malonylhexoside isomer (**13**). Compound **11** showed a protonated ion peak at  $m/z$  503.1185 (**Fig. 29B, left**). EPI analysis of **11** showed the diagnostic peaks at  $m/z$  459 and 417 suggested the loss of  $CO_2$  and malonyl groups, respectively (**Fig. 29B, right**) (Cuyckens and Claeys 2004). The transition from the ion peak at  $m/z$  459 to the ion peak at  $m/z$  255 revealed a loss of hexoside, leaving the characteristic aglycone peak at  $m/z$  255  $[M\text{-malonylhexose}+H]^+$ , which is here defined as a dihydroxyflavone. On the basis of the mass analysis, compound **11** has been tentatively characterized as dihydroxyflavone-malonylhexoside. Compound **12** showed a molecular ion peak at  $m/z$  487.1236 (**Fig. 29C, left**), which is 16 mass units less than **11** indicating that **12** has one OH group less. In the EPI spectrum (**Fig. 29C, right**), **12** showed signal

peaks at  $m/z$  443 and 401 refereeing to the loss  $\text{CO}_2$  and malonyl units, respectively. EPI of **12** showed also a peak at  $m/z$  239 corresponding to  $[\text{M-malonylhexose}+\text{H}]^+$  which is the aglycone part and defined as monohydroxyflavone. Therefore, compound **12** has been determined as monohydroxyflavone-malonylhexoside. Compound **13** displayed a similar molecular mass as of **11**, so it has been assigned as an isomer of **11**. Malonylated flavonoids have not previously described in *Primula* and here is the first occurrence of such phyto-constituents in the genus.

**Table 4:** Flavonoids identified in the hydro alcoholic extract of *P. boveana* using HPLC-HRMS and EPI analysis

Nr	$R_t$ (min)	Compound Name	Molecular formula	Exact mass of the $[\text{M}+\text{H}]^+$ ion		Error (ppm)	Fragment peaks as protonated ions
				Observed	Calculated		
1	19.9	Quercetin-trihexoside	$\text{C}_{33}\text{H}_{40}\text{O}_{22}$	789.2088	789.2084	- 0.5	627,487, 465, 325, 303
2	20.6	Quercetin-hexoside-dirhamnoside	$\text{C}_{33}\text{H}_{40}\text{O}_{20}$	757.2189	757.2185	- 0.5	611, 465, 303
3	21.0	Kaempferol-trihexoside	$\text{C}_{33}\text{H}_{40}\text{O}_{21}$	773.2138	773.2134	- 0.5	611, 287
4	21.4	Kaempferol-hexoside-dirhamnoside	$\text{C}_{33}\text{H}_{40}\text{O}_{19}$	741.2239	741.2236	- 0.4	595, 287
5	22.1	Quercetin-hexoside-rhamnoside	$\text{C}_{27}\text{H}_{30}\text{O}_{16}$	611.1603	611.1606	- 0.4	303
6	22.9	kaempferol-hexoside-rhamnoside	$\text{C}_{27}\text{H}_{30}\text{O}_{15}$	595.1658	595.1657	- 0.1	287
7	23.4	kaempferol-hexoside-rhamnoside (isomer)	$\text{C}_{27}\text{H}_{30}\text{O}_{15}$	595.1658	595.1657	- 0.1	287
8	24.6	Dihydroxy flavone- <i>O</i> -hexoside	$\text{C}_{21}\text{H}_{20}\text{O}_9$	417.1180	417.1180	0.0	255
9	25.5	Flavone- <i>O</i> -hexoside	$\text{C}_{21}\text{H}_{20}\text{O}_8$	401.1233	401.1230	- 0.7	239
10	26.5	Dihydroxy flavone-hexoside	$\text{C}_{21}\text{H}_{20}\text{O}_9$	417.1180	417.1180	0.0	255
11	26.7	Dihydroxy flavone-malonylhexoside	$\text{C}_{24}\text{H}_{22}\text{O}_{12}$	503.1186	503.1184	- 0.3	459, 417, 255
12	27.4	Flavone- <i>O</i> -malonylhexoside	$\text{C}_{24}\text{H}_{22}\text{O}_{11}$	487.1236	487.1234	- 0.4	443, 401, 239
13	27.5	Dihydroxyflavone- malonylhexoside	$\text{C}_{24}\text{H}_{22}\text{O}_{12}$	503.1185	503.1184	- 0.2	459, 417, 255
14	29.0	Dihydroxyflavone	$\text{C}_{15}\text{H}_{10}\text{O}_4$	255.0652	255.0651	- 0.3	--
15	31.3	Trimethoxy-monohydroxyflavone	$\text{C}_{18}\text{H}_{16}\text{O}_6$	329.1020	329.1019	- 0.3	--
16	32.9	Monohydroxy-methoxyflavone	$\text{C}_{16}\text{H}_{12}\text{O}_4$	269.0808	269.0808	0.0	--
17	34.6	2'-Hydroxy flavone	$\text{C}_{15}\text{H}_{10}\text{O}_3$	239.0703	239.0702	- 0.4	--
18	35.8	Trimethoxy flavone	$\text{C}_{18}\text{H}_{16}\text{O}_5$	313.1071	313.1070	- 0.3	--
19	36.5	5,6,2',6'Tetramethoxyflavone	$\text{C}_{19}\text{H}_{18}\text{O}_6$	343.1176	343.1176	0.0	--
20	37.1	Dihydroxy-methoxy flavone	$\text{C}_{16}\text{H}_{12}\text{O}_5$	285.0758	285.0757	- 0.3	--
21	39.5	Unsubstituted flavone	$\text{C}_{15}\text{H}_{10}\text{O}_2$	223.0753	223.0753	0.0	--
22	40.7	2'-Methoxyflavone	$\text{C}_{16}\text{H}_{12}\text{O}_3$	253.0859	253.0859	0.0	--
23	43.7	Dimethoxy-hydroxyflavone	$\text{C}_{17}\text{H}_{14}\text{O}_5$	299.0914	299.0914	0.0	--
24	44.8	Dimethoxy-hydroxyflavone	$\text{C}_{17}\text{H}_{14}\text{O}_5$	299.0914	299.0914	0.0	--
25	46.1	Monohydroxy-methoxyflavone (isomer)	$\text{C}_{16}\text{H}_{12}\text{O}_4$	269.0808	269.0808	0.0	--

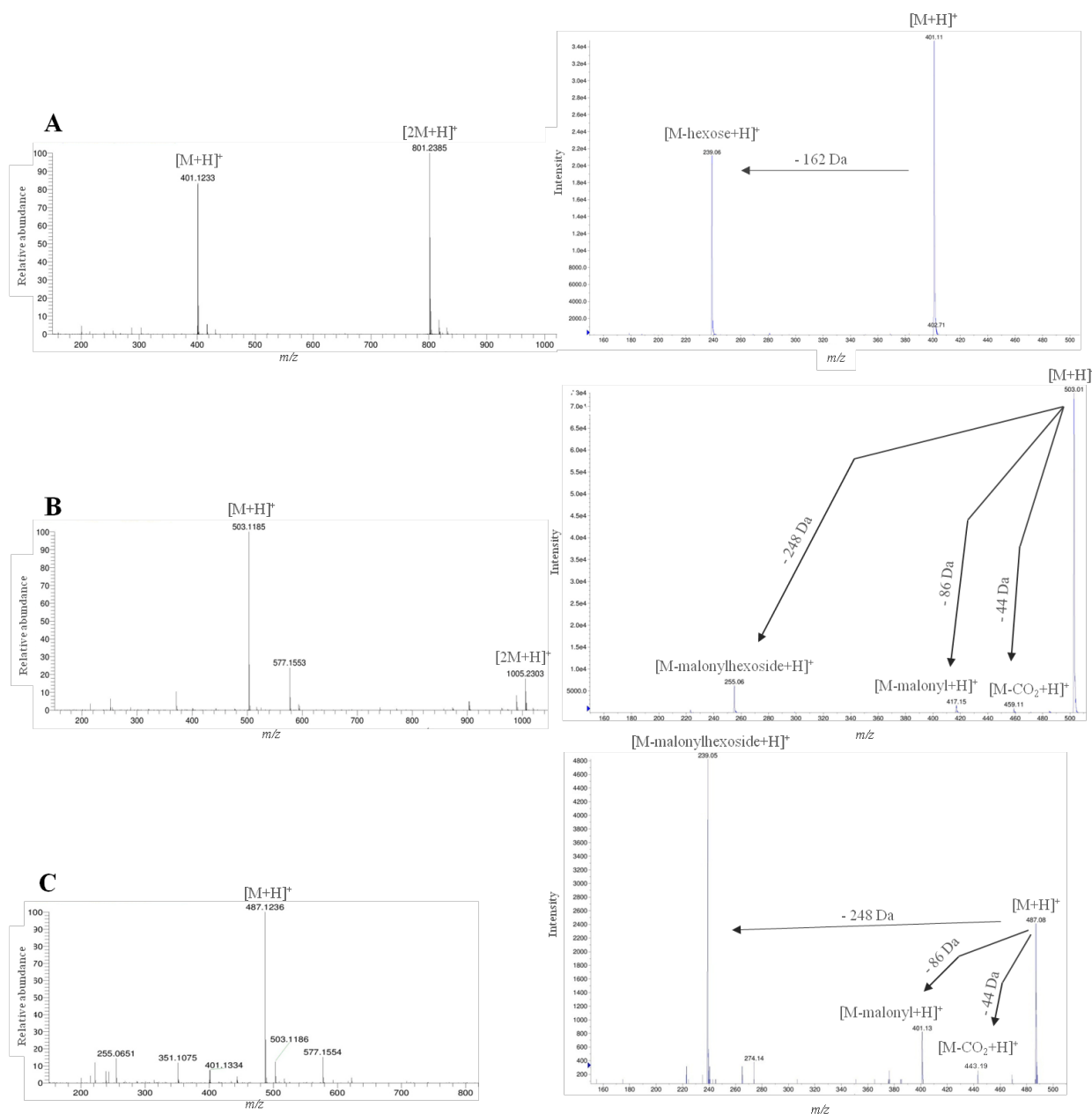


**Fig. 29.** HRESIMS spectra of compound **9** (A), **11** (B) and **12** (C) (left); the corresponding EPI spectra of each molecular ion peak (right).

### Flavonoids aglycones

The remained compounds (**13** - **25**) didn't show any sugar or organic acid residues (Table 4) and are defined as less polar flavonoids. The unsubstituted flavone (**21**) and monomethoxyflavone (**22**) were the predominant metabolites. The compounds were shown to bear a varying number of OH and OMe groups. The HRMS data (**Appendix 17**) obtained for these metabolites were comparable to those reported in literature for the epicuticular flavonoids from *Primula* plants. Furthermore, based on the NMR analysis of the active metabolites discussed

in section (4.1.3), compounds **17**, **19**, and **22** were identified as 2'-hydroxyflavone, 5,6,2',6'-tetramethoxyflavone, and 2'-methoxyflavone, respectively.

## 5. Discussion

### 5.1. Biological evaluation and active metabolites identification in *P. veris* flowers and *P. boveana* leaves

Given that *Primula* plants are known to accumulate versatile metabolites, their biological/chemical investigation would provide valuable information for the evidence-based herbal medicine. So, in this study, we sought to track the antibacterial and anti-AChE/BChE metabolites occurring in the medium polar extracts of two *Primula* species, *P. veris* and *P. boveana*. As a modern streamlined hyphenation with many unparalleled features, HPTLC-EDA was sought to study the titled plants.

The first bioactivity screened was the antibacterial bioassay, in which two bacterial strains, *A. fischeri* (Gram-negative) and *B. subtilis* (Gram-positive) were used. The results of the HPTLC-antibacterial bioassays showed that two bacterial inhibitors existed in the extract of *P. veris*, while four active metabolites were detected in the *P. boveana* extract. Growth inhi-



bition in *A. fischeri* was observed as dark spots vs. a luminescent background. While in *B. subtilis*, the inhibition was detected as white spot against the purple background due to reduction of MTT into formazan by viable cells (**Fig. 30**) (Dewanjee et al. 2015).

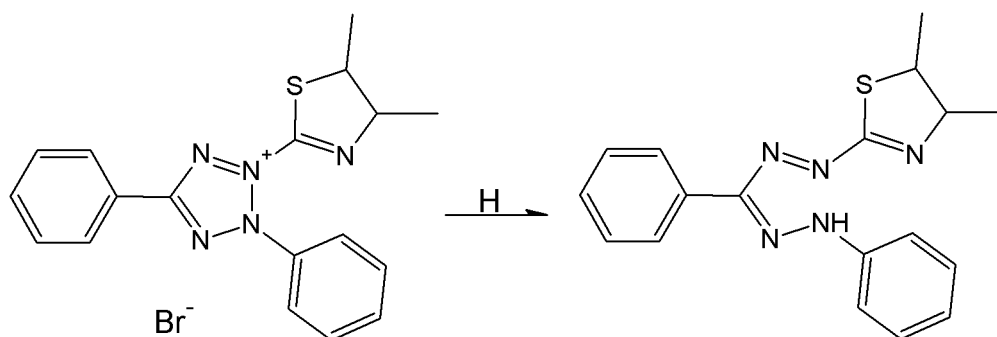


**Fig. 30.** Reduction of MTT into purple formazan by *B. subtilis* bacteria

The polarity of the detected active metabolites could be easily anticipated from the used developing system (hexane : EtOAc, 7:3, *V/V*), which indicated their lipophilic tendency. The direct mass analysis on HPTLC has permitted the assignment of such metabolites, which further confirmed by the NMR measurements.

In *P. veris*, the two active bands were determined as PUFAs, linoleic (C18:2, **Pv1**) and linolenic acids (C18:3, **Pv2**). Primulaceae is one of the higher plant families that are known to accumulate several PUFAs (Sayanova et al. 1999; Sayanova et al. 2003). Both acids have been previously described among the principle fatty acids occurring in *P. macrophylla* and *P. macrocalyx* (Tsydendambaev et al. 2004; Kosenkova et al. 2008). Production of PUFAs in plants has been suggested to correlate with stress exposure, *i.e.* biotic/abiotic. Alteration of the membrane fluidity in stress-resistant plants has been linked to the release of  $\alpha$ -linolenic acid (Upchurch 2008). Iba (2002) concluded that PUFAs play an important role in plants survival towards low temperature conditions, basically, through controlling the formation of chloroplast membranes. The antibacterial potential of PUFAs, including linoleic and linolenic acids, has been covered in earlier reviews (McGaw et al. 2002). The antibacterial activity of linoleic acid in Neem oil has recently been reported using direct bioautography (Krüzselyi et al. 2016). Chang et al. have studied the mechanism of antibacterial action of linoleic acid (Zheng et al. 2005). They concluded that linoleic acid principally targets the fatty acid synthesis in bacteria through inhibition of enoyl-acyl carrier protein reductase, which found to be inhibited by some other related compounds like linolenic, palmitoleic acid, and oleic acid. Their study also demonstrated the importance of unsaturation and the free acid group of lino-

leic acid as essential structural components for inhibition of the enoyl-acyl carrier protein reductase. Besides the unsaturation, the chain length was also found as crucial structural feature for effectiveness of fatty acid towards inhibition of sporulation in *B. subtilis* (Strauch et al. 1992). Extracts of *P. veris* flowers prepared by three different solvents (ether, ethanol, water) showed inhibitory activity with varying degrees against ten types of bacteria with ethanolic extract demonstrated a distinct inhibition to *Enterococcus faecalis*, *Bacillus cereus*, and *Pseudomonas fluorescens* (Xu and Lee 2001).

With regard to *P. boveana*, the four detected active metabolites (**Pb1** - **Pb4**) were determined as lipophilic flavonoids in nature. Their structures were confirmed by means of HRMS and NMR analysis as follow: unsubstituted flavone (**Pb1**), 2'-methoxyflavone (**Pb2**), 2'-hydroxyflavone (**Pb3**), and 5,6,2',6'-tetramethoxyflavone (**Pb4**). Under the used application volumes, all four compounds have successfully inhibited *A. fischeri* growth, while *B. subtilis* was found sensitive to only **Pb1** and **Pb2**. Lipophilic flavonoids are abundantly produced by *Primula* species and generally referred to epicuticular flavonoids, so to be distinguished from the tissue-type flavonoids which in common regarded as more polar metabolites. Primulas accumulate epicuticular flavonoids leaded by unsubstituted flavone, which is substituted with many OH and/or OMe groups at different positions. The most common sites for these substituents are 5, 2', and 8 (Colombo et al. 2017). Some compounds are known to be shared by several *Primula* plants, e.g. unsubstituted flavone, 2'-hydroxyflavone, 5-hydroxyflavone, 5,8-dihydroxyflavone, 2'-methoxyflavone, and 5,2-dihydroxyflavone. These literature findings strongly support our results of structural definition of the active metabolites detected in *P. boveana*. In this study, the unsubstituted flavone was the most profound inhibitor as revealed by its relevant zone of inhibition. In literature, unsubstituted flavone has displayed inhibitory activity against methicillin-resistant *Staphylococcus aureus* (MRSA) (Xu and Lee 2001). The unsubstituted flavone also found as the principle metabolite responsible for the antileishmanial and cytotoxic activities of the chloroform-soluble fraction of *P. macrophylla* (Najmus-Saqib et al. 2009). In a susceptibility testing, Bakar et al. (2012) have studied the impact of combination of nine different flavonoids (including the unsubstituted flavone) with vancomycin or oxacillin against vancomycin-intermediate *Staphylococcus aureus*. They found that only unsubstituted flavone was able to provoke a synergistic effect with both antibiotics, while other flavonoids have shown an additive action. Therefore, they concluded that unsubstituted flavone is worth to undergo further interaction studies at the molecular level. In another study conducted by Basile et al. (2010) aimed to track the antimicrobial principles in

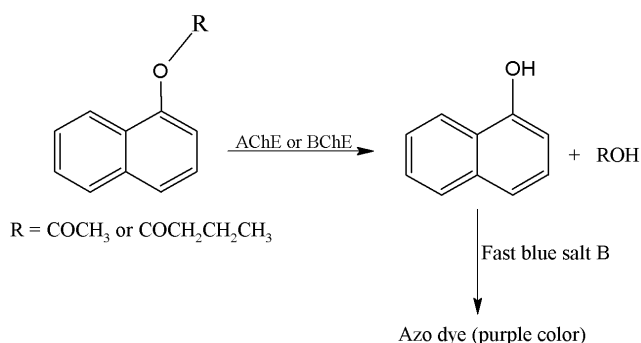
*Feijoa sellowiana* Berg. fruit extract, unsubstituted flavone was identified as the active metabolite present in the extract. Through their bioactivity-guided study on the fruit extract, unsubstituted flavone has significantly inhibited different types of bacterial strains, including *Helicobacter pylori*, and fungi. These literature reviews regarding the antibacterial attributes of unsubstituted flavone would also verify its distinct antibacterial potential discussed in our results.

Flavonoids are a large class of plant secondary metabolites, they occur in almost each organ of the plant. They perform several physiological functions in plants; induction of their biosynthesis is thought of as one of the defense mechanisms that the plant uses to fight against attacking pathogens. This property has been receiving a growing interest for the possible contribution of such naturally abundant chemicals as useful antimicrobial agents in humans (Cushnie and Lamb 2005; Jucá et al. 2018). Due to their diverse structural features, these compounds show variable physicochemical properties, which usually influence their antimicrobial behavior. However, the hydrophobic characteristic was determined as a crucial property for the effectiveness of flavonoids as antibacterial (Echeverría et al. 2017), and this could indicate that disturbing the bacterial cell membrane rigidity is one of the underlying mechanism of actions of flavonoids (Wu et al. 2013).

The second activity investigated was the AChE/BChE inhibition. So far, the activity of the genus *Primula* as ChE inhibitors has not been very well studied. To our knowledge, in one study, *P. officinalis* (L.) Hill (*syn.* of *P. veris*) flowers extract showed a moderate inhibition to AChE and BChE (Wszelaki et al. 2010). So, the obtained biological results would provide useful information for the use of such plants in treatment of the relevant diseases, *e.g.* AD and Myasthenia gravis.

The active compounds in the examined extract showed up as white zones against a purple background as previously described by Marston et al. (Marston et al. 2002) and based on the reaction showed in **Fig. 31**.

**Fig. 31.** Enzymatic reaction of AChE and BChE on the corresponding substrate with formation of an azo dye.



The results of AChE/BChE inhibition assay on *P. veris* revealed that linoleic and linolenic acids were also the main AChE/BChE inhibitors present in the extract. PUFAs are essential fatty acids that should be provided to our bodies from external sources, *e.g.* vegetable oils. In brain, PUFAs are essential for a proper neuronal transmission since they generally serve as building components of the neurons. Incorporation of PUFAs into neuronal membranes enhances the membrane fluidity and integrity; as a result, improve the neurotransmission, which is useful in cognitive function (Jicha and Markesbery 2010). Therefore, the beneficial role of PUFAs in treatment of neurodegenerative diseases like AD has been reported in some studies (Willis et al. 2009; Bentsen 2017). Diets rich in docosahexaenoic acid, a major PUFA, was suggested to be helpful in treatment of many neurological disorders, *e.g.* AD and depression (Farooqui and Horrocks 2001). The implication of PUFAs as ChE inhibitors have been also established through some studies that used dietary oils contained varying amount of PUFAs (Willis et al. 2009). Ren et al. (2006) found that the PUFAs-rich fraction of the centipede *Scolopendra subspinipes mutilans* L. Koch displayed an AChE inhibitory activity. The finding that promoted the authors to investigate the AChE potential of some other related PUFAs including linoleic and linolenic acids. Their results concluded that the inhibitory activity is linked to some structural prerequisites, a chain length of more than 16 carbon atoms, the presence of at least one saturation, and the intact acidic group, are all found essential for execution of the inhibition action by PUFAs. Moreover, the docosahexaenoic acid was the most active among the screened PUFAs, with activity found 200 times as higher as the standard reference, physostigmine. However, linoleic acid inhibited AChE in a concentration-dependent pattern.

In *P. boveana*, compounds (**Pb1** - **Pb4**) inhibited BChE, while AChE has been inhibited only by **Pb1** & **Pb2**. Flavonoids as omnipotent chemicals have and continue to inspire researchers to explore their multiactivities. Flavonoids have been acknowledged as enzyme modulators. They could efficiently modulate many phase I and phase II metabolic enzymes (Miron et al. 2017); they showed inhibitory activity towards many enzymes related to several pathogenesis (Guerrero et al. 2012). As a part from the well-known AChE/BChE inhibitors from alkaloid origin, flavonoids have recently emerged as a new class of compounds capable of inactivating this group of enzymes (Uriarte-Pueyo and Calvo 2011). Inhibition of AChE/BChE is linked to the treatment of many neurodegenerative diseases, in particular, AD (Khan et al. 2018). This enzyme inhibitory capability along with some other bioactivities like anti-amyloidogenic, anti-oxidant, and anti-inflammatory properties have strongly promoted the

use of flavonoids as comparably safe candidates for prevention and/or symptomatic relief of AD (Baptista et al. 2014; Bakhtiari et al. 2017).

The AChE-inhibitors interactions at the molecular level have been discussed by Roseiro et al. (2012). The peripheral anionic site at the entrance point of the active site gorge of the enzyme was suggested to be the position at which the inhibitors usually affect modulation of the enzyme. Moreover, the pattern that flavonoids usually orient themselves inside the AChE gorge active site was found similar to that usually adopted by the known inhibitor, donepezil.

Apparently, unsubstituted flavone (**Pb1**) was found as a potent antibacterial and AChE/BChE inhibitor. So an attempt to evaluate its AChE inhibitory potency compared to the well-known standard inhibitor, Riv, was carried out through the AChE inhibition equivalency study. The results were very encouraging, as the inhibitory activity exerted by **Pb1** in the *P. boveana* extract was found half as strong as of Riv. This result paves the way for further studies considering the possible implementation of unsubstituted flavone in treatment of the relevant diseases such as AD. The compound is ubiquitous in nature and considered as comparably safe and cheap chemical when compared to other drugs used in this regard.

In conclusion, this part of the study was designed with the purpose of searching for potential inhibitors to bacteria and AChE/BChE from natural sources. For many reasons, an interest in shifting to natural counterparts has attracted many researchers. Some of these reasons could be explained by the big worry surrounding the rapid bacterial resistance to the available antibiotics, the significantly growing number of people diagnosed with AD, the adverse effects associated with the administered synthetic drugs. Our results have determined the major active metabolites in both bioassays as being belonging to rather ubiquitous natural products. However, our study possesses the novelty with regard to some aspects:

- The type of the plant species as demonstrated by *P. boveana*, which has not been previously evaluated for its biological activity.
- The type of bioactivity screened or the microorganism used: as the current study is considered as the first report dealing with targeted tracking of the AChE/BChE inhibitors in both species.
- The bioactivity information collected: as clearly indicated by the multibioactivities of unsubstituted flavone, 2'-methoxyflavone.
- The bioanalytical technique used for EDA of the studied extracts.

## 5.2. Biological evaluation and active metabolites identification in *A. pubescens*

In the second part of the PhD study, we aimed to investigate the hydro-alcoholic extract of *A. pubescens* for the presence of active AChE inhibitors. The part is distinguished from the former section in using a different botanical species that is known to produce a different group of secondary metabolites in its tissue. Thus, providing wider insights with regard to the ChE inhibitory activity of diverse groups of natural products that are not related to alkaloids.

Bioactivity-guided screening of the plant extract has been also accomplished through the HPTLC-EDA procedures. The HPTLC-AChE inhibition assay led to identification of three inhibitors, two of which are here described as newly isolated natural compounds. The active metabolites were determined as derivatives of antirrhinoside iridoids and their structures were identified as follow: 6-*O*-, 6'-*O*-di-*trans*-cinnamoyl-antirrhinoside (**A1**), 6-*O*-foliamenthoyl-(6'-*O*-cinnamoyl)-antirrhinoside (**A2**) and 5-*O*-, 6-*O*-difoliamenthoyl-antirrhinoside (**A3**). The structures of the new metabolites (**A1** & **A3**) were determined based on extensive analysis of their NMR and MS spectroscopic data. Whereas, the structure of **A2** was furnished by interpretation of its HRMS and HRMS<sup>2</sup> spectrometric data.

*A. pubescens* belongs to family Plantaginaceae, which is known to harbor species producing diverse chemical phyto-constituents. Iridoids are one of the major secondary metabolites produced by Plantaginaceae plants. Plants of the genus *Anarrhinum* also reported to accumulate iridoid glycosides in their arial parts. The iridoid glycosides described so far in the genus are derived primarily from antirrhinoside or mussaenosidic acid (Dawidar et al. 1989; Salah El Dine et al. 2011; Mahran et al. 2018) with the former is being esterified with cinnamic and/or foliamenthoic acids, hence, substantiate our structures assumption for the active metabolites.

Iridoids demonstrated important biological functions resulting from their inhibitory actions on many biological enzymes. The antitumor activity of aucubin and geniposide have been also proposed to be due to their potent inhibition to topoisomerase I, leading to DNA damage (Gálvez et al. 2005). Also, several iridoids from plants that are known in Mexico for their ethnomedical value as anti-inflammatory have been tested by Ramírez-Cisneros et al. (2015) against cyclooxygenase-1 (COX-1) and cyclooxygenase-2 (COX-2) enzymes; loganic acid was found the most active compound. With regard to AChE, iridoids have been also reported to inhibit such enzyme. Loganin obtained from the fruits of *Cornus officinalis* inhibited

AChE in hippocampus of mice by as much as 45% compared to control groups (Lee et al. 2009). Likewise, *E*-harpagoside and 8-*O-E*-*p*-methoxycinnamoylharpagide isolated from *Scrophularia buergeriana* exhibited AChE inhibition activity to a level similar to that observed with donepezil; this characteristic potential was suggested to be the reason behind the cognitive function improvement in mice (Jeong et al. 2008). Moreover, iridoid compounds isolated of *Patrinia scabiosaefolia* showed inhibition to AChE (Liu et al. 2017). Catalpol, an iridoid with a structure that is very similar to antirrhinoside, also proposed to have AChE inhibitory activity (Zhang et al. 2013). In view of the foregoing enzymes modulating activities of iridoids, our AChE inhibitory findings deemed to be warranted.

What is more in our study is that it reports, for the first time, the AChE inhibitory potential of antirrhinoside-derived iridoids and further delivering some structure activity relationships as deduced from the AChE inhibition equivalency study performed at a fixed applied amount (20 µg/band). The results revealed that compound **A3** at this concentration showed peaks area that seems to be below the detection limit. Compound **A3** differs from **A1** & **A2** in that it has the 5-OH position esterified with another foliamenthoyl unit. Even though replacement of the cinnamoyl moiety (compound **A1**) by this structural unit increased activity of compound **A2** by approximately 4 times. In contrast, esterification of 5-OH with a second monoterpene moiety has dramatically lowered the activity, meaning that the free 5-OH is essential to maintain the AChE inhibition of antirrhinosides derivatives.

In summary, the second part of this PhD study described the isolation of three AChE inhibitors from *A. pubescens* extract, with two of these metabolites are considered as precedently not reported natural products. The study therefore integrates and verifies several previous reports proposing the beneficial neuroprotective role of iridoids and their promising roles in treatment of many related diseases in particular AD. It is worth to mention that AChE inhibition is currently the main therapy available for alleviating AD. It also details the structure elucidation of the known metabolite (**A2**) based on its tandem mass data, thus, would be of a privilege as a reference for any upcoming researches dealing with chemical profiling of the genus or any of related chemical classes in terms for example of the fragmentation behavior and CE.

### 5.3. HPTLC-GUS inhibition assay hyphenation

This experiment shapes the third part of the current PhD study. The overall object was to integrate the HPTLC to GUS inhibition assay as a new hyphenation technique in an effort to rapidly refer to the individual GUS inhibitory activity of each component in complex matrices.

Glucuronidation is a principle phase II process through which the body gets rid of many harmful xenobiotics. However, the reverse reaction could happen and leads to release of the active parent compounds, causing their re-absorption into the body through the intestinal lumen. This retrograded process is a deglucuronidation reaction; mediated through GUS of the gut bacteria (Cheng et al. 2015). Prolonged exposure of the body to these harmful xenobiotics evidently established as a predisposing factor for several pathological events such as intestinal injuries and various types of cancer. Hydrolysis of the glucuronide-conjugates of many important drugs by GUS of bacteria housed the gastrointestinal tract have been reported, *e.g.* Irinotecan and NSAID (LoGuidice et al. 2012).

While these examples represent medicinal candidates, microbial GUS has been evidenced to aggravate the deleterious effects of some food products including heterocyclic amines. Heterocyclic amines are food-borne carcinogens that are excreted from body *via* phase II glucuronidation process, *e.g.* 2-amino-3-methylimidazo[4,5-f]quinoline; however, in the intestine, microbial GUS hydrolyses the conjugated products, and thus enhancing their genotoxicity (Carmody and Turnbaugh 2014).

Collecting together the aforementioned harmful consequences traced to the hydrolytic activity of microbial GUS on xenobiotics-glucuronide conjugates, several studies have been focusing on developing drug candidates targeting such enzyme inhibition. For the purpose of detecting and evaluating the GUS inhibitors, many conventional methods are available. Nevertheless, these methods could only evaluate the GUS inhibitory activity of the total mixture, *e.g.* plant extract without giving any definite information about the activity of the individual compounds unless they are further separated. Therefore, samples pretreatment is necessary, rendering these methods rather tedious and time/material consuming interventions. The reaction in general is carried out in Eppendorf or in well plates followed by spectrophotometric measurements at a selected wavelength. Hence, imparting other limitations to these methods such as difficulty in dissolving lipophilic compounds in a solvent that is compatible with the



aqueous enzyme solution, and the possible interference from the dissolving solvents either on the enzyme activity or the results readout.

In view of the above stated challenges, it would be worthwhile developing a new method for detection of GUS inhibitors in complex mixtures. In this part of the study, we successfully linked the HPTLC to the GUS inhibition assay. Thus, allowing efficient chromatographic separation of the mixture components followed by *in situ* assay application on the developed autograms.

The detection method used in this study depended on the enzymatic reaction previously described by Jefferson (1987) employing X-Gluc as a substrate (**Fig. 32**)

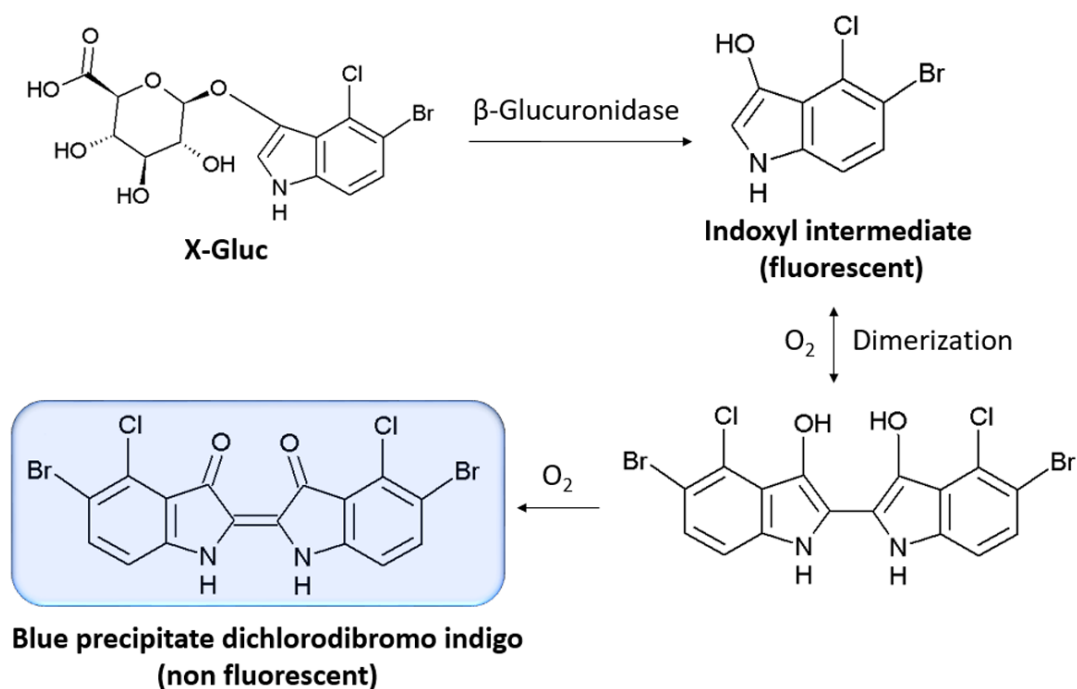


**Fig. 32.** GUS enzymatic reaction using X-Gluc as a substrate.

The active inhibitors shown up as white spots against a blue background, permitting their colorimetric detection. Given that fluorescent intermediates are formed during the enzymatic reaction, fluorometric detection is also feasible. So, the method could provide two methods of detection. Ramallo et al. (2015) has reported a dual readout assay for detection of AChE inhibitors using indoxyl acetate as a substrate, which is closely related to X-Gluc and liberate colorless fluorescent intermediates, as well. It is noteworthy to mention that X-Gluc is generally regarded as chromogenic as well as fluorogenic substrate for GUS and routinely used as a histochemical reagent (Jefferson 1987; Frampton et al. 1988). However, while developing this method, we devoted more focus to the colorimetric detection as being the prevalent approach in most of the HPTLC-EDA protocols; it also doesn't need any sophisticated instru-

mentations for documentation since the active inhibitor are easily observable under white light.

In order to bring our method to the up-to-date means of HPTLC derivatization, all applied solutions (enzyme and substrate) were delivered to the HPTLC *via* the piezoelectric spraying technology using the TLC derivatizer (Azadniya and Morlock 2019). This recently introduced technology to the field of planar chromatography carries several advantages over the classically used automated immersion technique. The new micro droplet spraying technology ensures the homogenous transfer of all solutions to the plate; it allows chemical/material worry-free workflow, as it doesn't need large amounts of solutions. Typically in our method, 3.0 mL was the maximum used volume to spray a plate of 10 x 20 cm. while, in automated dipping, approximately 100 mL solution is needed for a plate of the same area; this is considered a major obstacle enzymatic assays which in general seen as expensive material. One such superiority for using the piezoelectric derivatization is that studied plates are sprayed while horizontally positioned, thus, avoiding a shift of the inhibitory bands and ensures a good resolution of adjacent compounds.

The method has been optimized with respect to the detection wavelength, enzyme concentration, reaction time, and the effect of using HPTLC plates with and without fluorescent indicator. For all of these parameters, the reaction temperature was kept at 37 °C and pH 7.0 which repeatedly used working conditions in GUS assay (Jefferson 1987; Sekikawa et al. 2002). Also, SL was used as a standard inhibitor and the collected peak areas of the inhibition zones were used as a criterion for optimization experiments.

The optimum wavelength for colorimetric detection was found between 610 - 650 nm as deduced from the UV-Vis absorption spectrum for the background acquired at 200 - 800 nm. This range is acceptable for visible detection range of the blue indigo, which showed absorption maximum at 610 nm (Seixas de Melo et al. 2004). It is well known that indigo derivatives experience another absorption maxima in the UV range, which probably explains the observed absorption peaks at 306 nm. The optimum GUS concentration was determined as 25 U/mL (3.0 mL used for each run). In view of the conventional assays, Sekikawa et al. (2002) used 5 U of GUS from *E. coli* per reaction mixture, while Karak et al. (2017) used 98.6 U of bovine liver GUS for every reaction mixture. Accordingly, our developed method has significantly lowered the amount of the enzyme used. With regard to the reaction time,

60 min incubation after substrate application was found superior to 20 and 40 min as revealed from the statistical analysis of the collected data for peak areas of inhibition. Another attempt was made to inspect a longer reaction time at 2 h. The statistical analysis showed a significant difference between 1 & 2 h reaction times, indicating that 2 h is better. However, that would be at the expenses of the whole experiment time. So, 1 h reaction time was found as entirely reasonable for the developed method. In classical procedures of GUS assay using *p*-nitrophenyl- $\beta$ -D-glucuronide as a substrate, the reaction is usually terminated by addition of alkali after varied reaction times, but commonly from 50 - 60 min (Karak et al. 2017; Kim et al. 1999). The influence of fluorescent indicator on the colorimetric as well as fluorometric detection of the developed method was also studied using two types of HPTLC of plates, *i.e.* with and without fluorescent indicator. The results showed a significant difference between the plate types under both detection methods; fluorescent HPTLC plates yield better peak areas. Meaning, for the current assay, HPTLC plates with fluorescent indicator are preferred. The method has been validated in terms of LOD, linearity, and specificity. A range of SL concentrations have been applied such that we can determine the lowest concentration that could be detected with  $S/N \geq 3$ . In our method the lowest concentration applied and provided  $S/N = 4$  was 62 ng/band. The method showed also a linear regression within the range of 62 - 1000 ng/band that fits to a second order polynomial equation. The specificity of the established method has been also confirmed using different substrate, which demonstrated no results, *i.e.* background acquired no color.

Up to this point, an optimized hyphenation protocol for linking the GUS inhibition assay to HPTLC has been efficiently established and validated to some terms using a standard reference inhibitor (SL) that was applied directly without chromatographic development. So, a verification study was performed to evaluate the capacity of the newly developed protocol to detect the active inhibitors present in a complex mixture after being chromatographed. Thereof, two representatives of botanical material were used, *P. boveana* and SFLG. Both plant materials were selected with the view of their chemical constituents. Also, a particular attention was given to investigate the compatibility of the developed workflow with different developing systems composed of some commonly used solvents and the impact of including an acid as a modifier.

In *P. boveana*, the non-polar metabolites (**Pb1** & **Pb2**) developed with hexane : EtOAc (7:3, *V/V*) have been readily detected without prior neutralization of the plates. Flavonoids are prevalent bioactive compounds. They demonstrated inhibitory activity against many en-

zymes, nonetheless, few is known regarding their GUS inhibitory properties. In a previous study, Weng et al. (2017) have evaluated the inhibition activity of 30 flavonoids against *E. coli* GUS with additional structure activity relationship analysis. Their results showed that flavones without glucosyl or methoxyl modification displayed strong inhibitory effects against *E. coli* GUS with two flavonoids, scutellarein and luteolin, were found the most potent inhibitors and activity described as higher than the standard inhibitor, SL.

The second botanical model studied was SFLG. Silymarin is a collective term for flavonolignan constituents in *Silybum marianum*, Asteraceae (milk thistle). The extract of the plant has a wide scope of therapeutic applications. While, the antioxidant, anti-inflammatory, and chemopreventive activities have been proved for plant extract (Katiyar 2005); hitherto, the most known from literature and evidently established is its beneficial roles in hepatic disorders including, hepatitis, cirrhosis and fibrosis (Abenavoli et al. 2010; Csupor et al. 2016). One major compound was observed in the SFLG extract after application of the optimized assay and marked as **SFLG1**. The influence of using different MP composed of various solvents and with varying FA proportions was also studied. The plates were studied with and without prior neutralization as well. With MP1 (8.5 % FA), the assay didn't work at all unless the plates were neutralized in advance. In contrast, with MP2 (2.6 % FA) the assay is still able to provide the inhibition information.

Many active metabolites reside in the polar fraction of plant extract and, in many cases, the use of acidic MP is practically indispensable for their separation. Acidic MP is a serious impediment for microbiological or enzymatic assays being hyphenated with planar chromatography. The acid is retained on the plate and difficult to remove with the conventional methods of drying, *e.g.* using hair dryer, thus, impair the applied (bio)assay. In accordance, neutralization of the developed chromatogram was found as a determinant intervention for accomplishment of the assay. Jamshidi-Aidji and Morlock (2015) have discussed several methods of neutralization for plates being developed in acid-containing MP. They concluded that a buffer, in their case citric acid-phosphate (0.2 M) at pH 7.8, worked efficiently and retained the optimum pH of the plate at  $7 \pm 0.2$  to accommodate the applied microbial and enzymatic (bio)assay. Similarly, Hage and Morlock (2017) implied the neutralization step for bioprofiling of Salicaceae bud extracts and, for this, they immersed the plates into 2% sodium hydroxide solution. Thus, as clearly observed in both plant samples used, the current assay can tolerate FA inclusion up to certain proportions under which it can work to some degrees. The maximum that the current assay can tolerate has not attempted and could be the objective of

further studies. Nevertheless, our visual observation of the results favors the application of neutralization step if acidic MPs are to be used.

The extensive mass spectrometric analysis represented by HRMS and HRMS<sup>2</sup> measurements together with the help of the literature comparison (Brinda et al. 2012; Kuki et al. 2012a, 2012b) have fundamentally assisted in structure identification of this metabolite as silychristin. Basically, silymarin contains two silychristin diastereomers A & B and it was not possible to be distinguished from their MS data primarily, because of their comparable mass fragmentation pattern (Shibano et al. 2007), thus, herein collectively named as silychristin. The mass spectrometry has been extensively used to characterize the major constituents of silymarin, and it is well defined that the fragmentation behavior of such components is energy-dependent. Therefore, a range of collision energies (10 - 50 V) was applied and the occurrence as well as relative abundance of the diagnostic peaks was used for identification of the active metabolite. The optimal CE was found as 20 V, which is in accordance with the previously set values. To date, only single study have coupled the HPTLC to (bio)assays and mass spectrometry for profiling of the active metabolites in milk thistle (Taha et al. 2015); the authors have only identified the active metabolite in the extract as silybin through the low resolution MS analysis and comparison with standard. So, our current findings considered as the first report for linking HPTLC to HRMS/tandem HRMS for analysis of silymarin.

Silymarin as an inhibitor to GUS has been previously studied. Kim et al. (1994) have evaluated the GUS inhibition potential of three metabolites isolated from silymarin (silybin was one of them) and concluded that silybin considerably inhibited the enzyme. The hepatoprotective outcomes as a result of the GUS inhibition has been proposed through establishment of such activity in plants used to treat liver disorders (Karak et al. (2017)). A strong clue of the hepatoprotective potential of GUS inhibitors has been also determined for lactic acid bacteria, which significantly inhibited GUS of intestinal microflora (Han et al. 2005).

So, the selection of the plant for the verification study seems meaningful and the results would promote our knowledge with respect to the evaluation of the individual GUS inhibitory potential of this medicinally important plant. Besides, the results could offer a piece of evidence to support hepatoprotective characteristics of the GUS inhibitors. A part from the HPTLC-GUS assay findings, the MS analysis of silychristin and the fragmentation behavior at varying CE, importantly facilitate its determination in the total milk thistle extract.

In conclusion, this part of the study describes for the first time an efficient, optimized protocol for linking planar chromatography to *in situ* evaluation of GUS inhibitory activity. By means of this new hyphenation, sample mixtures can be evaluated in parallel for the presence of the enzyme inhibitors. It provides the possibility of dual output of the results (colorimetric and fluorometric). A number of concerned aspects have been addressed and discussed during the method verification like using different MPs, impact of FA as a modifier at different percentages, and important mass interpretation of the active metabolites.

#### **5.4. HPLC-HRMS and EPI analysis for identification of flavonoids constituents in *P. boveana* leaves**

*P. boveana* is a wild plant growing endemically in mountainous Saint Catherine region in Egypt. *P. boveana* is the only species representing the genus *Primula* in Egypt (El-Karemy and Hosni 1993). According to the 2014 IUCN report, the total number of the mature individuals was estimated as less as 165 (IUCN 2014). The report indicated that several impacts generally attribute to the remarkable reduction in the population of the titled plant; with the climate changes, marked by long drought periods, were impacting the most. In general consensus, synthesis and biogenesis of secondary metabolites in plants depend on numerous factors and greatly influenced as the plants are exposed to imminent stresses/threats. Verma and Shukla (2015) have reviewed the importance of the environmental factors, biotic and abiotic, as key players on the production of secondary metabolites in plants. Considering its critically endangered status and the pressing exogenous factors, *P. boveana* is worth chemically investigating with the purpose of possible revealing a plant-specific chemical profile.

As a time and material saving method, LC coupled to mass analysis was preferred to study *P. boveana* (80% methanol extract). Following the LC-MS protocol mentioned in the methodology section (3.6), a total of 25 flavonoid compounds have been tentatively identified. The LC-HRMS analysis suggested the elemental composition for each resolved peak with mass errors of less than 0.7 ppm, and then the tentative structures were assigned based on the fragmentation pattern affected by CID MS/MS. The characterized metabolites represented varied structures of flavonoid aglycones as well as glycosyl conjugates. Thirteen of these metabolites were defined as glycoconjugated flavonoids with three of them showed an additional acylation with malonyl unit. The characteristic loss of 86 Da in EPI measurement unam-

biguously indicated the presence of such malonyl group. These three metabolites have been tentatively assigned as: two isomers of dihydroxyflavone-*O*-malonylhexoside (**11**, Rt 26.7 min & **13**, 27.5 min) and flavone-*O*-malonylhexoside (**12**, Rt 27.4 min). Transfer of the malonyl moiety to flavonoid molecules is basically catalyzed by the action of malonyltransferase and preferably linked to the OH of the sugar residue (Kogawa et al. 2007). In general, malonylated flavonoids glycoconjugates show broad structure variations in terms of attachment position of the malonyl group on the glycone part (Muth et al. 2008). Malonylated flavones and flavonols have been previously reported, however, in genus *Primula* the occurrence of such compounds was not reported in literature. One more structure (**9**, Rt 25.5 min) that seen distinct to the studied plant species and, to our knowledge, previously not described to any of the *Primula* species. The simplicity of the MS data of **9** has largely helped to confirm its structure as flavone-*O*-hexoside. The compound showed a transition from *m/z* 401 to *m/z* 239, suggesting a loss of one hexoside unit with the remaining flavonoid aglycone assigned as monohydroxy flavone. Whereas, the exact position of the OH group on the aglycone moiety was not determined, it might be centered at the C-2' as formerly found in section (4.1.3). Noteworthy, several flavone-*O*-hexoside structures have been reported in literature, e.g. flavone-3-*O*-glucoside (Thirugnanasambantham et al. 1990; Miyakoshi et al. 2010), flavone-6-*O*-glucoside and flavone-7-*O*-glucoside. The above-discussed metabolites are considered species-specific and importantly distinguish *P. boveana* from other *Primula* species. The rest of the glycoconjugated metabolites were dominated by two different aglycones, kaempferol and quercetin, that being glycosylated by either di- or tri-saccharides. The consecutive loss of the sugar in the EPI spectra has determined the building units of the glycone units. The fact that *Primula* plants are capable of producing wide range of flavonoids that are glycosylated with different mono saccharides (glucopyranoside, galactopyranoside, and rhamnopyranoside), disaccharides (rutinoside, gentiobioside, robinobioside, neohesperidoside, and sophoroside), and tri-saccharides has made the definite assignment of the metabolites depending only on MS analysis a considerable challenge.

Beside the glycoconjugated flavonoids, 12 more compounds were identified as free flavonoid aglycones. Initial attempts were made to collect the EPIMS data for their protonated ion peaks but the results were not enough informative. So, their identification was chiefly based on their HRMS data, compounds determined in section 4.1.3, and the literature reviews. Unsubstituted flavone and 2'-methoxyflavone dominated the identified compounds. *Primulas* are well known to accumulate diverse lipophilic flavonoids leaded in principle by the unsubsti-

tuted flavone. The lipophilic flavonoids that frequently occur in *Primula* have some structural peculiarities as they show hydroxylation and/or methoxylation at unusual positions within the flavone molecule (Bhutia and Valant-Vetschera 2012). These free flavonoid aglycones are generally termed as epicuticular flavonoids as they always deposit on the outer surfaces of arial parts of the plant, with many relevant protection as well as adaptation functions (Cuadra and Harborne 1996; Isshiki et al. 2014). As a result of their unusual structural pattern, their underlying a biosynthetic pathway is rather confusing and it is assumed that these compounds are biosynthesized from still unknown pathway (Elser et al. 2016).

In conclusion, the HPLC-HRMS and EPI-MS/MS analyses have proven their capability to provide valuable structural information for constituents of a complex mixture. The initial assumption, that the tough growing conditions and the pressing environmental impacts on *P. boveana* could impose unique chemical features to the plant, has been gotten to the point. While the titled plant displays chemical profile that partially in harmony with this previously reported for many other *Primula sp.*, it is still reserving a particular capacity to accumulate other new metabolites. These new structural findings (represented by compounds **9**, **11-13**) and their occurrence could be explained as a kind of the survival or adaptation mechanisms that the plant uniquely utilizes.



## Summary

The aimed at the biological and chemical investigations of two plant species, *P. boveana*, and *A. pubescens* that endemically grow in St. Catherine, Egypt, along with the well-known medicinally important species, *P. veris*. Considering the scarce nature of the endemic species, biological-chemical hyphenated systems were found the most suitable for their analysis. Therefore, the study involved:

- 1) Guided isolation of the bacterial and/or ChE inhibitors from *P. boveana*, *P. veris*, and *A. pubescens* by means of HPTLC-EDA-HRMS technique.
- 2) Development of a new HPTLC-GUS inhibition assay hyphenation.
- 3) Utilization of HPLC-HRMS and tandem MS for flavonoids profiling in *P. boveana*.

For the *Primula sp.*, the bacterial and AChE/BChE inhibitory activities of their medium polar extracts were evaluated. The two species are here studied for the first time using HPTLC-EDA-HRMS hyphenation. The results revealed the presence of two major active metabolites in *P. veris*, which clearly inhibited the tested bacteria (*A. fischeri* and *B. subtilis*) and ChE (AChE and BChE). HPTLC-HRMS allowed their structure characterization as linoleic and linolenic acids. While in *P. boveana*, four metabolites have been detected and variably showed bacterial and/or ChE inhibition. After isolation of these four metabolites, they were structurally identified by means of <sup>1</sup>H NMR analysis. Two of them (unsubstituted flavone and 2'-methoxy flavone) have inhibited both bacteria tested (*A. fischeri* and *B. subtilis*) as well as AChE and BChE. While the other two (2'-hydroxy- and 5,6,2',6'-tetramethoxyflavone) displayed inhibition to only *A. fischeri* bacteria and BChE. These bioactivity findings evidenced the multipotent properties of some naturally occurring compounds. Furthermore, HPTLC-AChE inhibition equivalency study on the unsubstituted flavone, as a principle inhibitor, was carried out; it revealed that the unsubstituted flavone as exists in 10 µg dry powder of *P. boveana* inhibited AChE equivalently to 4.5 µg the standards inhibitor, Riv.

With regard to *A. pubescens*, HPTLC-AChE inhibition assay led to characterization of three inhibitors from the 80% methanolic extract of the plant. The metabolites were assigned as antirrhinose-derived iridoid glucosides. Whereas the AChE inhibitors of many iridoids have been previously reported, this study describes for the first time the AChE inhibitory activity of the antirrhinose class of iridoids. Based on the extensive spectroscopic analysis,

two of the identified metabolites are here described as newly isolated natural compounds and their structures were determined as 6-*O*-, 6'-*O*-di-*trans*-cinnamoyl-antirrhinose and 5-*O*-, 6-*O*-difoliamenthoyl-antirrhinose while, the third compound was identified as 6-*O*-foliamenthoyl-(6'-*O*-cinnamoyl)-antirrhinose, which is a previously known compound. The AChE inhibition equivalency study performed on the isolated metabolites revealed that 6-*O*-foliamenthoyl-(6'-*O*-cinnamoyl)-antirrhinose is the most active amongst the three compounds and the free 5-OH is essential to maintain higher AChE inhibitory activity of antirrhinose derivatives.

The second part of the study reports the hyphenation of GUS inhibition assay to HPTLC for a streamlined detection of the enzyme inhibitors in complex mixtures. The classical methods are usually performed on the total mixtures or extracts without pointing to the activity of the individual components unless being separated in advance, which is seen as a major concern as it requires more time as well as material. So, with the newly developed hyphenation, the GUS inhibition activity of each component of the mixture could be *in situ* evaluated after being resolved on the HPTLC. Thus, offers a time/material effective method of biological analysis. The detection reaction of the method relied on the enzymatic cleavage of the substrate, X-Gluc, followed by oxidative dimerization to give the indigo blue as the final product. GUS inhibitors were shown up as white zones against the blue background. In addition, a fluorescent detection of the inhibition zones is also possible due to the highly fluorescent intermediates. Thus, the utilized reaction presents a dual readout of the results, putting it steps superior to other commonly used reactions. The optimum wavelength of colorimetric detection (610 - 650 nm), enzyme concentration (25 U/mL, *i.e.* 0.375 U/cm<sup>2</sup>), reaction time (60 min), and plate type (with fluorescent indicator) were all assessed and discussed in the view of the literature data. In our method the lowest concentration applied and provided S/N  $\geq 3$  was 62 ng/band with S/N of 4. The method showed a good linearity and specificity. Furthermore, the newly developed hyphenation was verified through application on two plant extracts, *P. boveana* and SFLG. The optimized protocol proved its efficiency to detect the GUS inhibitors in complex mixtures being separated under different chromatographic systems, advanced our understanding of the appropriate MP used, and how to overcome the inevitable loss of the enzymatic reaction when an acid is used as a modifier. With the help of HPTLC-HRMS/MS, the structures of the active GUS inhibitors were assigned.

Finally, the third part of the study addressed the HPLC-HRMS and EPIMS-based characterization of flavonoids in *P. boveana* extract. *Primula* plants are known to accumulate diverse scaffolds of flavonoid structures. Nevertheless, the chemical analysis of *P. boveana* has

not thoroughly reported. The elemental composition and the CID MS/MS measurements permitted tentative assignment of 25 compounds in total. Thirteen of these metabolites were defined as glycoconjugated flavonoids with three of them have shown an additional acylation with a malonyl unit, so far, no previous reports on the occurrence of the malonylated flavonoids in any plants of the genus is available. Also, flavone-*O*-hexoside has never been described in any species of the genus. The rest of the metabolites (12 compounds) are defined based on their accurate mass analysis and determined as epicuticular flavonoids, *i.e.* produced on the outer surfaces of the arial parts of the plant. These were flavonoid aglycones showing different degrees of hydroxylation and/or methoxylation. Obviously, *P. boveana* displayed some phyto-constituent particularities, which expressed more in the glycoconjugated metabolites and these chemical profiling, could correlate to the survival and/or defense mechanisms that the plant uses to tolerate the stressing influences.

To summarize, the presented study has revealed many unprecedentedly reported biological as well as chemical findings. It supported the evidence-based herbal medicine approach for treatment of many major human diseases like infection and AD. The study not only considered as a proof of principle for the potential of the previously developed HPTLC-EDA hyphenations, but also offered a new coupling approach.

## Deliverables

### Manuscripts accepted/submitted from this PhD study

- (1) Mahran E., El Gamal I., Keusgen M., Morlock G. (2019) Effect-directed analysis by high performance thin layer chromatography for bioactive metabolites tracking in *Primula veris* flower and *Primula boveana* leaf extracts. *Journal of Chromatography A* (Accepted, in print).
- (2) Mahran E., Morlock G., Keusgen M. (2019) Guided isolation of new iridoid glucosides from *Anarrhinum pubescens* by high-performance thin-layer chromatography-acetylcholinesterase assay. *Journal of Chromatography A* (Accepted, in print).
- (3) Mahran E., Keusgen M., Morlock G. New planar assay for a streamlined detection and quantification of  $\beta$ -glucuronidase inhibitors and application to botanical extracts. (In submission).

### Conference and workshops

- Poster, June 2019: "67th ASMS Conference on Mass Spectrometry and Allied Topics", Atlanta, GA, USA.
- Oral presentation, June 2019: "48th International Symposium on High-Performance Liquid Phase Separations and Related Techniques", Milan, Italy.
- Oral presentation, November 2018: "24th International Symposium for High-Performance Thin-Layer Chromatography" Bangkok, Thailand.
- Workshop, October 2018: "Scifinder on campus". Philipps University of Marburg, Germany.
- Conference attendance, August 2017 "Engineering of Functional Interfaces" Marburg, Germany.

## References

- Abdelaal M, Fois M, Fenu G, Bacchetta G (2018) Critical checklist of the endemic vascular plants of Egypt. *Phytotaxa* 360:19–34
- Abenavoli L, Capasso R, Milic N, Capasso F (2010) Milk thistle in liver diseases: past, present, future. *Phytother Res* 24:1423–1432.
- Aniszewski T. *Alkaloids-Secrets of life: alkaloid chemistry, biological significance, applications and ecological role*. Elsevier, 2007.
- Apel L, Kammerer D, Stintzing F, Spring O (2017) Comparative metabolite profiling of triterpenoid saponins and flavonoids in flower color mutations of *Primula veris* L. *Int J Mol Sci* 18:153.
- Atanasov et al. (2015) Discovery and resupply of pharmacologically active plant-derived natural products: A review. *Biotechnol Adv* 33:1582–1614.
- Ayyad MA, Fakhry AM, Moustafa AR (2000) Plant biodiversity in the Saint Catherine area of the Sinai peninsula, Egypt. *Biodivers Conserv* 9:265–81.
- Azadniya E, Morlock GE (2019) Automated piezoelectric spraying of biological and enzymatic assays for effect-directed analysis of planar chromatograms, *in print*.
- Azadniya E, Morlock GE (in submission) Equivalency calculation of enzyme inhibiting unknowns *in situ* the adsorbent of the effect-directed autogram.
- Bakar NS, Zin NM, Basri DF (2012) Synergy of flavone with vancomycin and oxacillin against vancomycin-intermediate *Staphylococcus aureus*. *Pak J Pharm Sci* 25:633–638.
- Bakhtiari M, Panahi Y, Ameli J, Darvishi B (2017) Protective effects of flavonoids against Alzheimer's disease-related neural dysfunctions. *Biomed Pharmacother* 93:218–229.
- Baptista FI, Henriques AG, Silva AM, Wiltfang J, da Cruz e Silva OA (2014) Flavonoids as therapeutic compounds targeting key proteins involved in Alzheimer's disease. *ACS Chem Neurosci* 5:83–92.
- Başbülbül G, Özmen A, Biyik HH, Şen Ö (2008) Antimitotic and antibacterial effects of the *Primula veris* L. flower extracts. *Caryologia* 61:88–91.
- Basile A, Conte B, Rigano D, Senatore F, Sorbo S (2010) Antibacterial and antifungal properties of acetic extract of *Feijoa sellowiana* fruits and its effect on *Helicobacter pylori* growth. *J Med Food* 13:189–95.
- Batra P, Sharma AK (2013) Anti-cancer potential of flavonoids: recent trends and future Perspectives. *3Biotech* 3:439–459.
- Bawri A, Gajurel PR, Khan ML (2014) New distributional records of *Primula* species in Arunachal Pradesh, India. *Biosci Discov* 5:6–10.
- Baynes RE, Hodgson E (Eds.). *A textbook of modern toxicology*, John Wiley & Sons, 2010, pp. 143–145.
- Beninger CW, Cloutier RR, Monteiro MA, Grodzinski B (2007) The distribution of two major iridoids in different organs of *Antirrhinum majus* L. at selected stages of development. *J Chem Ecol* 33:731–747.
- Bentsen H (2017) Dietary polyunsaturated fatty acids, brain function and mental health. *Microb Ecol Health Dis* 2:1281916.
- Bhardwaj C, Hanley L (2014) Ion sources for mass spectrometric identification and imaging of molecular species. *Nat Prod Rep* 31:756–67.

- Bhutia TD, Valant-Vetschera KM (2012) Diversification of exudate flavonoid profiles in further *Primula* spp. *Nat Prod Commun* 7.
- Blaskó G, Xun L, Cordell GA (1988) Studies in the Thymelaeaceae, V. 2'-Hydroxyflavone from *Daphnopsis sellowiana*: Isolation and Synthesis. *J Nat Prod* 51:60–65.
- Bolus L (2000) *Flora of Egypt*, Vol. II. Al Hadara Publishing, Cairo, pp. 58-59.
- Brinda BJ, Zhu HJ, Markowitz JS (2012) A sensitive LC–MS/MS assay for the simultaneous analysis of the major active components of silymarin in human plasma. *J Chromatogr B* 902:1–9.
- Budzianowski J, Morozowska M, Wesolowska M (2005) Lipophilic flavones of *Primula veris* L. from field cultivation and *in vitro* cultures. *Phytochemistry* 66:1033–9.
- Budzianowski J, Morozowska M, Wesolowska M (2005) Lipophilic flavones of *Primula veris* L. from field cultivation and *in vitro* cultures. *Phytochemistry* 66:1033–1039.
- Caputi L, Aprea E (2011) Use of terpenoids as natural flavouring compounds in food industry. *Recent Pat Food Nutr Agric* 3:9–16.
- Carmody RN, Turnbaugh PJ (2014) Host-microbial interactions in the metabolism of therapeutic and diet-derived xenobiotics. *J Clin Invest* 124:4173–4181.
- Chahar MK, Sharma N, Dobhal MP, Yogesh C, Joshi YC (2011) Flavonoids: A versatile source of anticancer drugs. *Pharmacogn Rev* 5:1–12.
- Cheng TC, Chuang KH, Roffler SR, Cheng KW, Leu YL, Chuang CH, Huang CC, Kao CH, Hsieh YC, Chang LS, Cheng TL (2015) Discovery of specific inhibitors for intestinal *E. coli*  $\beta$ -glucuronidase through *in silico* virtual screening. *Sci World J* 2015:2015.
- Colombo PS, Flamini G, Rodondi G, Giuliani C, Santagostini L, Fico G (2017) Phytochemistry of European *Primula* species. *Phytochemistry* 143:132–144.
- Cragg GM, Newman DJ (2013) Natural products: A continuing source of novel drug leads. *Biochim Biophys Acta* 1830:3670–3695.
- Csupor D, Csorba A, Hohmann J (2016) Recent advances in the analysis of flavonolignans of *Silybum marianum*. *J Pharm Biomed Anal* 130:301–317.
- Cuadra P, Harborne JB (1996) Changes in epicuticular flavonoids and photosynthetic pigments as a plant response to UV-B radiation. *Z Naturforsch C* 51:671–80.
- Cushnie TT, Lamb AJ (2005) Antimicrobial activity of flavonoids. *Int J Antimicrob Agents* 26:343–56.
- Cuyckens F, Claeys M (2004) Mass spectrometry in the structural analysis of flavonoids. *J Mass Spectrom* 39:1–5.
- Cuyckens F, Claeys M (2004) Mass spectrometry in the structural analysis of flavonoids. *J Mass Spectrom* 39:1–5.
- Dawidar AM, Esmirly ST, Al-Hajar AS, Jakupovic J, Abdel-Mogib M (1989) Two iridoid glucoside esters from *Anarrhinum orientale*. *Phytochemistry* 28:3227–9.
- Dewanjee S, Gangopadhyay M, Bhattacharya N, Khanra R, Dua TK (2015) Bioautography and its scope in the field of natural product chemistry. *J Pharma Anal* 5:75-84.
- Dewick PM, *Medicinal natural products: a biosynthetic approach*. John Wiley & Sons, 2002.
- DIN EN ISO 11348-1 (2009) Part 1, Section 5, Water quality-determination of the inhibitory effect of water samples on the light emission of *Vibrio fischeri* (Luminescent Bacteria Test), Beuth-Verlag, Berlin, 2009.

- Dinda B, Debnath S, Banik R (2011) Naturally occurring iridoids and secoiridoids. An updated review, part 4. *Chem Pharm Bull* 59:803–33.
- Echeverría J, Opazo J, Mendoza L, Urzúa A, Wilkens M (2017) Structure-activity and lipophilicity relationships of selected antibacterial natural flavones and flavanones of Chilean flora. *Molecules* 22:608.
- EL Hadidi MN, Hosni HA (1996) Biodiversity in the flora of Egypt. pp 785–787.
- El-Karemy ZA, Hosni HA (1993) Systematic studies on the Egyptian species of the family Primulaceae With 3 Plates. *Feddes Rept* 104:327–334.
- Elser D, Gilli C, Brecker L, Valant-Vetschera KM (2016) Striking diversification of exudate profiles in selected *Primula Lineages*. *Nat Prod Commun* 11.
- EMA, European Medicines Agency (2012) Assessment report on *Primula veris* L. and/or *Primula elatior* (L.) Hill, radix.
- Farooqui AA, Horrocks LA (2001) Plasmalogens, phospholipase A 2, and docosahexaenoic acid turnover in brain tissue. *J Mol Neurosci* 16:263–272.
- Fenn JB, Mann M, Meng CK, Wong SF, Whitehouse CM (1990) Electrospray ionization—principles and practice. *Mass Spectrom Rev* 9:37–70.
- Frampton EW, Restaino L, Blaszkowski N (1988) Evaluation of the  $\beta$ -glucuronidase substrate 5-bromo-4-chloro-3-indolyl- $\beta$ -D-glucuronide (X-Gluc) in a 24-hour direct plating method for *Escherichia coli*. *J Food Prot* 51:402–404.
- Fuchs A, Bowers MD (2004) Patterns of iridoid glycoside production and induction in *Plantago lanceolata* and the importance of plant age. *J Chem Ecol* 30:1723–41.
- Gálvez M, Martín-Cordero C, Jesús Ayuso M (2005) Iridoids as DNA topoisomerase I poisons. *J Enzyme Inhib Med Chem* 20:389–392.
- Ganeshpurkar A, Saluja AK (2017) The pharmacological potential of rutin. *Saudi Pharm J* 25:149–64.
- Glavnik V, Vovk I, Albrecht A (2017) High performance thin-layer chromatography–mass spectrometry of Japanese knotweed flavan-3-ols and proanthocyanidins on silica gel plates. *J Chromatogr A* 1482:97–108.
- Gousiadou C, Gotfredsen CH, Matsa M, Hadjipavlou-Litina D, Skaltsa H (2013) Minor iridoids from *Scutellaria albida* ssp. *albida*. Inhibitory potencies on lipoxygenase, linoleic acid lipid peroxidation and antioxidant activity of iridoids from *Scutellaria sp.* *J Enzyme Inhib Med Chem* 28:704–710.
- Guerram M, Jiang ZZ, Zhang LY (2012) Podophyllotoxin, a medicinal agent of plant origin: past, present and future. *Chin J Nat Med* 10:161–9.
- Guerrero L, Castillo J, Quiñones M, Garcia-Vallvé S, Arola L, Pujadas G, Muguerza B (2012) Inhibition of angiotensin-converting enzyme activity by flavonoids: structure-activity relationship studies. *PloS one* 7:e49493.
- Hage S, Morlock GE (2017) Bioprofiling of Salicaceae bud extracts through high-performance thin-layer chromatography hyphenated to biochemical, microbiological and chemical detections. *J Chromatogr A* 1490:201–211.
- Haines JR, Covert TC, Rankin CC (1993) Evaluation of indoxyl-beta-D-glucuronide as a chromogen in media specific for *Escherichia coli*. *Appl Environ Microbiol* 59:2758–2759.
- Han SY, Huh CS, Ahn YT, Lim KS, Baek YJ, Kim DH (2005) Hepatoprotective effect of lactic acid bacteria, inhibitors of  $\beta$ -glucuronidase production against intestinal microflora. *Arch Pharm Res* 28:325.

- Handjieva NV, Ilieva EI, Spassov SL, Popov SS, Duddeck H (1993) Iridoid glycosides from *Linaria* species. *Tetrahedron* 49:9261–9266.
- Hegazy A, Lovett-Doust J (2016) *Plant ecology in the Middle East*. Oxford University Press, London, 339
- Heim KE, Tagliaferro AR, Bobilya DJ (2002) Flavonoid antioxidants: chemistry, metabolism and structure-activity relationships. *J Nutr Biochem* 13:572–84.
- Hodek P, Tepla M, Krizkova J, Sulc M, Stiborova M (2009) Modulation of cytochrome P450 enzyme system by selected flavonoids. *Neuro Endocrinol Lett* 1:67–71.
- Hodgson E (2010) Introduction to biotransformation (metabolism). In: *Hayes' Handbook of Pesticide Toxicology* (pp. 865-875). Academic Press.
- Huck CW, Huber CG, Lagoja IM, Ongania KH, Scherz H, Bonn GK, Popp M (1999) Isolation and structural elucidation of 3',4',5'-trimethoxyflavone from the flowers of *Primula veris*. *Planta Med* 65:491.
- Huck CW, Huber CG, Ongania KH, Bonn GK (2000) Isolation and characterization of methoxylated flavones in the flowers of *Primula veris* by liquid chromatography and mass spectrometry. *J Chromatogr A* 18:453–62.
- Iba K (2002) Acclimative response to temperature stress in higher plants: approaches of gene engineering for temperature tolerance. *Annu Rev Plant Biol* 53:225–245.
- Isshiki R, Galis I, Tanakamaru S (2014) Farinose flavonoids are associated with high freezing tolerance in fairy primrose (*Primula malacoides*) plants. *J Integr Plant Biol* 56:181–188.
- IUCN, International Union for Conservation of Nature's Red List of Threatened Species <https://www.iucnredlist.org/species/163968/1015883>
- Jaberian H, Piri K, Nazari J (2013) Phytochemical composition and *in vitro* antimicrobial and antioxidant activities of some medicinal plants. *Food Chem* 136:237–44.
- Jamshidi-Aidji M, Morlock GE (2015) Bioprofiling of unknown antibiotics in herbal extracts: Development of a streamlined direct bioautography using *Bacillus subtilis* linked to mass spectrometry. *J Chromatogr A* 1420:110–118.
- Jefferson RA (1987) Assaying chimeric genes in plants: the GUS gene fusion system. *Plant Mol Biol Report* 5:387–405.
- Jeffree GM (1969) Demonstration of  $\beta$ -glucuronidase with naphthol AS-BI- $\beta$ -D-glucosiduronic acid by simultaneous coupling. *J Microsc* 89:55–62.
- Jensen SR, Franzyk H, Wallander E (2002) Chemotaxonomy of the Oleaceae: iridoids as taxonomic markers. *Phytochemistry* 60:213–231.
- Jeong EJ, Lee KY, Kim SH, Sung SH, Kim YC (2008) Cognitive-enhancing and antioxidant activities of iridoid glycosides from *Scrophularia buergeriana* in scopolamine-treated mice. *Eur J Pharmacol* 588:78–84.
- Jicha GA, Markesbery WR (2010) Omega-3 fatty acids: potential role in the management of early Alzheimer's disease. *Clin Interv Aging* 5:45.
- Jiménez A, Mansour H, Keller B, Conti E (2014) Low genetic diversity and high levels of inbreeding in the Sinai primrose (*Primula boveana*), a species on the brink of extinction. *Plant Syst Evol* 300: 1199–1208.
- Jucá MM, Cysne Filho FM, de Almeida JC, Mesquita DD, Barriga JR, Dias KC, Barbosa TM, Vasconcelos LC, Leal LK, Ribeiro JE, Vasconcelos SM (2018) Flavonoids: biological activities and therapeutic potential. *Nat Prod Res* 15:1–4.



- Kabera JN, Semana E, Mussa AR, He X (2014) Plant secondary metabolites: biosynthesis, classification, function and pharmacological properties. *J Pharm Pharmacol* 2:377–392.
- Kachlicki P, Piasecka A, Stobiecki M, Marczak L (2016) Structural characterization of flavonoid glycoconjugates and their derivatives with mass spectrometric techniques. *Molecules* 21:1494.
- Karak S, Nag G, De B (2017) Metabolic profile and  $\beta$ -glucuronidase inhibitory property of three species of *Swertia*. *Rev Bras Farmacogn* 27:105–111.
- Katiyar SK (2005) Silymarin and skin cancer prevention: anti-inflammatory, antioxidant and immunomodulatory effects. *Int J Oncol* 26:169–176.
- Khan H, Amin S, Kamal MA, Patel S (2018) Flavonoids as acetylcholinesterase inhibitors: Current therapeutic standing and future prospects. *Biomed Pharmacother* 101:860–870.
- Kim D, Jin Y, Park J, Kobashi K (1994) Silymarin and its components are inhibitors of  $\beta$ -glucuronidase. *Biol Pharm Bull* 17:443–445.
- Kim DH, Shim SB, Kim NJ, Jang IS (1999)  $\beta$ -Glucuronidase-inhibitory activity and hepatoprotective effect of *Ganoderma lucidum*. *Biol Pharm Bull* 22:162–164.
- Kogawa K, Kazuma K, Kato N, Noda N, Suzuki M (2007) Biosynthesis of malonylated flavonoid glycosides on the basis of malonyltransferase activity in the petals of *Clitoria ternatea*. *J Plant Physiol* 164:886–894.
- Koppelaar et al. (2005) MS detectors. 418A–427A.
- Kosenkova YS, Polovinka MP, Komarova NI, Korchagina DV, Morozov SV, Vyalkov AI, Kurochikina NY, Cheremushkina VA, Salakhutdinov NF (2008) Fatty-acid composition and secondary metabolites from slightly polar extracts of the aerial part of *Primula macrocalyx*. *Chem Nat Compd* 44:564–8.
- Kroll-Møller P, Pedersen KD, Gousiadou C, Kokubun T, Albach D, Taskova R, Garnock-Jones PJ, Gottfredsen CH, Jensen SR (2017) Iridoid glucosides in the genus *Veronica* (Plantaginaceae) from New Zealand. *Phytochemistry* 140:174–80.
- Krungkrai J, Krungkrai SR (2016) Antimalarial qinghaosu/artemisinin: The therapy worthy of a Nobel Prize. *Asian Pac J Trop Biomed* 6:371–375.
- Krüzelyi D, Nagy R, Ott PG, Móricz Á (2016) Rapid, bioassay-guided process for the detection and identification of antibacterial Neem oil compounds. *J Chromatogr Sci* 54:1084–1089.
- Kuki Á, Biri B, Nagy L, Deák G, Kalmár J, Mándi A, Nagy M, Zsuga M, Kéki S (2012) Collision induced dissociation study of the major components of silymarin. *Int J Mass Spectrom* 315:46–54.
- Kuki Á, Nagy L, Deák G, Nagy M, Zsuga M, Kéki S (2012) Identification of silymarin constituents: an improved HPLC-MS method. *Chromatographia* 75:175–180.
- Kumar S, Pandey AK (2013) Chemistry and biological activities of flavonoids: an overview. *The Scientific World Journal* 2013:1–16.
- Kurata S, Yamaguchi K, Nagai M (2005) Rapid discrimination of fatty acid composition in fats and oils by electrospray ionization mass spectrometry. *Anal Sci* 21:1457–65.
- Lampe JW, Li SS, Potter JD, King IB (2002) Serum  $\beta$ -glucuronidase activity is inversely associated with plant-food intakes in humans. *J Nutr* 132:1341–1344.
- Larson JR, Tingstad JE, and Swadesh JK., Introduction. In: Swadesh JK (Eds.), *HPLC practical and industrial applications*, CRC press, 2000, 1–57.
- Lee KY, Sung SH, Kim SH, Jang YP, Oh TH, Kim YC (2009) Cognitive-enhancing activity of loganin isolated from *Cornus officinalis* in scopolamine-induced amnesic mice. *Arch Pharm Res* 32:677–83.

- Lin D, Xiao M, Zhao J, Li Z, Xing B, Li X, Kong M, Li L, Zhang Q, Liu Y, Hong Chen H, Qin W, Wu H, Chen S (2016) An overview of plant phenolic compounds and their importance in human nutrition and management of type 2 Diabetes. *Molecules* 21:1374–1392.
- Liu Q, Luo L, Zheng L (2018) Lignins: Biosynthesis and biological functions in plants. *Int J Mol Sci* 19:2–16.
- Liu ZH, Hou B, Yang L, Ma RJ, Li JY, Hu JM, Zhou J (2017) Iridoids and bis-iridoids from *Patrinia scabiosaefolia*. *RSC Adv* 7:24940–9.
- LoGuidice A, Wallace BD, Bendel L, Redinbo MR, Boelsterli UA (2012) Pharmacologic targeting of bacterial  $\beta$ -glucuronidase alleviates nonsteroidal anti-inflammatory drug-induced enteropathy in mice. *J Pharmacol Exp Ther* 341:447–454.
- Mahrn E, Hosny M, El-Hela A, Boroujerdi A (2018) New iridoid glycosides from *Anarrhinum pubescens*. *Nat Prod Res* 11:1–8.
- Majid A, Hassan S, Hussain W, Khan A, Hassan A, Khan A, Khan T, Ahmad T, Rehman MU (2014) In vitro Approaches of *Primula vulgaris* Leaves and Roots Extraction against Human Pathogenic Bacterial Strains. *World Applied Sciences Journal* 30:575–80.
- Mansour HH, Jiménez A, Keller B, Nowak DM, Conti E (2013) Development of 13 microsatellite markers in the endangered Sinai primrose (*Primula boveana*, Primulaceae). *Appl Plant Sci* 1: 1200515.
- March R, Brodbelt J (2008) Analysis of flavonoids: tandem mass spectrometry, computational methods, and NMR. *J Mass Spectrom* 43:1581–617.
- Marston A, Kissling J, Hostettmann K (2002) A rapid TLC bioautographic method for the detection of acetylcholinesterase and butyrylcholinesterase inhibitors in plants. *Phytochem Anal* 13:51–54.
- Martins A, Vieira H, Gaspar H, Santos S (2014) Marketed marine natural products in the pharmaceutical and cosmeceutical industries: Tips for success. *Mar Drugs* 12:1066–1101.
- McGaw LJ, Jäger AK, Van Staden J, Houghton PJ (2002) Antibacterial effects of fatty acids and related compounds from plants. *S Afr J Bot* 68:417–423.
- Medhe S (2018) Ionization Techniques in Mass Spectrometry: A Review. *Mass Spectrom Purif Tech* 4:126.
- Miron A, Aprotosoiaie AC, Trifan A, Xiao J (2017) Flavonoids as modulators of metabolic enzymes and drug transporters. *Ann N Y Acad Sci.* 1398:152–167.
- Miyakoshi S, Azami S, Kuzuyama T (2010) Microbial glucosylation of flavonols by *Cunninghamella echinulata*. *J Biosci Bioeng* 110:320–321.
- Moberg LJ (1985) Fluorogenic assay for rapid detection of *Escherichia coli* in food. *Appl. Environ Microbiol* 50:1383–7.
- Moon BH, Lee YS, Shin CS, Lim YH (2005) Complete assignments of the  $^1\text{H}$  and  $^{13}\text{C}$  NMR data of flavone derivatives. *Bull Korean Chem Soc.* 26:603–608.
- Morlock G, Schwack W (2010) Hyphenations in planar chromatography. *J Chromatogr A.* 1217:6600–6609.
- Mostafa FA, Gamal MA, Sabrin IR, Ehab ES (2014) Antioxidant and anti-inflammatory activities of phenolic constituents from *Primula elatior* L. aerial part. *Int J Pharmacogn Phytochem Res* 6:74–78.
- Muth D, Marfisdén-Edwards E, Kachlicki P, Stobiecki M (2008) Differentiation of isomeric malonylated flavonoid glyconjugates in plant extracts with UPLC-ESI/MS/MS. *Phytochem Anal* 19:444–452.

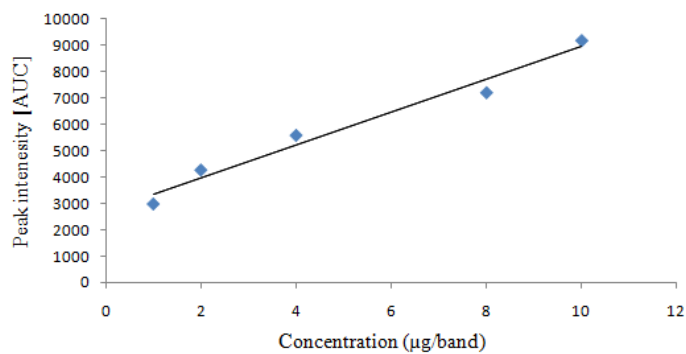
- Najmus-Saqib Q, Alam F, Ahmad M (2009) Antimicrobial and cytotoxicity activities of the medicinal plant *Primula macrophylla*. *J Enzyme Inhib Med Chem* 24:697–701.
- Newman DJ, Cragg GM (2012) Natural products as sources of new drugs over the 30 years from 1981 to 2010. *J Nat Prod* 75:311–335.
- Newman DJ, Cragg GM (2016) Natural products as sources of new drugs from 1981 to 2014. *J Nat Prod* 79:629–661.
- Orčić D, Francišković M, Bekvalac K, Svirčev E, Beara I, Lesjak M, Mimica-Dukić N (2014) Quantitative determination of plant phenolics in *Urtica dioica* extracts by high-performance liquid chromatography coupled with tandem mass spectrometric detection. *Food Chem* 143:48–53.
- Pan M, Laia C, Ho C (2010) Anti-inflammatory activity of natural dietary flavonoids. *Food Funct* 1:15–31.
- Panche A, Diwan AD, Chandra SR (2016) Flavonoids: an overview. *J Nutr Sci* 5:1–15.
- Park KS, Kim BH, Chang IM (2010) Inhibitory potencies of several iridoids on cyclooxygenase-1, cyclooxygenase-2 enzymes activities, tumor necrosis factor- $\alpha$  and nitric oxide production in vitro. *Evid Based Complement Alternat Med* 7:41–45.
- Patel KN, Patel JK, Patel MP, Rajput GC, Patel HA (2010) Introduction to hyphenated techniques and their applications in pharmacy. *Pharm Methods* 1:2–13.
- Patlolla JMR, Rao CV (2012) Triterpenoids for cancer prevention and treatment: current status and future prospects. *Curr Pharm Biotechnol* 13:147–55.
- Pellock SJ, Creekmore BC, Walton WG, Mehta N, Biernat KA, Cesmat AP, Ariyaratna Y, Dunn ZD, Li B, Jin J, James LI (2018) Gut microbial  $\beta$ -Glucuronidase inhibition *via* catalytic cycle interception. *ACS Cen Sci* 4:868–79.
- Pietta PG (2000) Flavonoids as Antioxidants. *J Nat Prod* 63:1035–1042.
- Pirouzpanah S, Hanaee J, Razavieh SV, Rashidi MR (2009) Inhibitory effects of flavonoids on aldehyde oxidase activity. *J Enzyme Inhib Med Chem* 24:14–21.
- Pitt JJ (2009) Principles and applications of liquid chromatography-mass spectrometry in clinical biochemistry. *Clin Biochem Rev* 30:19–34.
- Proença C, Freitas M, Ribeiro D, Oliveira EF, Sousa JL, Tomé SM, Ramos MJ, Silva AM, Fernandes PA, Fernandes E (2017)  $\alpha$ -Glucosidase inhibition by flavonoids: an *in vitro* and *in silico* structure–activity relationship study. *J Enzyme Inhib Med Chem* 32:1216–28.
- Ramallo IA, García P, Furlan RL (2015) A reversed-phase compatible thin-layer chromatography autoradiography for the detection of acetylcholinesterase inhibitors. *J Sep Sci* 38:3788–94.
- Ramírez-Cisneros MÁ, Rios MY, Aguilar-Guadarrama AB, Rao PP, Aburto-Amar R, Rodríguez-López V (2015) *In vitro* COX-1 and COX-2 enzyme inhibitory activities of iridoids from *Penstemon barbatus*, *Castilleja tenuiflora*, *Crescentia alata* and *Vitex mollis*. *Bioorg Med Chem Lett* 25:4505–8.
- Rates SMK (2001) Plants as source of drugs. *Toxicon* 39:603–613.
- Rathee P, Chaudhary H, Rathee S, Rathee D, Kumar V, Kohli K (2009) Mechanism of action of flavonoids as anti-inflammatory agents: A review. *Inflamm Allergy Drug Targets* 8:229–235.
- Ren Y, Houghton P, Hider RC (2006) Relevant activities of extracts and constituents of animals used in traditional Chinese medicine for central nervous system effects associated with Alzheimer's disease. *J Pharm Pharmacol* 58:989–996.
- Richards (2003) *Primula* Second Ed. Portland, OR, USA: Timber Press.

- Roberts AB, Wallace BD, Venkatesh MK, Mani S, Redinbo MR (2013) Molecular insights into microbial  $\beta$ -glucuronidase inhibition to abrogate CPT-11 toxicity. *Mol Pharmacol* 84:208–217.
- Roseiro LB, Rauter AP, Serralheiro ML (2012) Polyphenols as acetylcholinesterase inhibitors: structural specificity and impact on human disease. *Nut Aging* 1:99–111.
- Roseiro LB, Rauter AP, Serralheiro ML (2012) Polyphenols as acetylcholinesterase inhibitors: structural specificity and impact on human disease. *Nutr Aging* 1:99–111.
- Salah El Dine R, Abdel Monem AR, El-Halawany AM, Hattori M, Abdel-Sattar E (2011) HCV-NS3/4A protease inhibitory iridoid glucosides and dimeric foliamenthic acid derivatives from *Anarrhinum orientale*. *J Nat Prod* 74:943–8.
- Saxena PK, (Eds.) Development of plant-based medicines: conservation, efficacy and safety. Kluwer Academic Publishers, Dordrecht, 2001, pp 69–95.
- Sayanova O, Napier JA, Shewry PR (1999)  $\Delta$ 6-Unsaturated fatty acids in species and tissues of the Primulaceae. *Phytochemistry* 52:419–422.
- Sayanova OV, Beaudoin F, Michaelson LV, Shewry PR, Napier JA (2003) Identification of *Primula* fatty acid  $\Delta$ 6-desaturases with n-3 substrate preferences. *Febs Letters* 542:100–104.
- Seixas de Melo J, Moura AP, Melo MJ (2004) Photophysical and spectroscopic studies of indigo derivatives in their keto and leuco forms. *J Phys Chem A* 108:6975–81.
- Sekikawa C, Kurihara H, Goto K, Takahashi K (2002) Inhibition of  $\beta$ -Glucuronidase by Extracts of *Chondria crassicaulis*. *Bull Fish Sci Hokkaido Univ* 53:27–30.
- Sharpe AN, Parrington LJ, Diotte MP, Peterkin PI (1989) Evaluation of indoxyl- $\beta$ -d-glucuronide and hydrophobic grid membrane filters for electronic enumeration of *Escherichia coli*. *Food Microbiol* 6:267–280.
- Shibano M, Lin AS, Itokawa H, Lee KH (2007) Separation and characterization of active flavonolignans of *Silybum marianum* by liquid chromatography connected with hybrid ion-trap and time-of-flight mass spectrometry (LC-MS/IT-TOF). *J Nat Prod* 70:1424–1428.
- Singh S, Farswan M, Ali S, Afzal M, Al-Abbasi FA, Kazmi I, Anwar F (2014) Antidiabetic potential of triterpenoid saponin isolated from *Primula denticulate*. *Pharma Biol* 52:750–755.
- Slichenmyer WJ, Von DH (1991) Taxol: a new and effective anti-cancer drug. *Anticancer Drugs* 2:519–30.
- Sneider W. (Eds.) Drug discovery: A history. John Wiley & Sons; 2005.
- Snyder DT, Szalwinski LJ, Wells JM, Cooks RG (2018) Logical MS/MS scans: a new set of operations for tandem mass spectrometry. *Analyst* 143:5438–5452.
- Spangenberg B, Poole CF, Weins C. The Stationary Phase in Thin-Layer Chromatography, In: Spangenberg B, Poole CF, Weins C (Eds.), *Quantitative Thin-Layer Chromatography A Practical Survey*, Springer, Heidelberg, 2011, pp. 53–80.
- Stevenson PC, Nicolson SW, Wright GA (2017) Plant–pollinator interactions from flower to landscape: Plant secondary metabolites in nectar: impacts on pollinators and ecological functions. *Funct Ecol* 31:65–75.
- Stobiecki M, Staszko A, Piasecka A, Garcia-Lopez PM, Zamora-Natera F, Kachlicki P (2010) LC-MSMS profiling of flavonoid conjugates in wild Mexican lupine, *Lupinus reflexus*. *J Nat Prod* 7:1254–1260.
- Strauch MA, de Mendoza D, Hoch JA (1992) cis-Unsaturated fatty acids specifically inhibit a signal-transducing protein kinase required for initiation of sporulation in *Bacillus subtilis*. *Mol Microbiol* 6:2909–17.

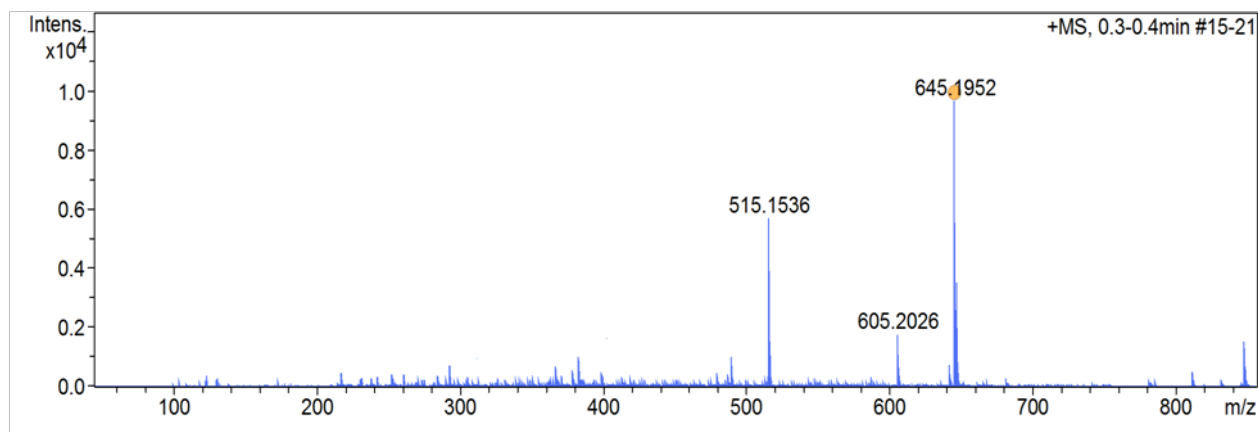
- Stylos E, Chatziathanasiadou MV, Syriopoulou A, Tzakos AG (2017) Liquid chromatography coupled with tandem mass spectrometry (LC–MS/MS) based bioavailability determination of the major classes of phytochemicals. *J Chromatogr B* 1047:15–38.
- Taha MN, Krawinkel MB, Morlock GE (2015) High-performance thin-layer chromatography linked with (bio)assays and mass spectrometry—A suited method for discovery and quantification of bioactive components? Exemplarily shown for turmeric and milk thistle extracts. *J Chromatogr A* 1394:137–147.
- Takshak S, Agrawal SB (2019) Defense potential of secondary metabolites in medicinal plants under UV-B stress. *J Photochem Photobiol B, Biol* 193:51–88.
- Taskova R, Evstatieva L, Handjieva N, Popov S (2002) Iridoid patterns of genus *Plantago* L. and their systematic significance. *Z Naturforsch C* 57:42–50.
- Taskova RM, Kokubun T, Ryan KG, Garnock-Jones PJ, Jensen SR (2010) Phenylethanoid and iridoid glycosides in the New Zealand snow hebes (*Veronica*, Plantaginaceae). *Chem Pharm Bull* 58:703–11.
- Thirugnanasambantham P, Viswanathan S, Mythirayee C, Krishnamurthy V, Ramachandran S, Kameswaran L (1990) Analgesic activity of certain flavone derivatives: a structure-activity study. *J Ethnopharmacol* 28:207–214.
- Tokalov SV, Kind B, Wollenweber E, Gutzeit HO (2004) Biological effects of epicuticular flavonoids from *Primula denticulata* on human leukemia cells. *J Agric Food Chem* 52:239–245.
- Tsimogiannis D, Oreopoulou V, Classification of phenolic compounds in plants; In: Watson (Eds.), polyphenols in plants (2nd edition) isolation, purification and extract preparation. Elsevier, 2019, pp. 263–284.
- Tsydendambaev VD, Christie WW, Brechany EY (2004) Vereshchagin AG. Identification of unusual fatty acids of four alpine plant species from the Pamirs. *Phytochemistry* 65:2695–703.
- Tundis R, Loizzo MR, Menichini F, Statti GA, Menichini F (2008) Biological and pharmacological activities of iridoids: recent developments. *Mini Rev Med Chem* 8:399–420.
- Tyler VE (1999) Phytomedicines: Back to the future. *J Nat Prod* 62:1589–1592.
- Upchurch RG (2008) Fatty acid unsaturation, mobilization, and regulation in the response of plants to stress. *Biotechnol Lett* 30:967–977.
- Uriarte-Pueyo I, I Calvo M (2011) Flavonoids as acetylcholinesterase inhibitors. *Curr Med Chem* 18:5289–5302.
- Veeresham C (2012) Natural products derived from plants as a source of drugs. *J Adv Pharm Technol Res* 3: 200–201.
- Verma N, Shukla S (2015) Impact of various factors responsible for fluctuation in plant secondary metabolites. *J Appl Res Med Aromat Plants* 2:105–113.
- Waksmundzka-Hajnos M, Sherma J (2010) High performance liquid chromatography in phytochemical analysis. CRC press.
- Wallace BD, Wang H, Lane KT, Scott JE, Orans J, Koo JS, Venkatesh M, Jobin C, Yeh LA, Mani S, Redinbo MR (2010) Alleviating cancer drug toxicity by inhibiting a bacterial enzyme. *Science* 330:831–835.
- Weng ZM, Wang P, Ge GB, Dai ZR, Wu DC, Zou LW, Dou TY, Zhang TY, Yang L, Hou J (2017) Structure-activity relationships of flavonoids as natural inhibitors against *E. coli*  $\beta$ -glucuronidase. *Food Chem Toxicol* 109:975–983.
- Willis LM, Shukitt-Hale B, Joseph JA (2009) Dietary polyunsaturated fatty acids improve cholinergic transmission in the aged brain. *Genes Nutr* 4:309.

- Wilm M (2011) Principles of electrospray ionization. *Mol Cell Proteomics* 10:M111–009407.
- Wink M (2018) Plant secondary metabolites modulate insect behavior-steps toward addiction?. *Front Physiol* 9:364.
- Wolfender JL, Queiroz EF, Hostettmann K (2006) The importance of hyphenated techniques in the discovery of new lead compounds from nature. *Expert Opin Drug Discov* 1:237–260.
- Wollenweber E, Mann K, Inuma M, Tanaka T, Mizuno M (1988) 8, 2'-Dihydroxyflavone from *Primula pulverulenta*. *Phytochemistry* 27:1483–6.
- Wszelaki N, Kuciun A, Kiss A (2010) Screening of traditional European herbal medicines for acetylcholinesterase and butyrylcholinesterase inhibitory activity. *Acta Pharm* 60:119–128.
- Wu J, Stewart JR, Sobsey MD, Cormency C, Fisher MB, Bartram JK (2018) Rapid detection of *Escherichia coli* in water using sample concentration and optimized enzymatic hydrolysis of chromogenic substrates. *Curr Microbiol* 1:1–8.
- Wu T, He M, Zang X, Zhou Y, Qiu T, Pan S, Xu X (2013) A structure–activity relationship study of flavonoids as inhibitors of *E. coli* by membrane interaction effect. *Biochim Biophys Acta Biomembr* 1828:2751–2756.
- Xiao ZP, Peng ZY, Peng MJ, Yan WB, Ouyang YZ, Zhu HL (2011) Flavonoids health benefits and their molecular mechanism. *Mini Rev Med Chem* 11:169–77.
- Xie Y, Yang W, Chen X, Xiao J (2014) Inhibition of flavonoids on acetylcholine esterase: binding and structure–activity relationship. *Food Funct* 5:2582–2589.
- Xu HX, Lee SF (2001) Activity of plant flavonoids against antibiotic-resistant bacteria. *Phytother Res* 15:39–43.
- Yang M, Sun J, Lu Z, Chen G, Guan S, Liu X, Jiang B, Ye M, Guo DA (2009) Phytochemical analysis of traditional Chinese medicine using liquid chromatography coupled with mass spectrometry. *J Chromatogr A* 1216:2045–2062.
- Yao LH, Jiang YM, Shi J, Tomás-Barberán FA, Datta N, Singanusong R, Chen SS (2004) Flavonoids in food and their health benefits. *Plant Foods Hum Nutr* 59:113–22.
- Zaghloul MS, Moustafa AA, Mauricio R, Mansour HMH (2016) Evolution and conservation of Sinai's primrose (*Primula boveana*): an endangered pre-glacial relict species growing on Sinai Mountain, Egypt. *Biogent J* 4:56–72.
- Zaynab M, Fatima M, Abbas S, Sharif Y, Umair M, Zafar MH, Bahadar K (2018) Role of secondary metabolites in plant defense against pathogens. *Microb Pathog* 124:198–2020
- Zhang X, Jin C, Li Y, Guan S, Han F, Zhang S (2013) Catalpol improves cholinergic function and reduces inflammatory cytokines in the senescent mice induced by D-galactose. *Food Chem Toxicol* 58:50–55.
- Zheng CJ, Yoo JS, Lee TG, Cho HY, Kim YH, Kim WG (2005) Fatty acid synthesis is a target for antibacterial activity of unsaturated fatty acids. *FEBS Lett* 579:5157–5162.

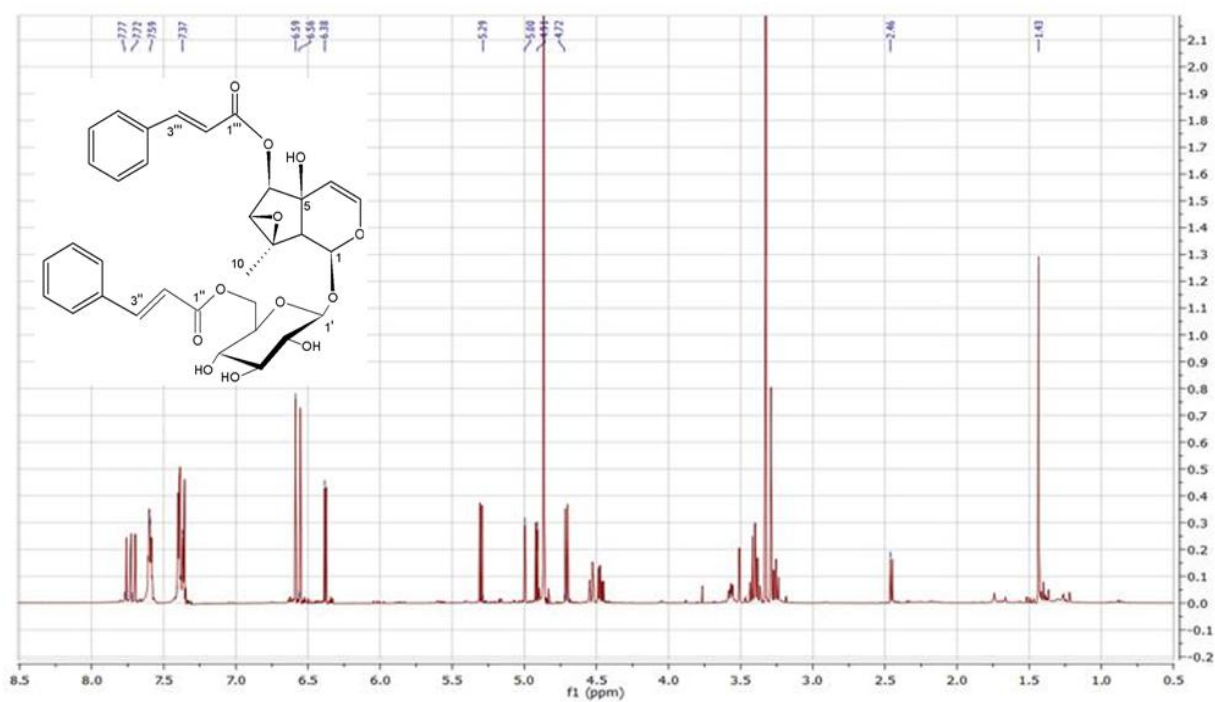
# Appendix



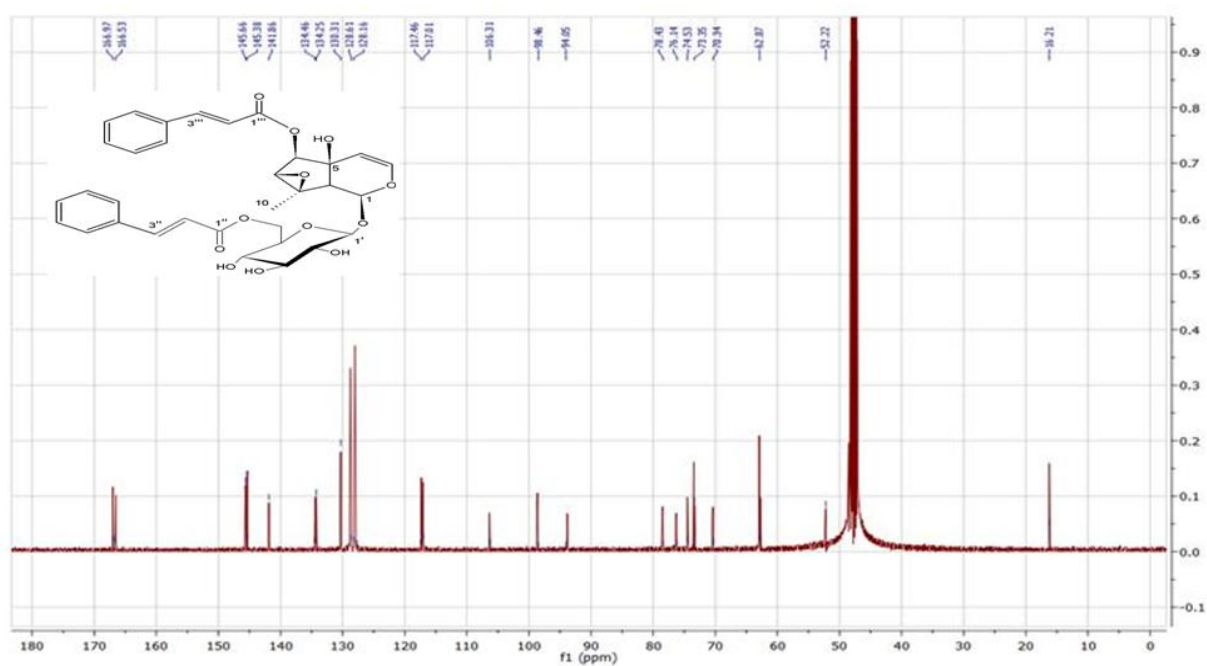
**Appendix 1.** Standard calibration curve of AChE inhibitory activity of Riv



**Appendix 2.** HRESIMS spectrum of compound A1

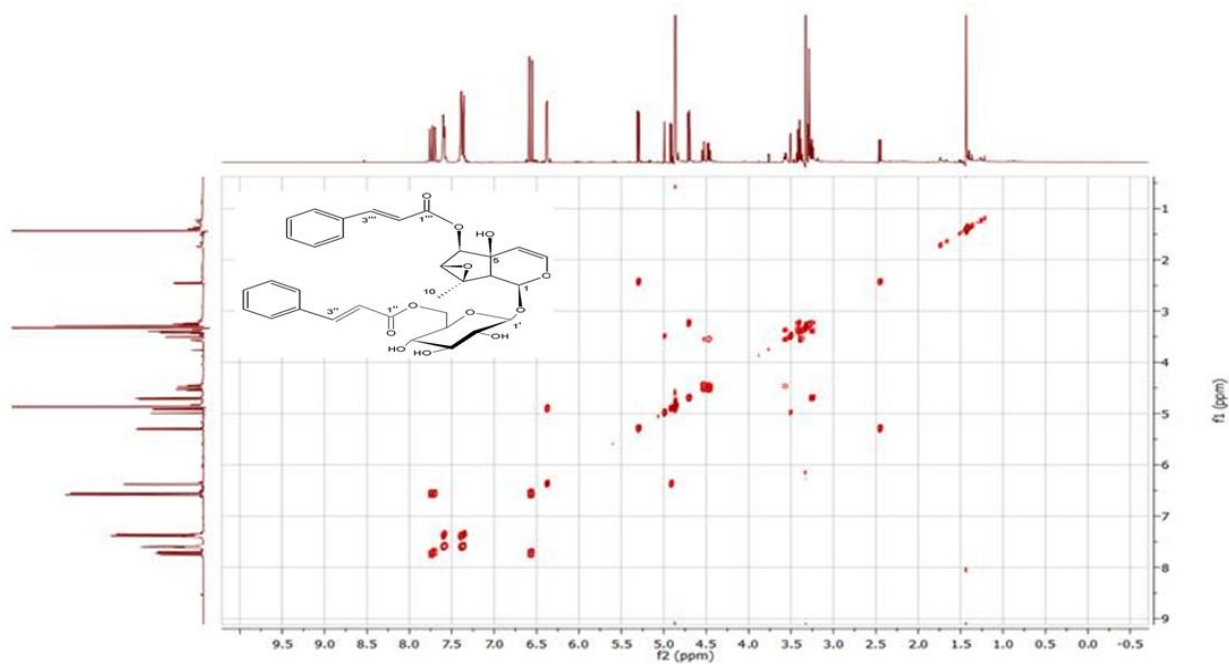


Appendix 3.  $^1\text{H}$  NMR spectrum (500 MHz) of compound A1 (in  $\text{CD}_3\text{OD}$ )

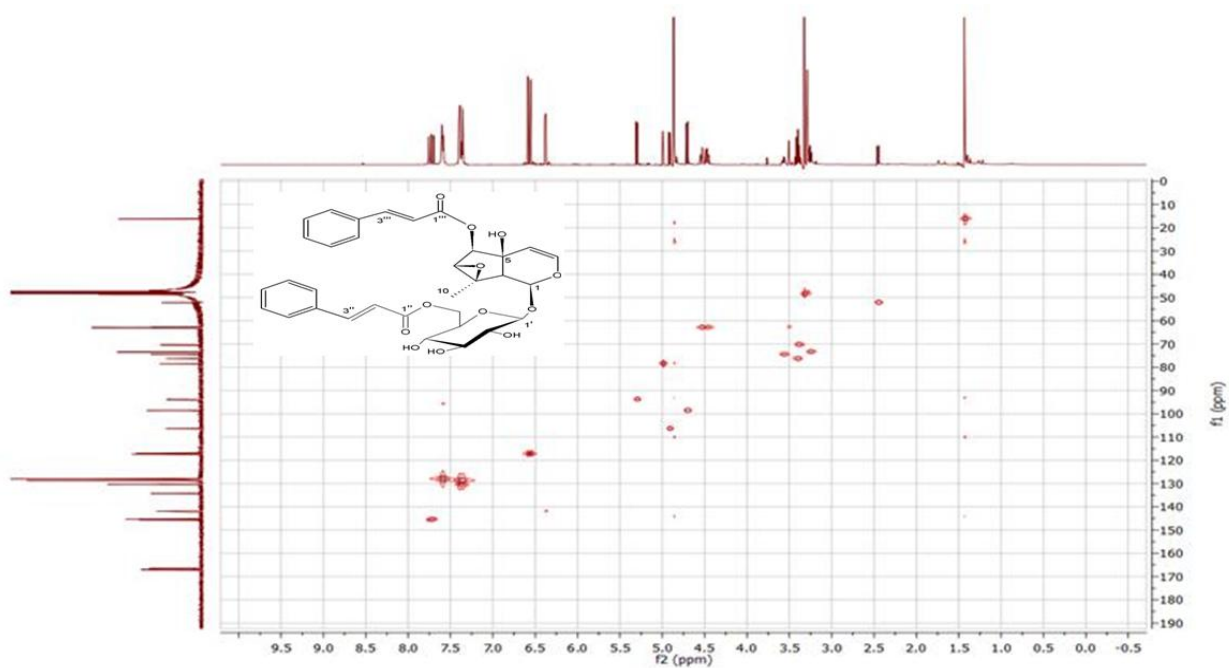


Appendix 4.  $^{13}\text{C}$  NMR (125 MHz) spectrum of compound A1 (in  $\text{CD}_3\text{OD}$ )

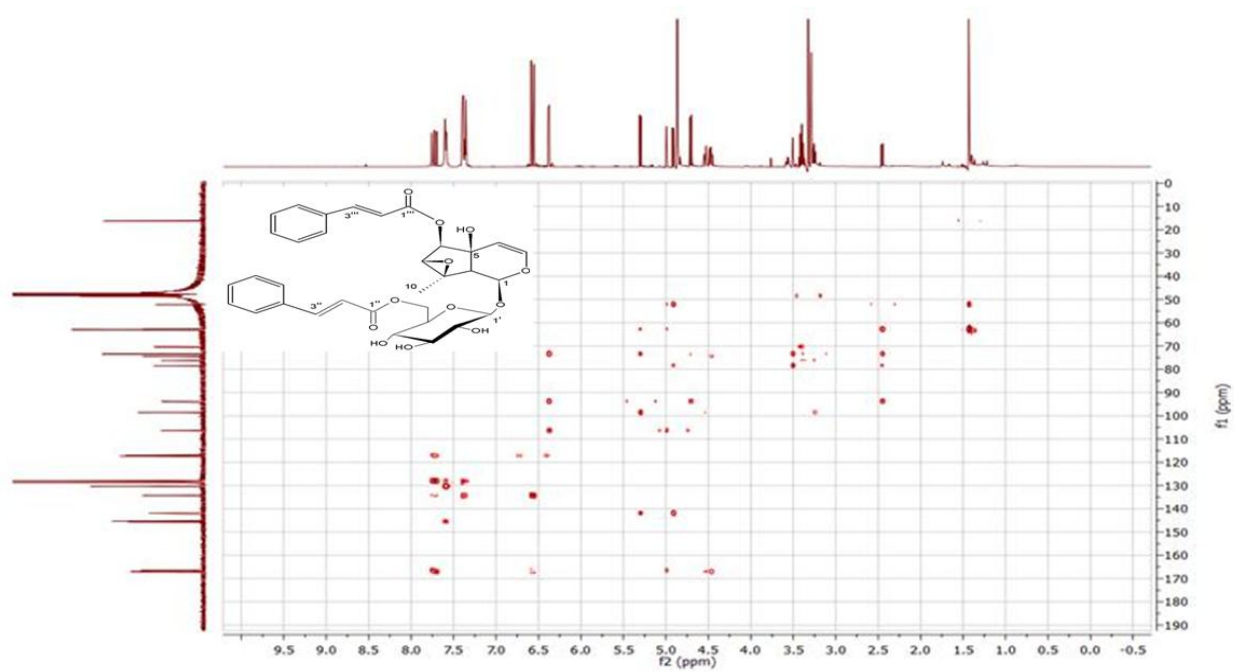




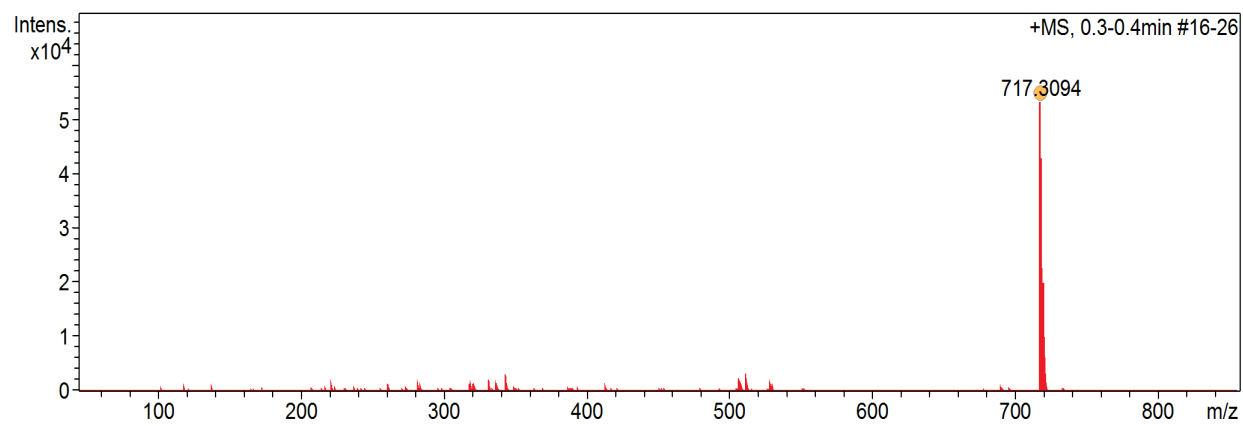
Appendix 5.  $^1\text{H}$ - $^1\text{H}$  COSY spectrum of compound A1



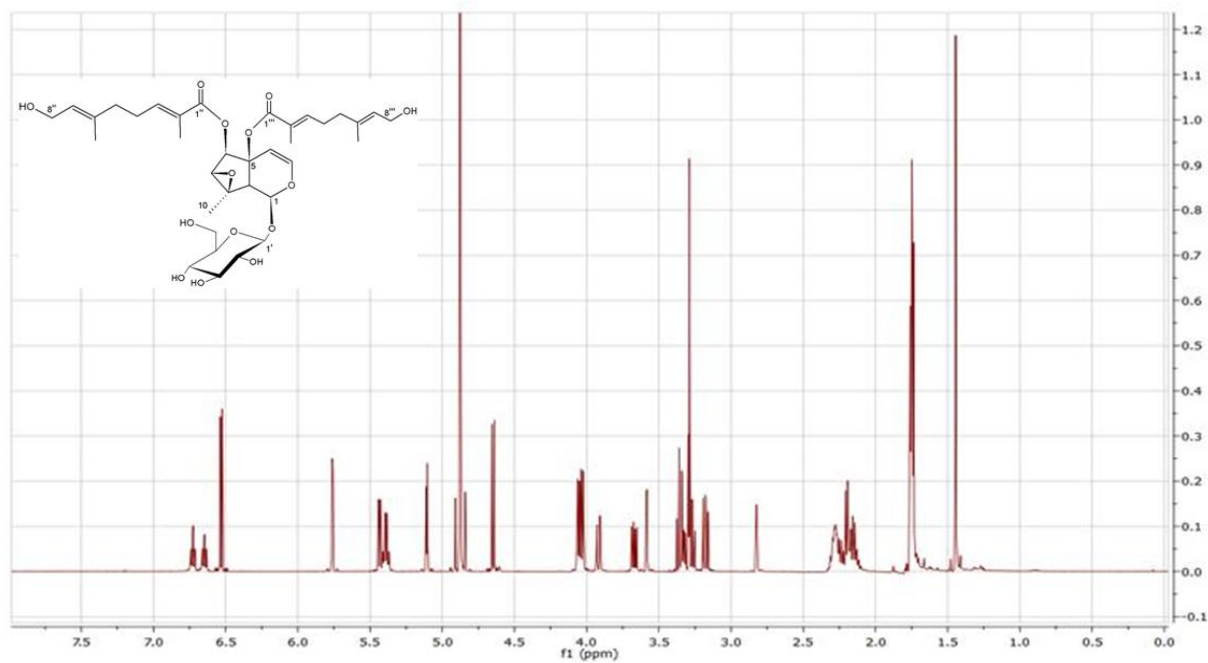
Appendix 6. HSQC spectrum of compound A1



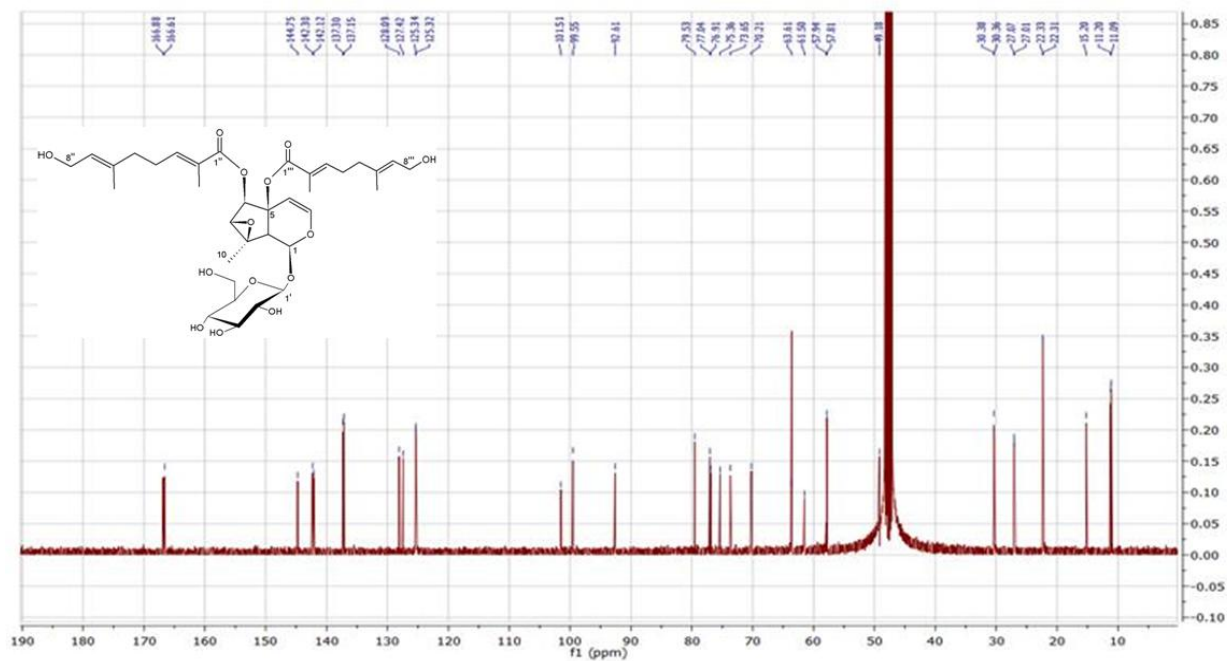
**Appendix 7.** HMBC spectrum of compound **A1**



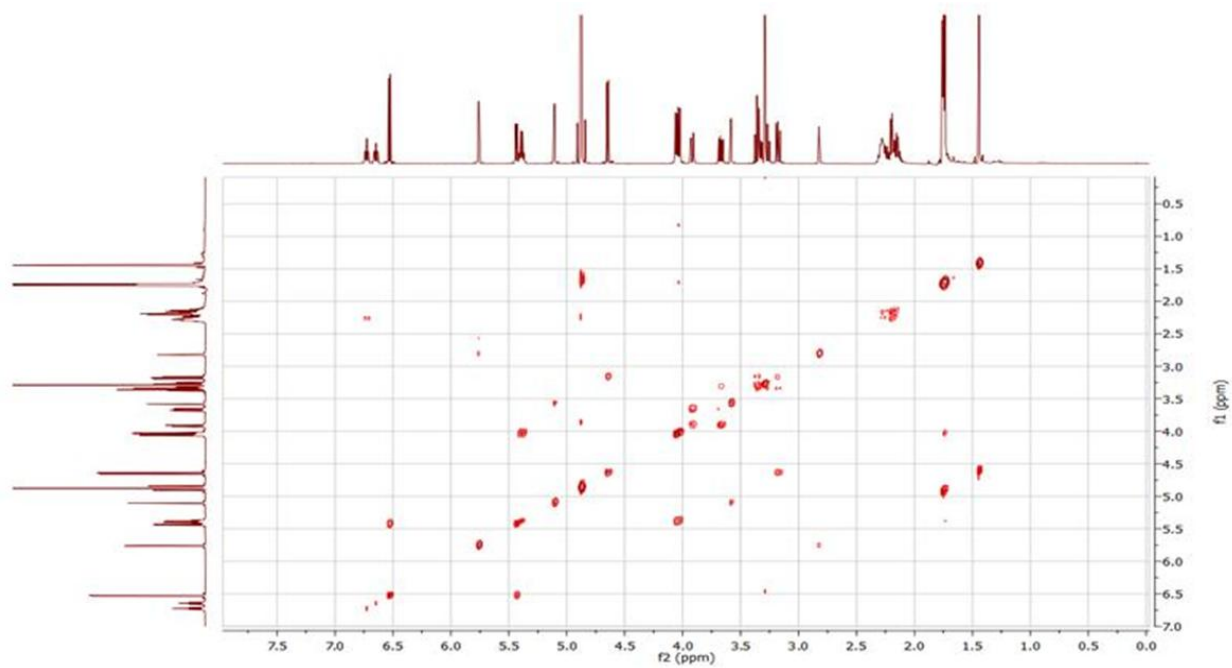
**Appendix 8.** HRESIMS spectrum of compound **A3**



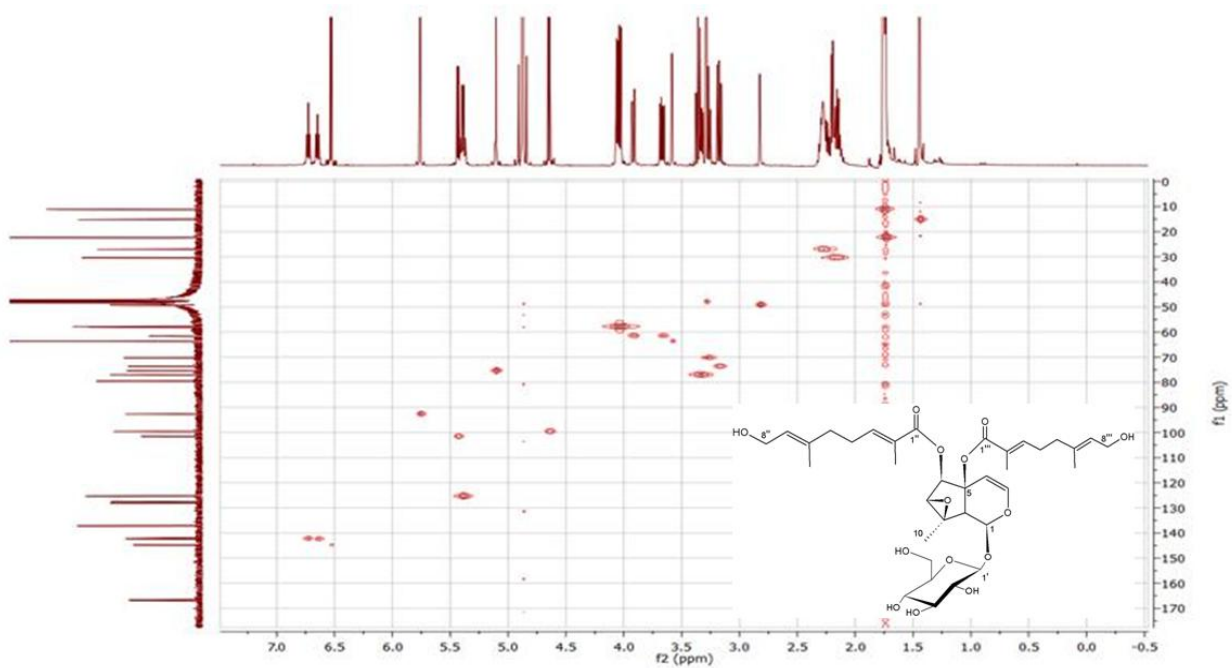
**Appendix 9.**  $^1\text{H}$  NMR spectrum (500 MHz) of compound 3 (in  $\text{CD}_3\text{OD}$ )



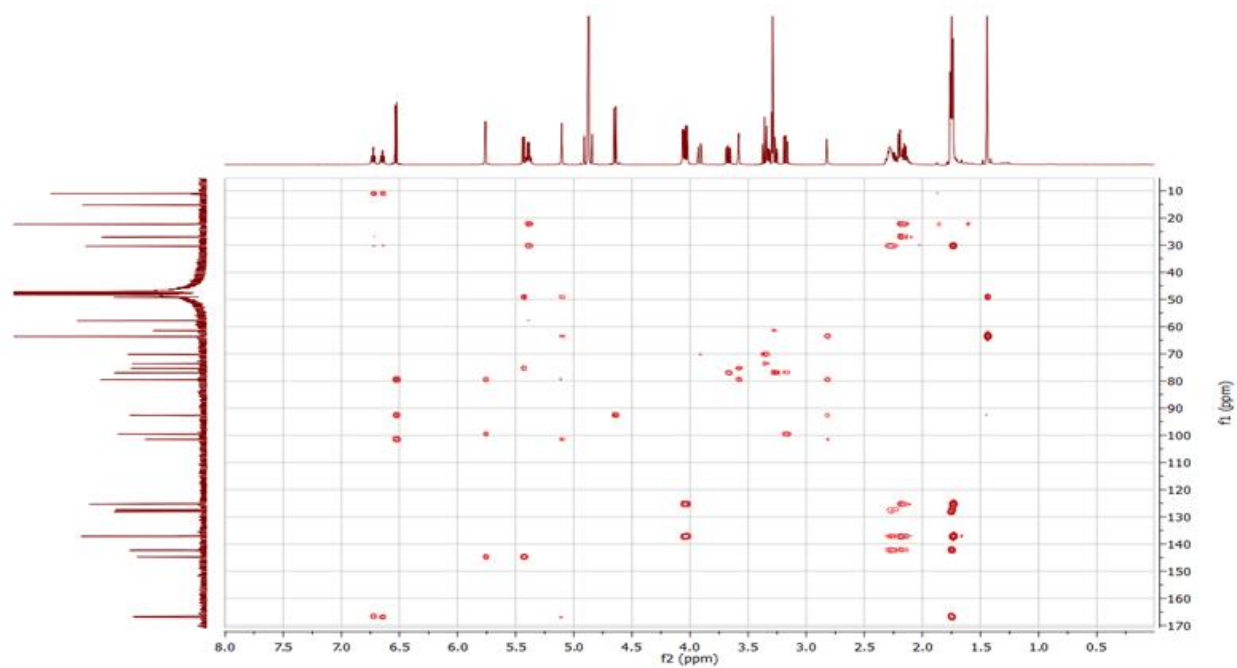
**Appendix 10.**  $^{13}\text{C}$  NMR (125 MHz) spectrum of compound A3 (in  $\text{CD}_3\text{OD}$ )



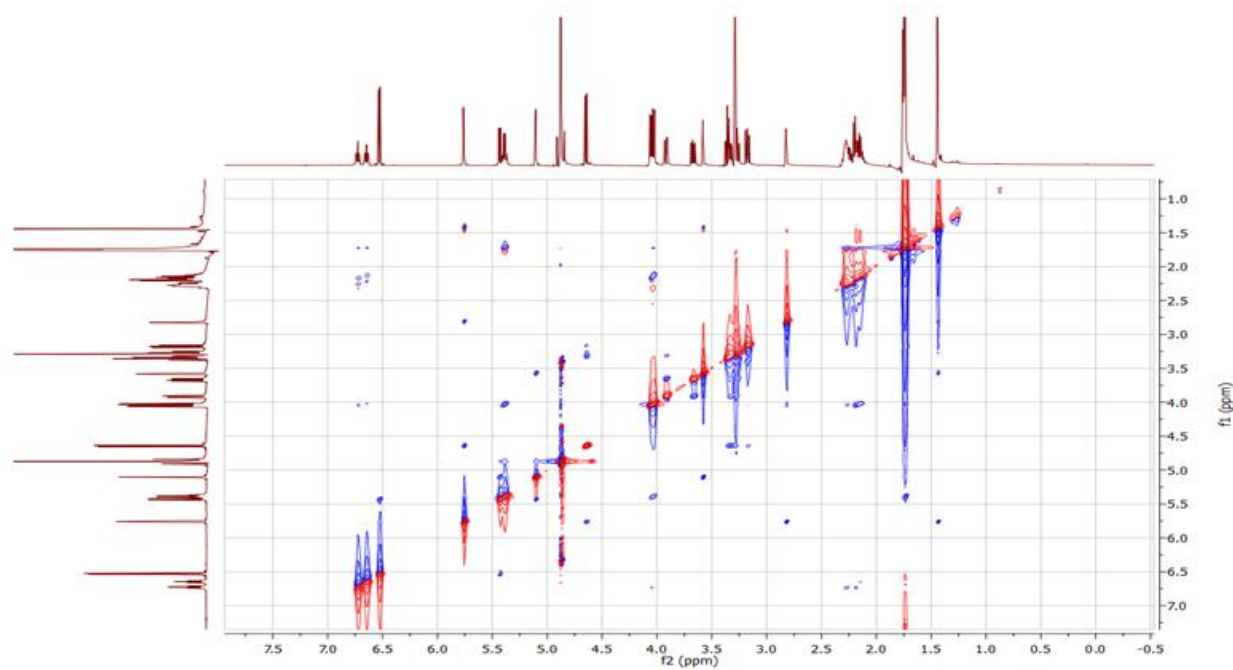
Appendix 11.  $^1\text{H}$ - $^1\text{H}$  COSY spectrum of compound A3



Appendix 12. HSQC spectrum of compound A3



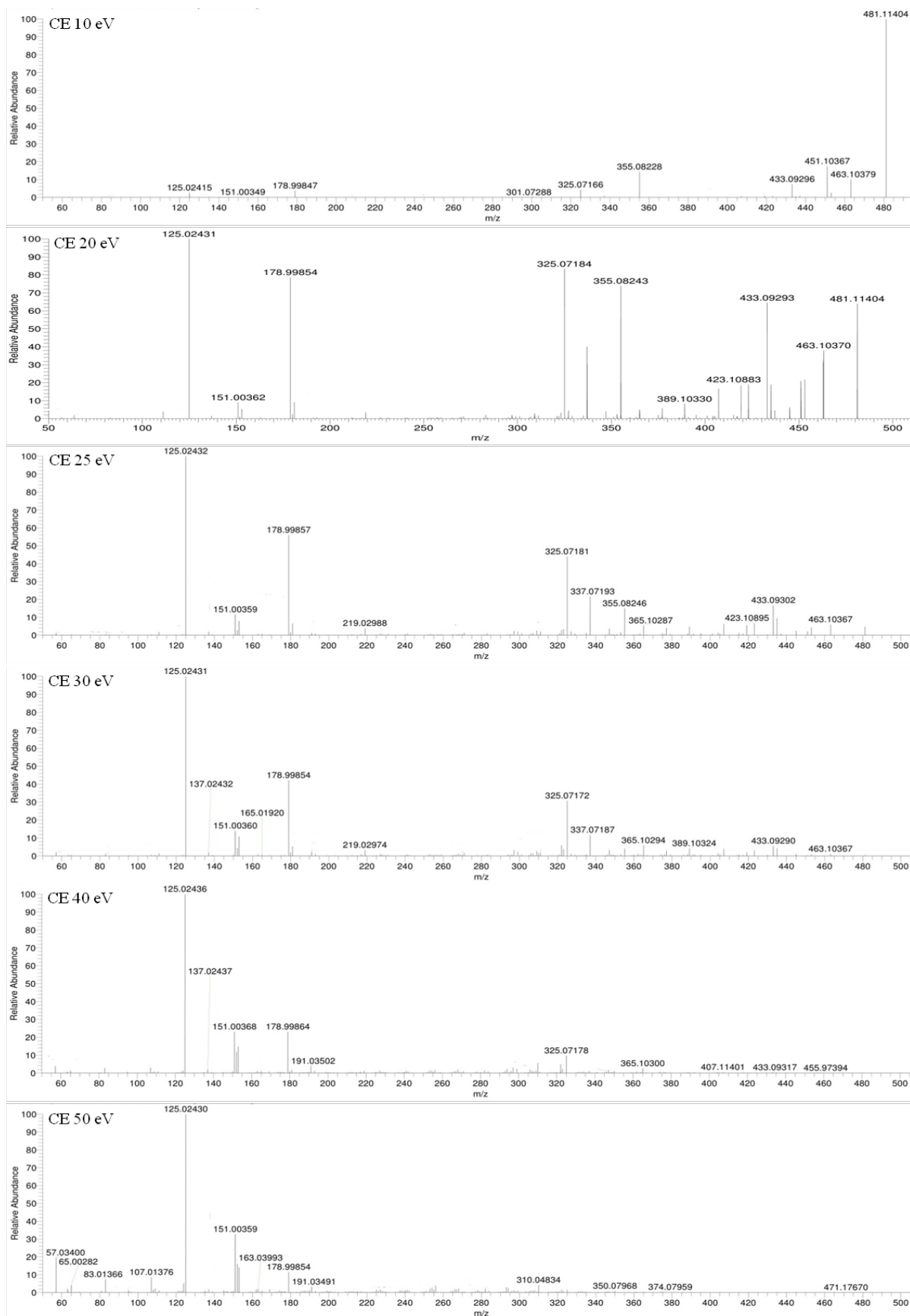
**Appendix 13.** HMBC spectrum of compound A3



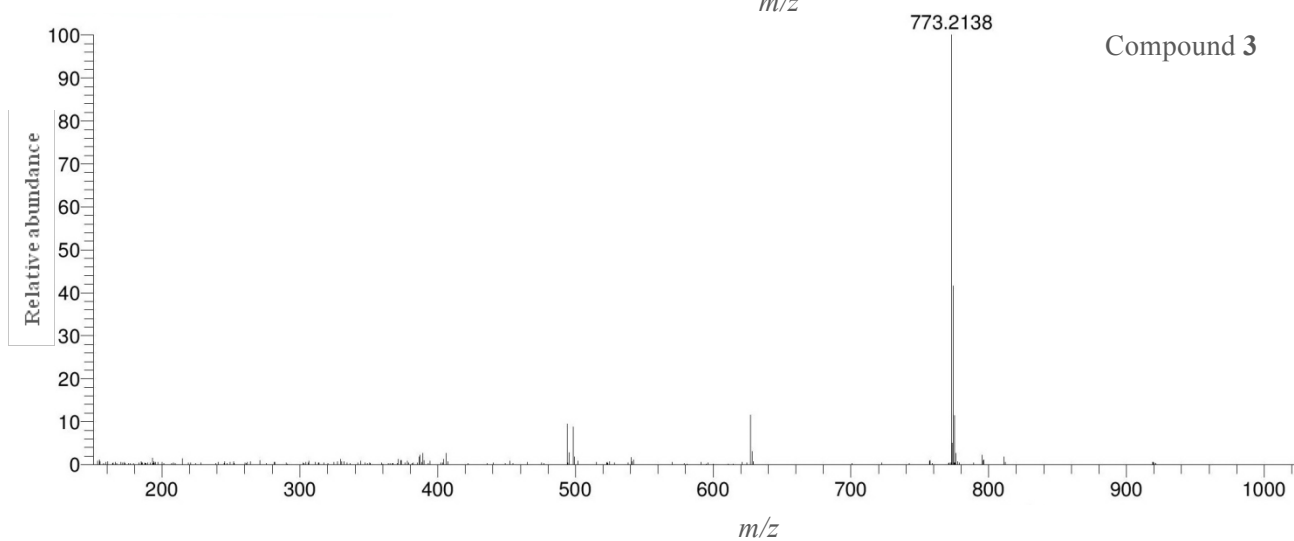
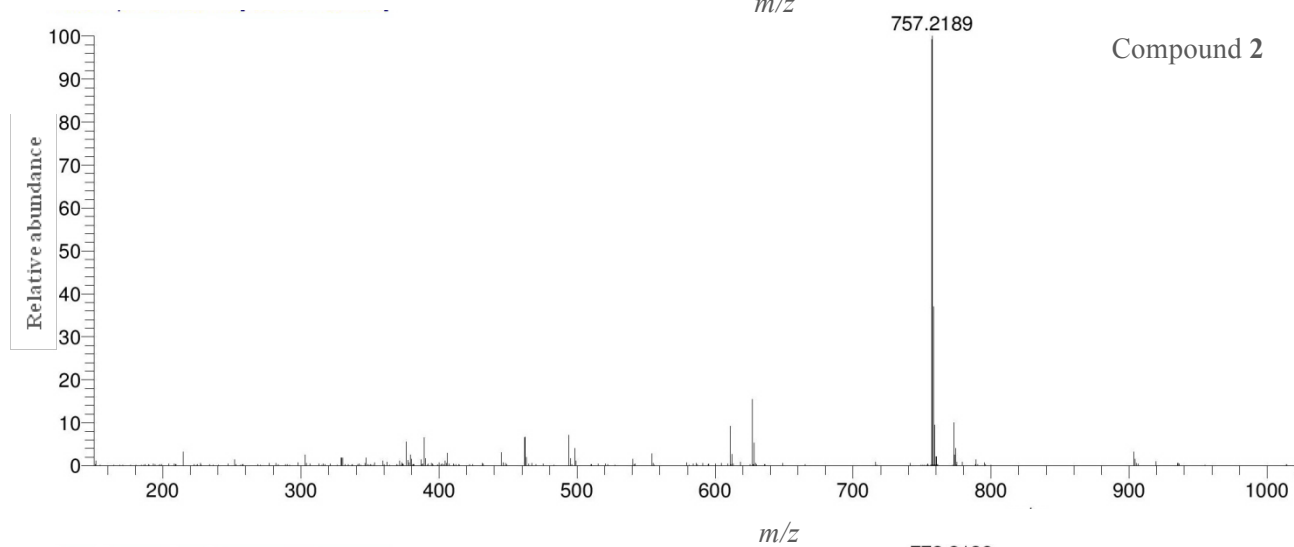
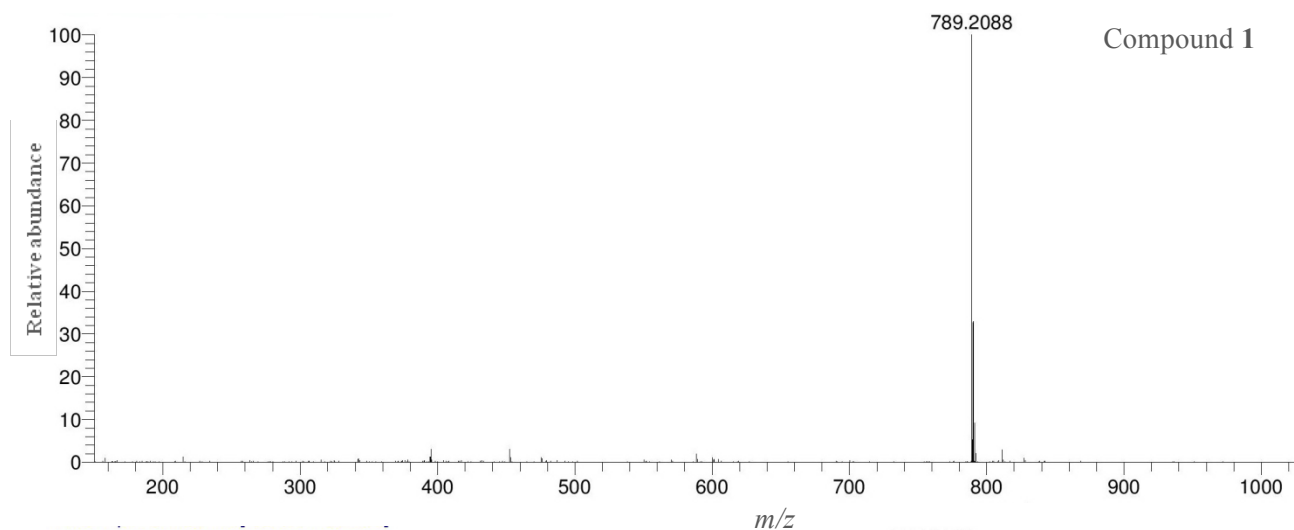
**Appendix 14.** NOESY spectrum of compound A3



**Appendix 15.** Specificity study of GUS inhibition assay using 2-naphthyl- $\beta$ -D-glucopyranoside as a substrate.

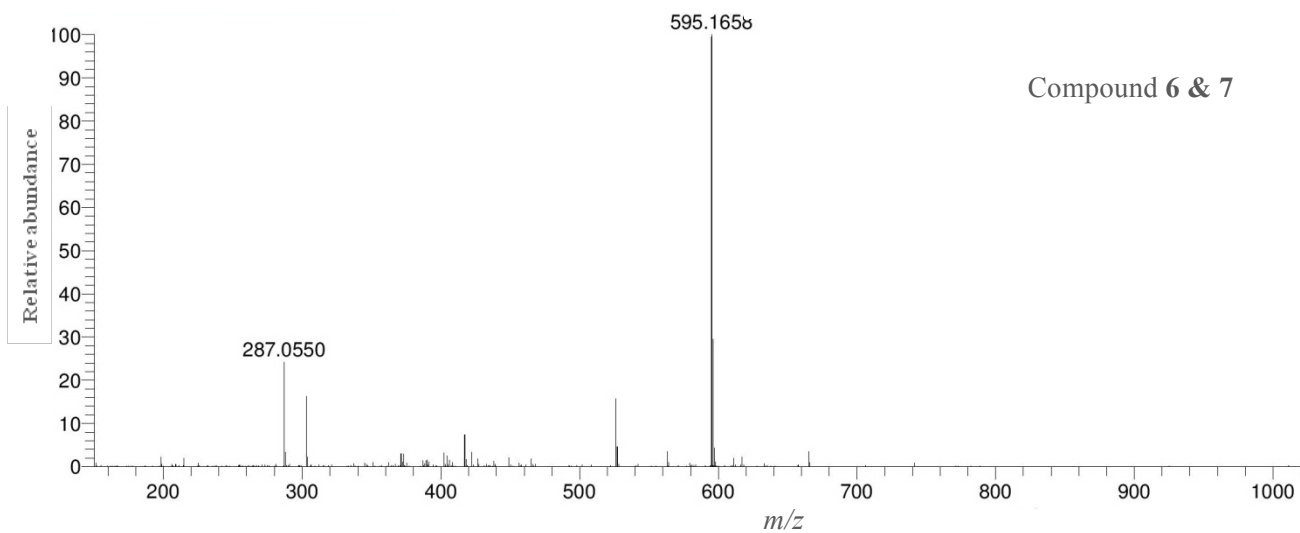
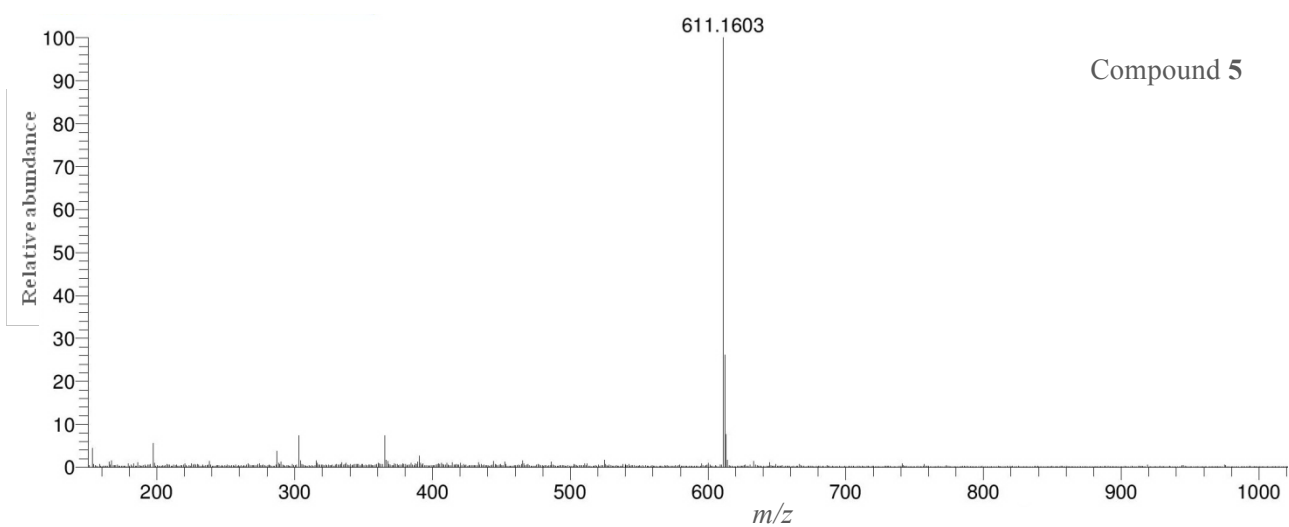
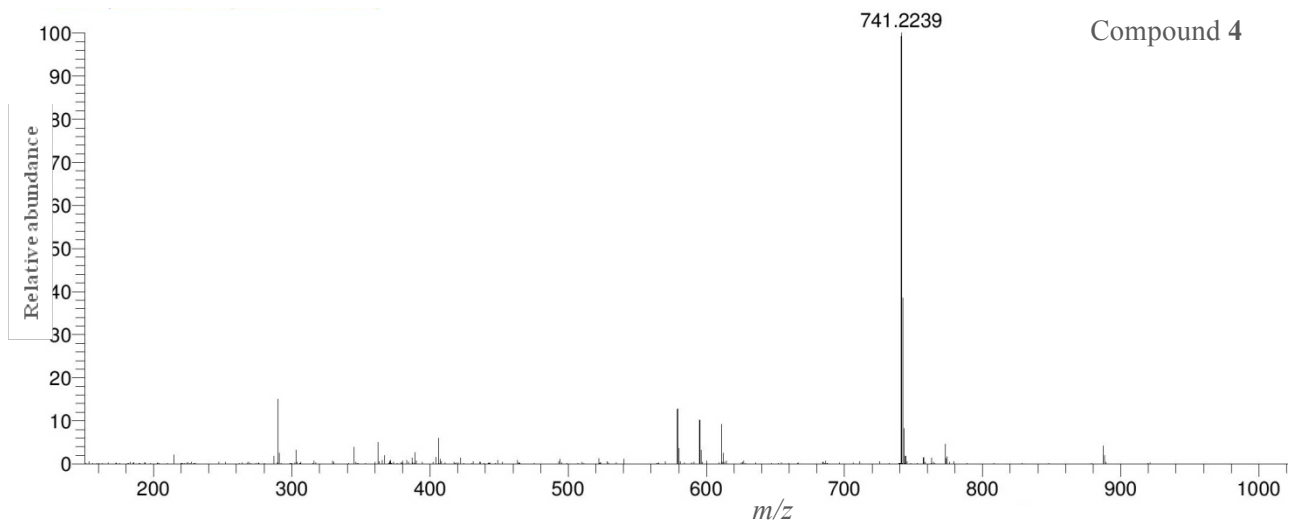


Appendix 16. HRMS<sup>2</sup> spectra of SFLG1 collected at different CE.

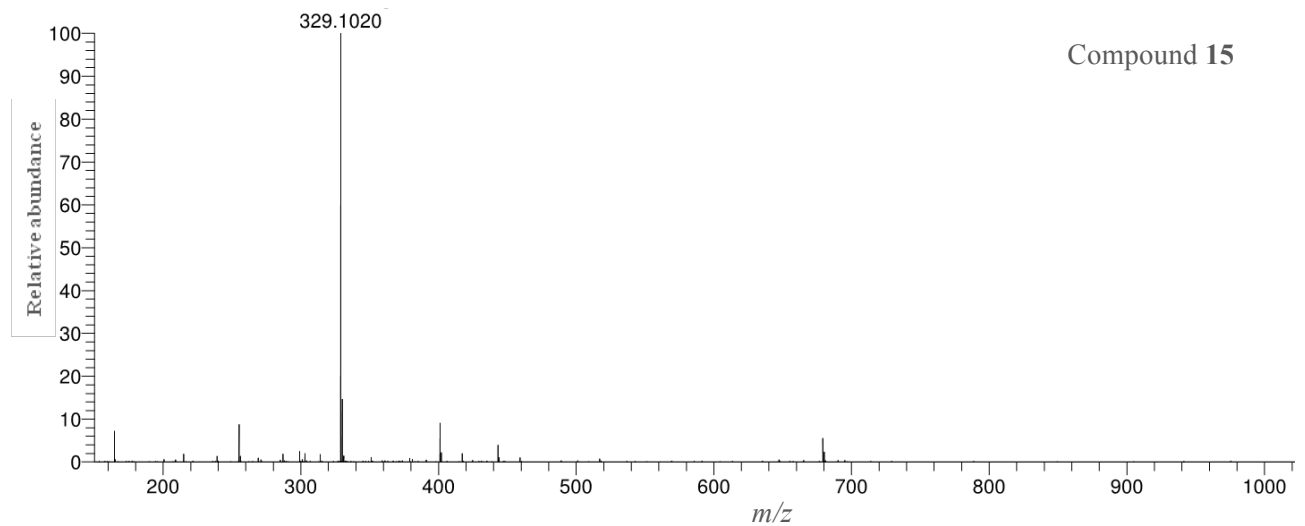
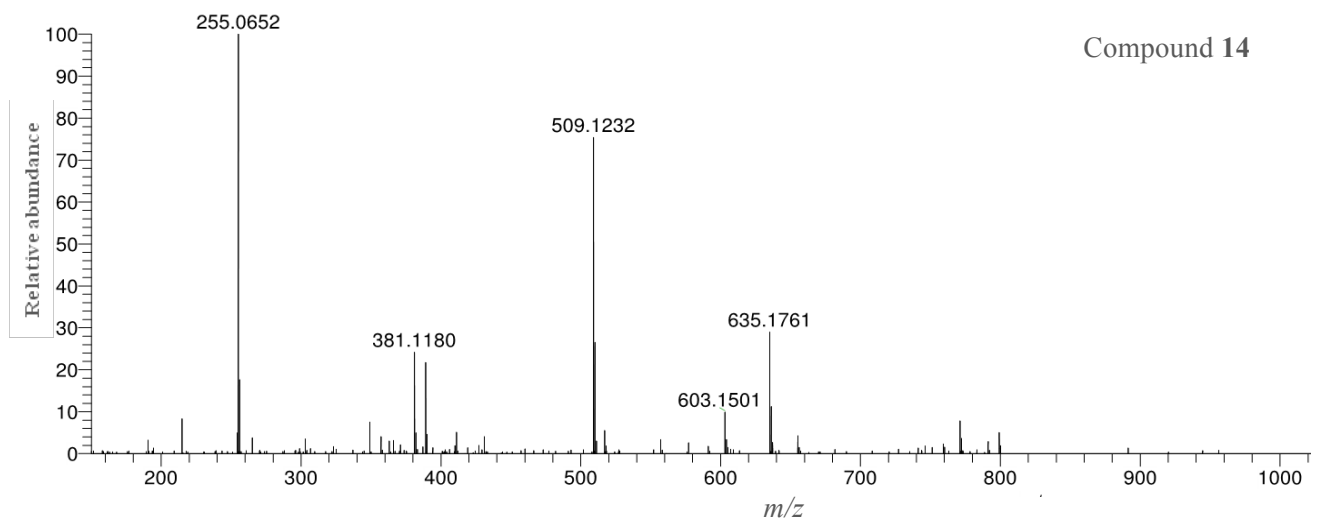
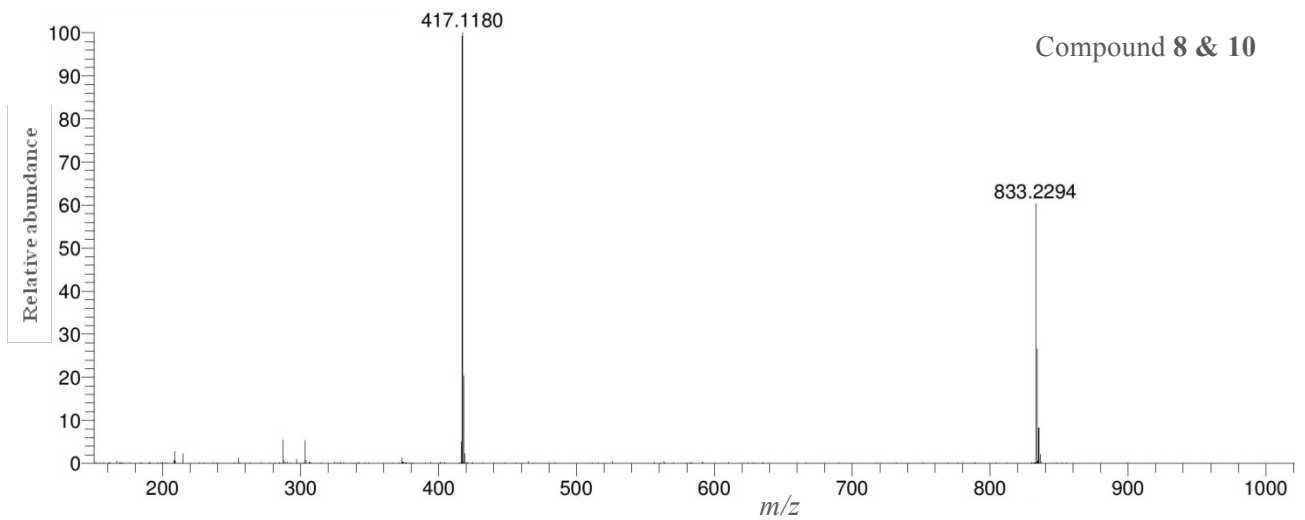


**Appendix 17.** ESIHRMS spectra for the flavonoids identified in hydro-alcoholic extract of *P. boveana*.

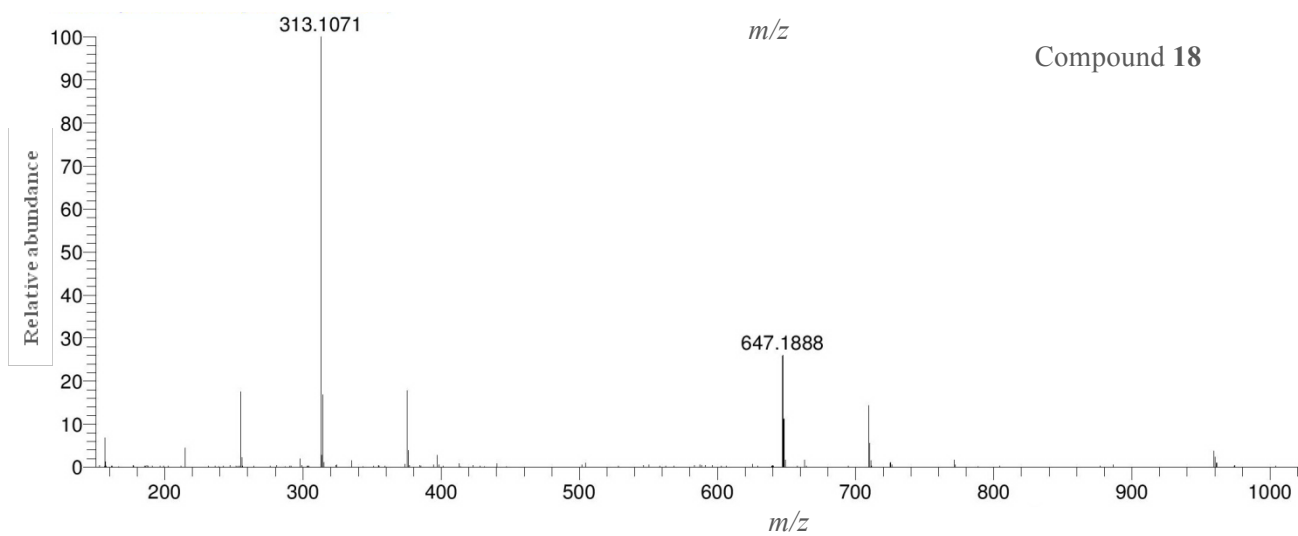
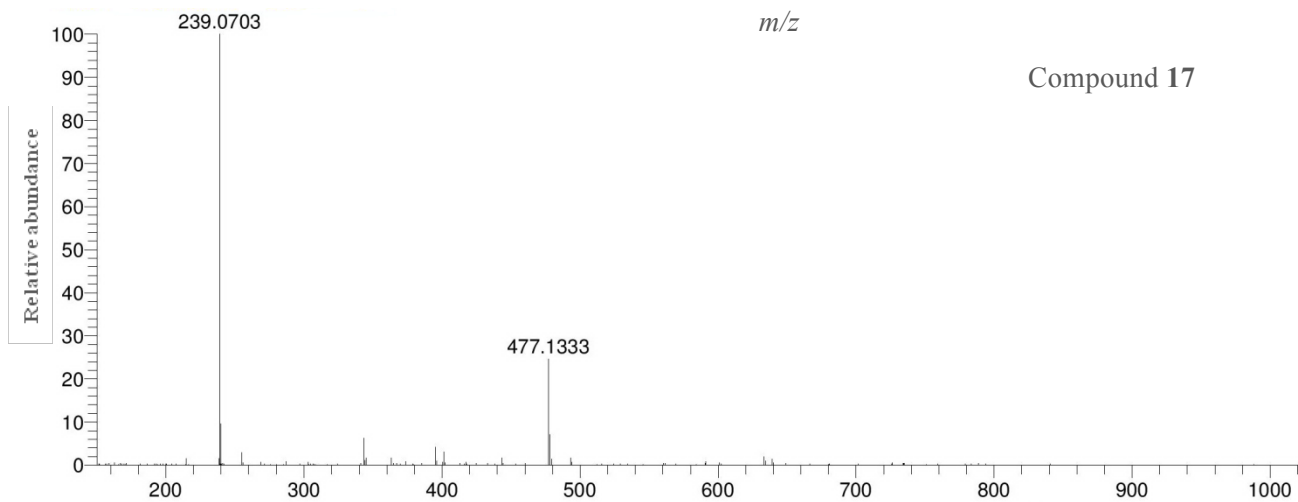
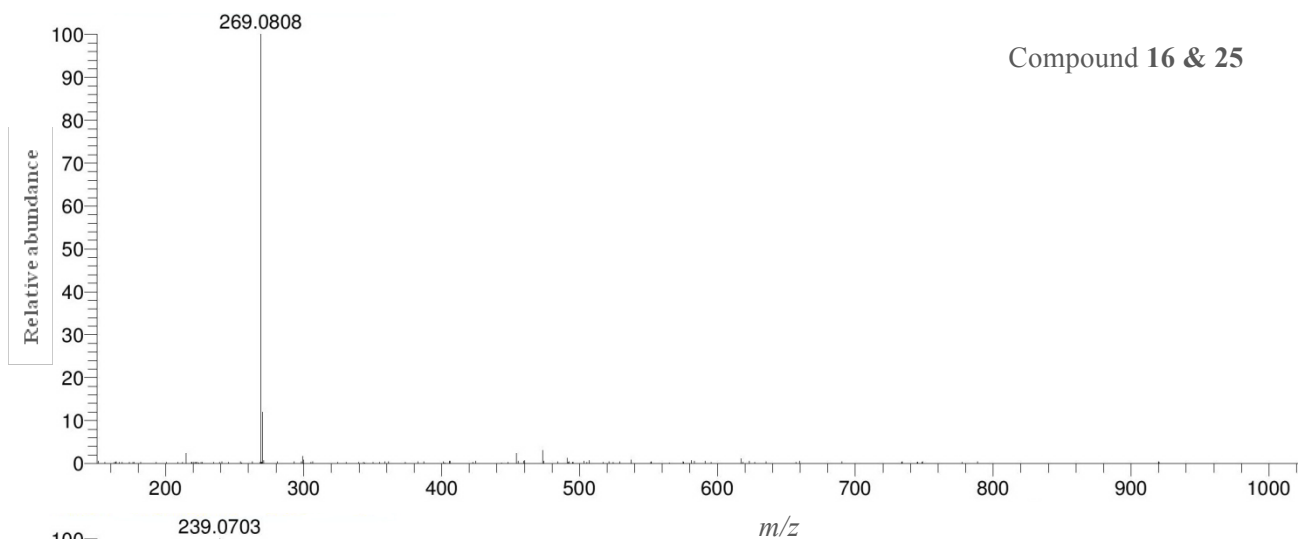




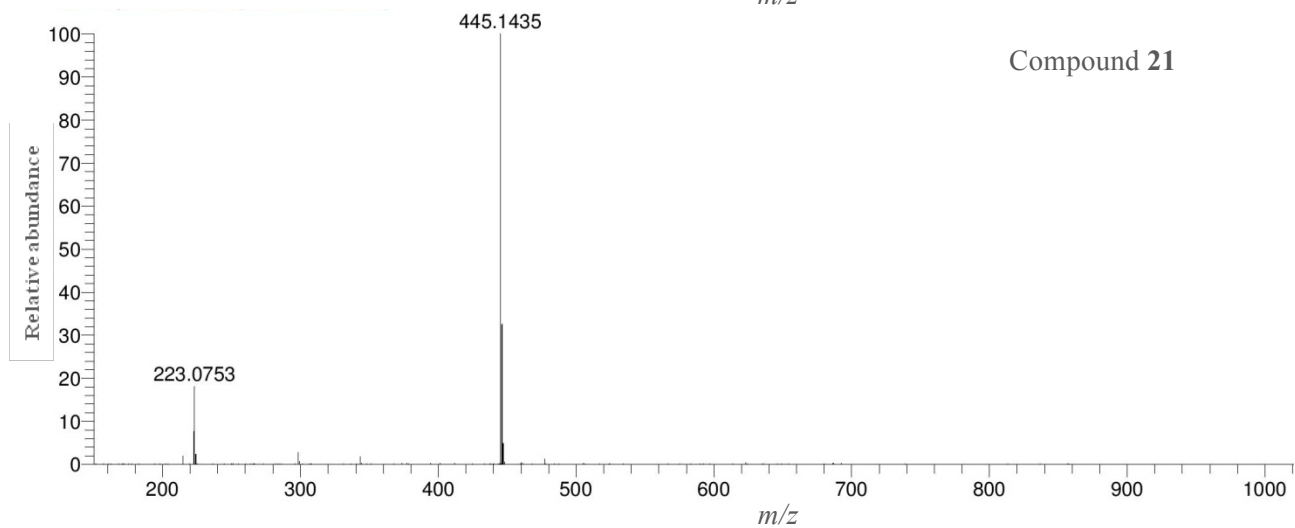
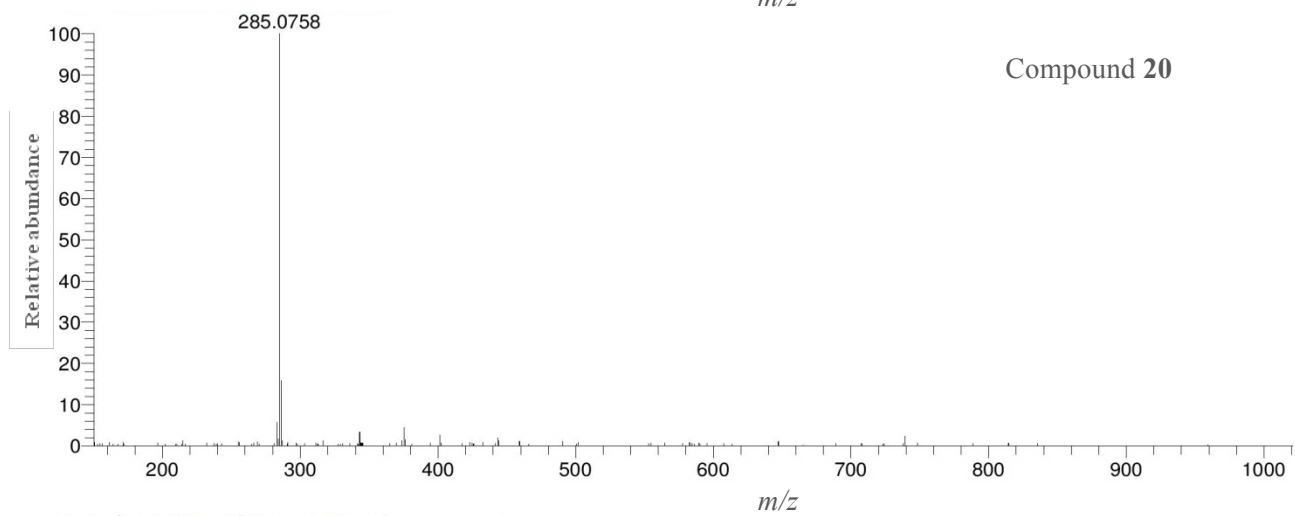
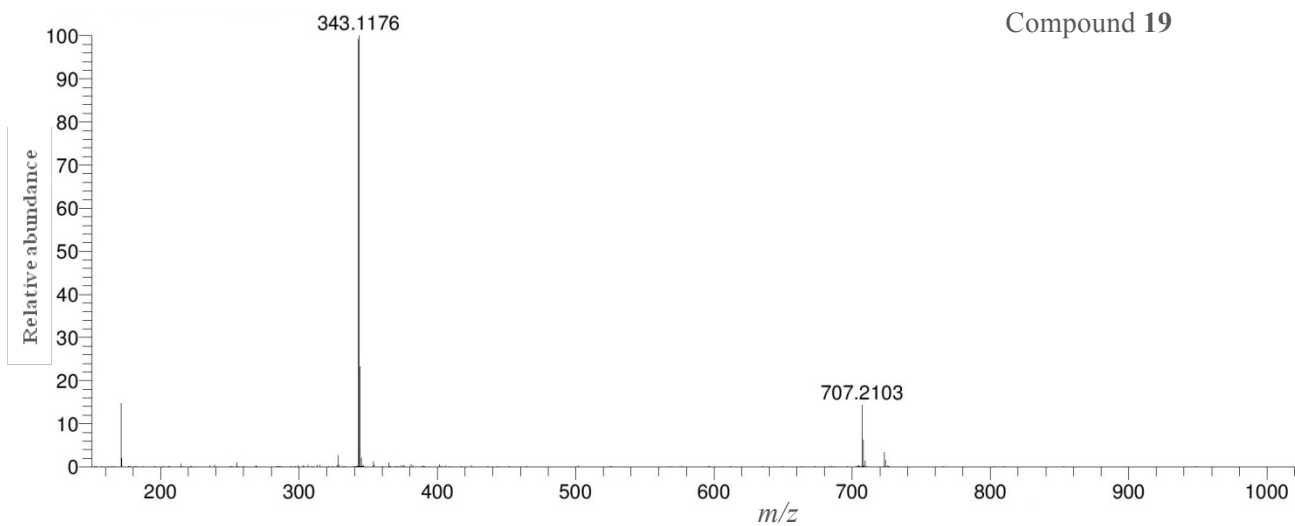
**Appendix 17.** (Continued) ESIHRMS spectra for the flavonoids identified in hydro-alcoholic extract of *P. boveana*.



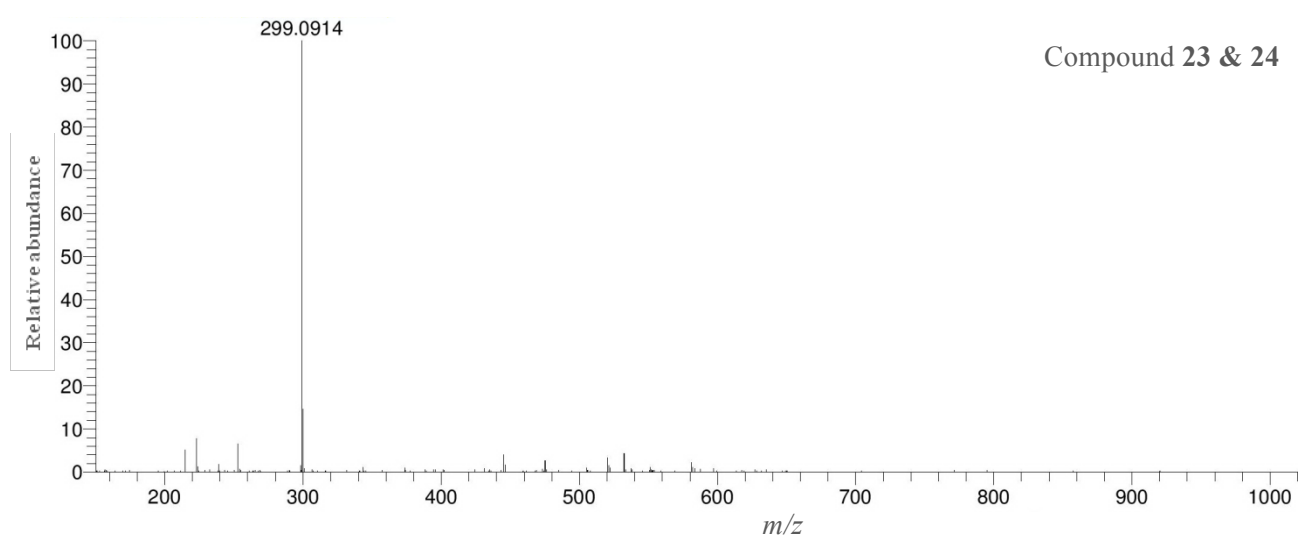
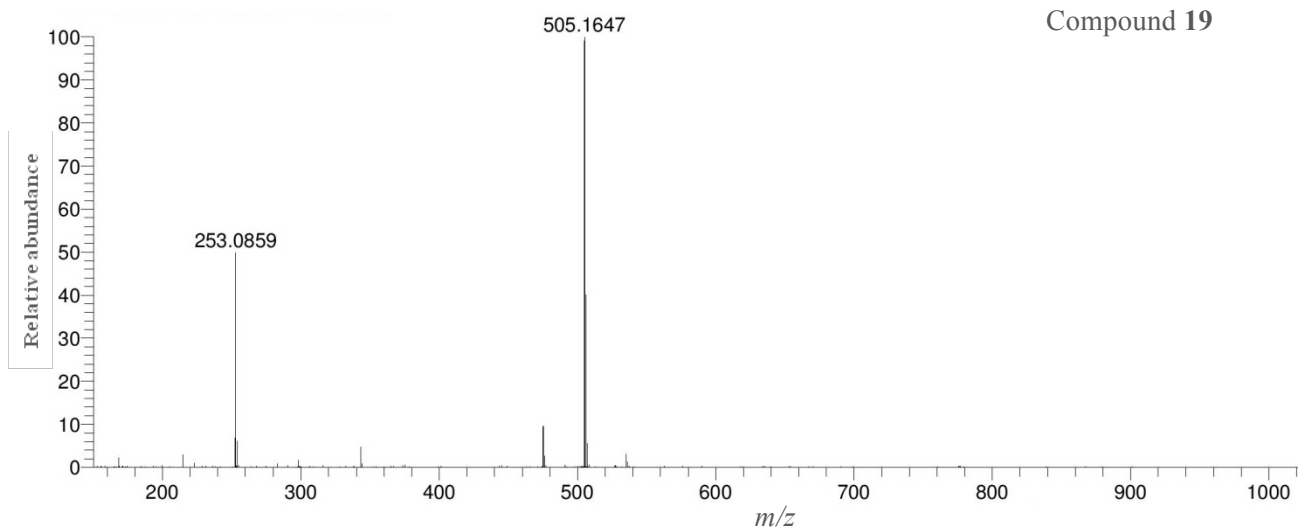
**Appendix 17.** (Continued) ESIHRMS spectra for the flavonoids identified in hydro-alcoholic extract of *P. boveana*.



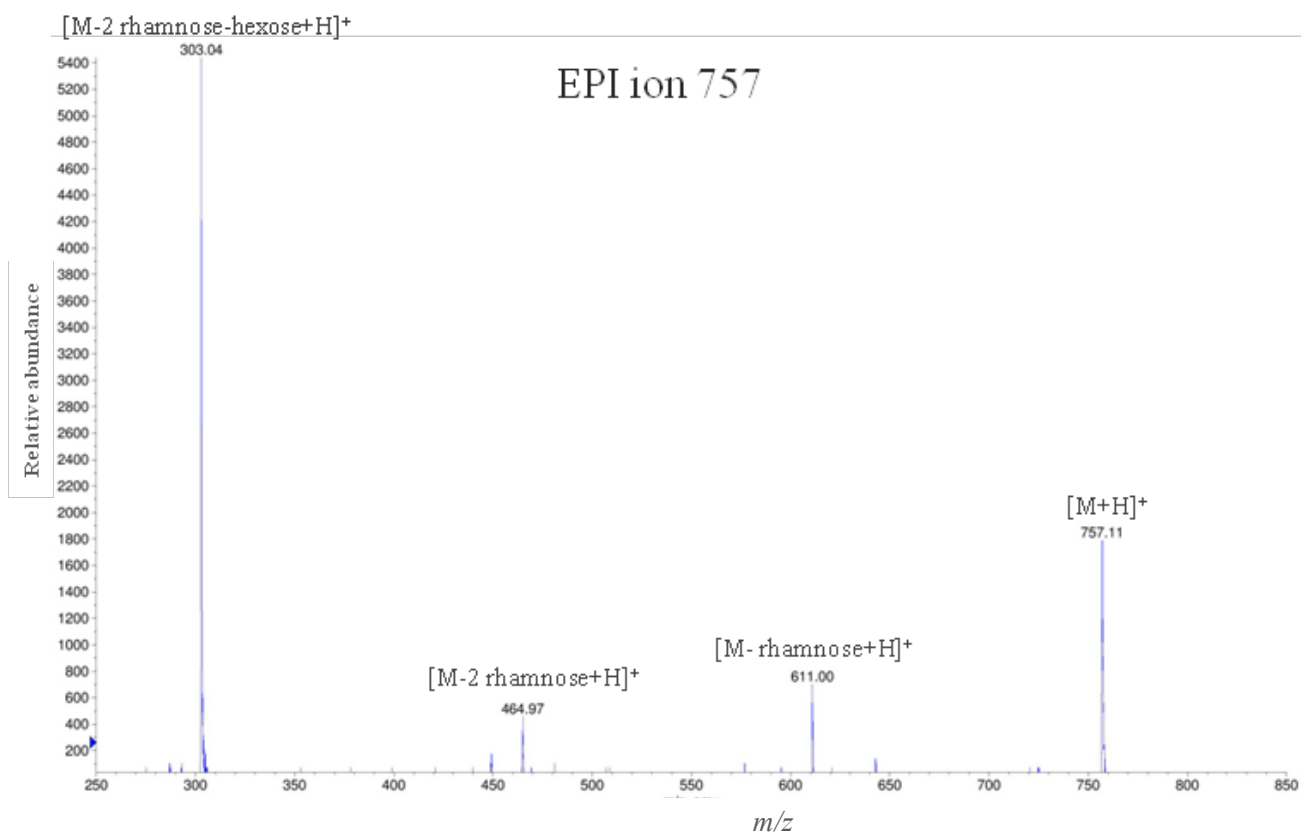
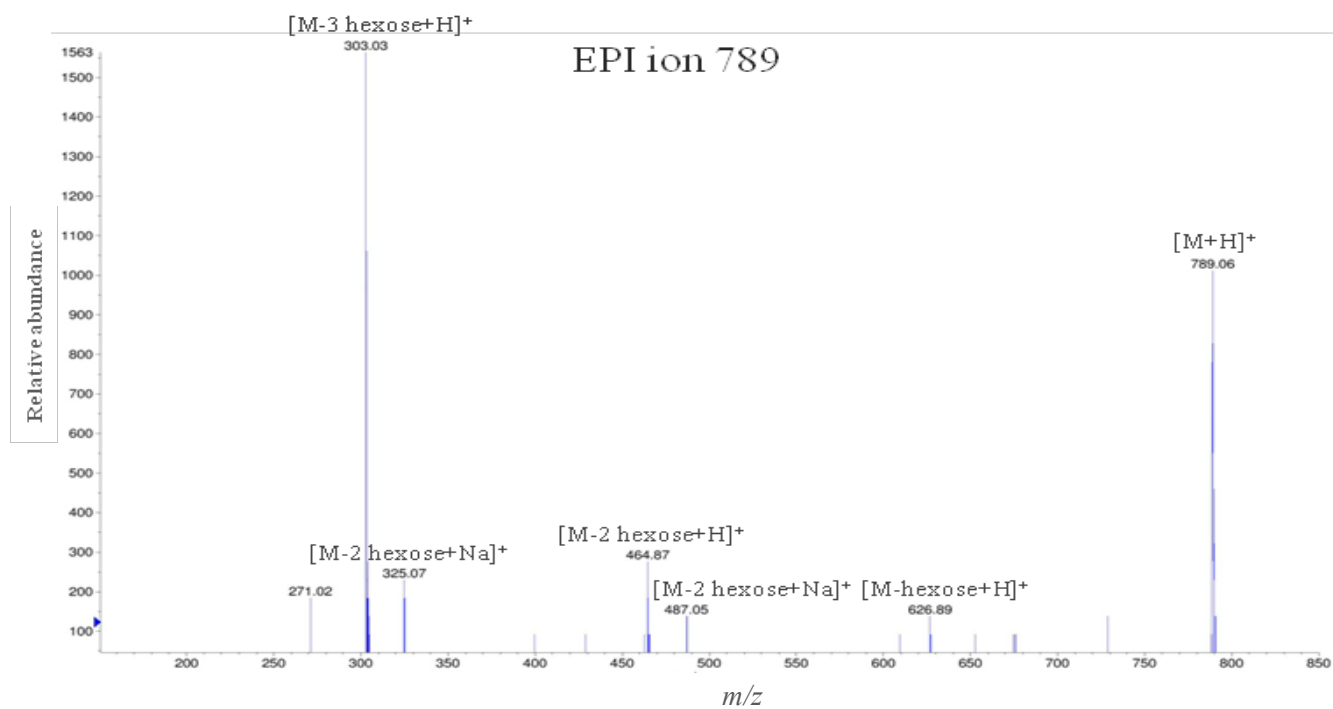
**Appendix 17.** (Continued) ESIHRMS spectra for the flavonoids identified in hydro-alcoholic extract of *P. boveana*



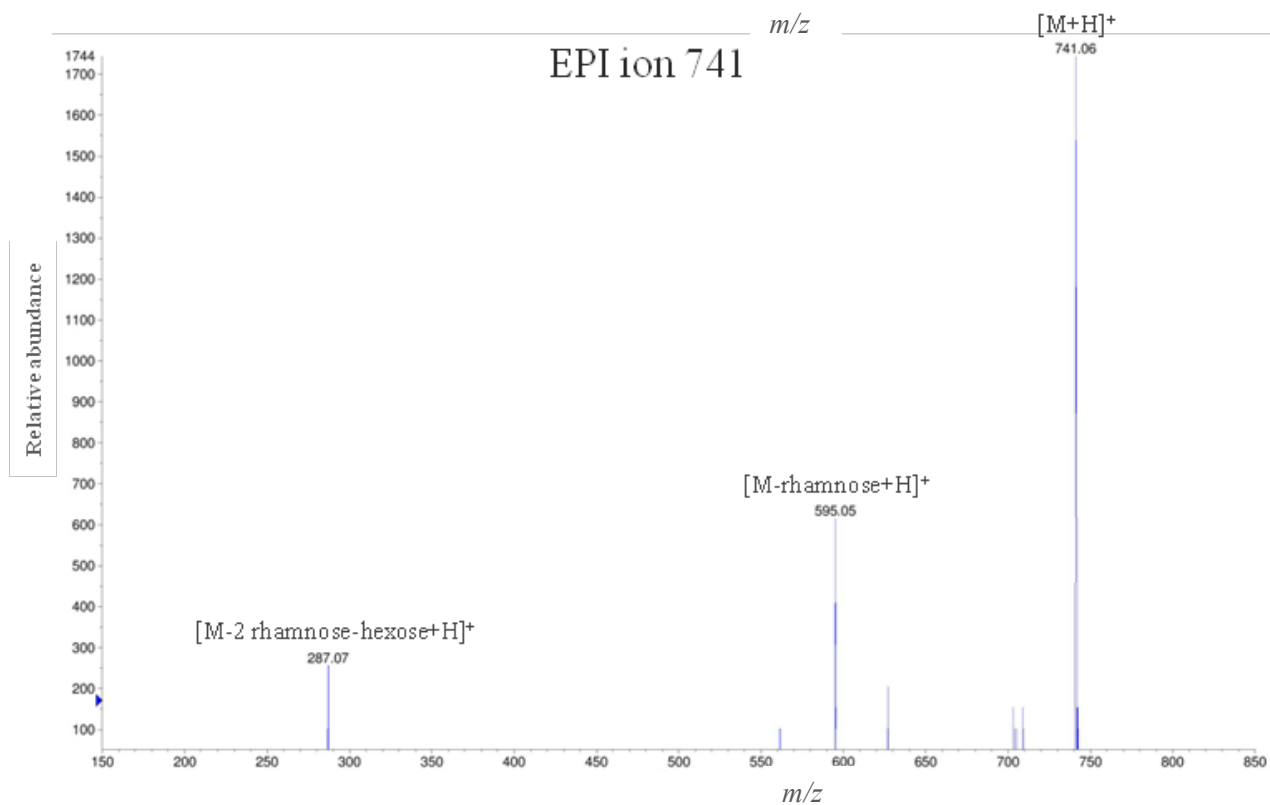
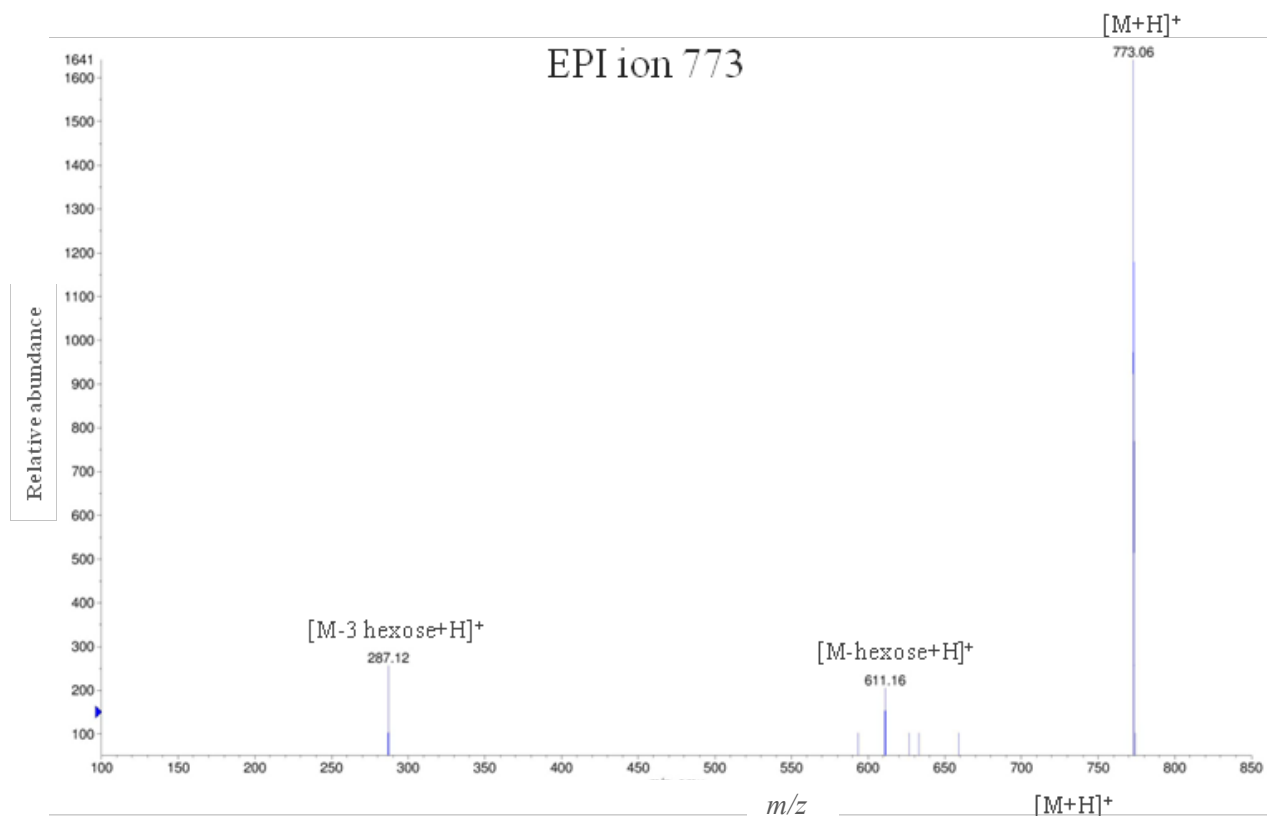
**Appendix 17.** (Continued) ESIHRMS spectra for the flavonoids identified in hydro-alcoholic extract of *P. boveana*



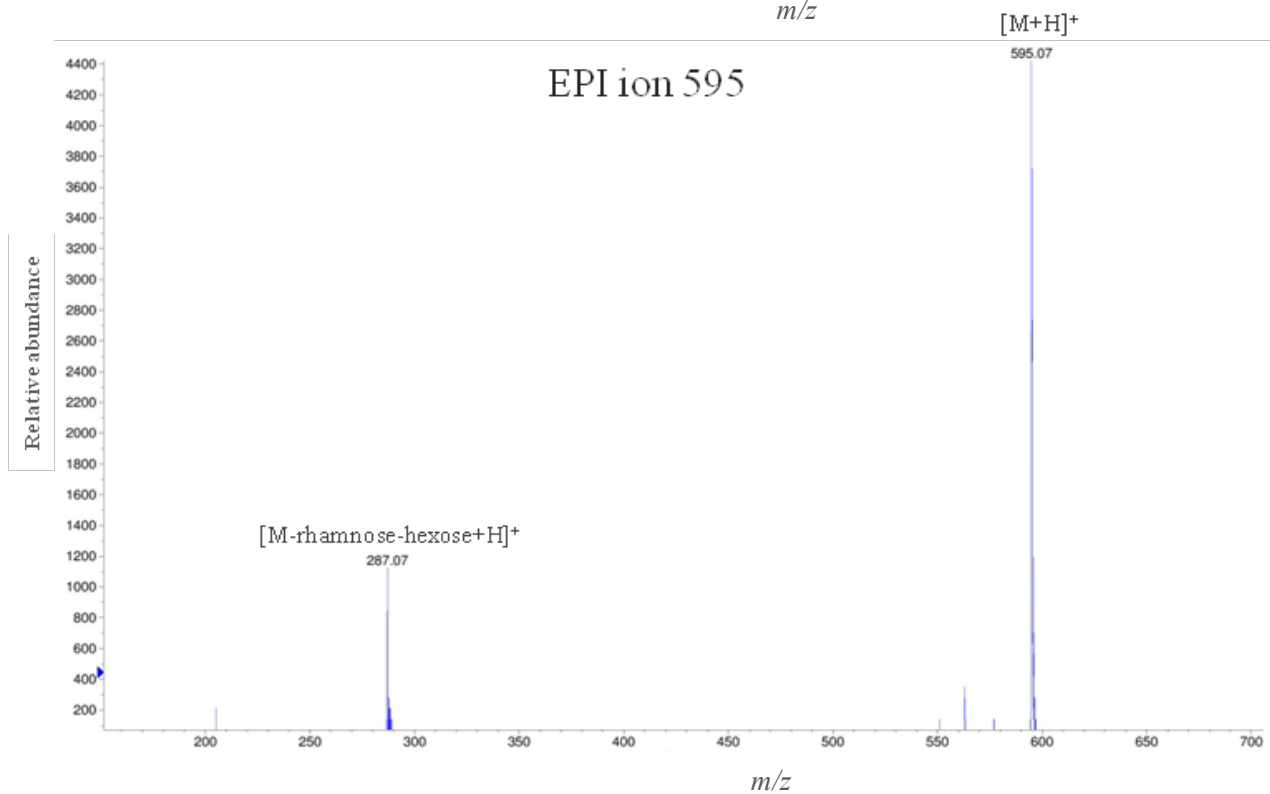
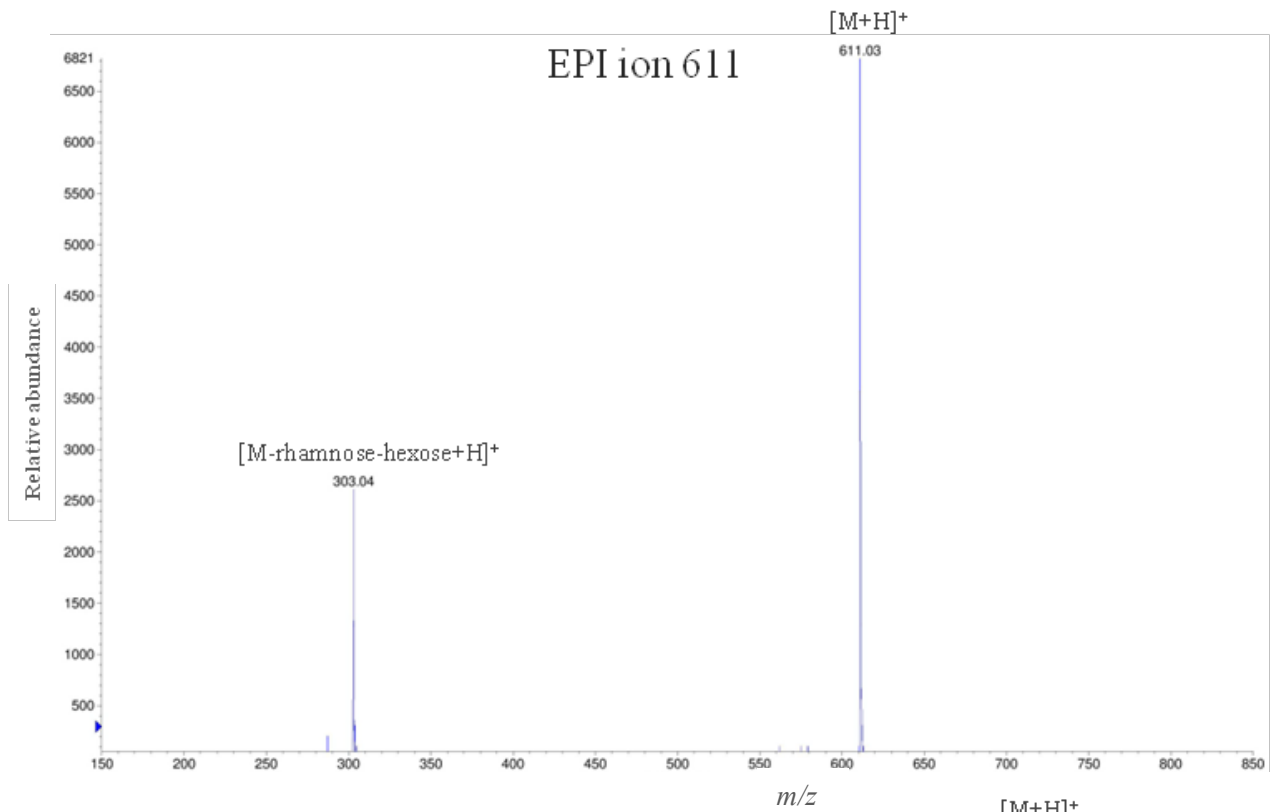
**Appendix 17.** (Continued) ESIHRMS spectra for the flavonoids identified in hydro-alcoholic extract of *P. boveana*



**Appendix 18.** EPI mass spectra (CE 10 V) of glycoconjugated flavonoids identified in hydro alcoholic extract of *P. boveana*.

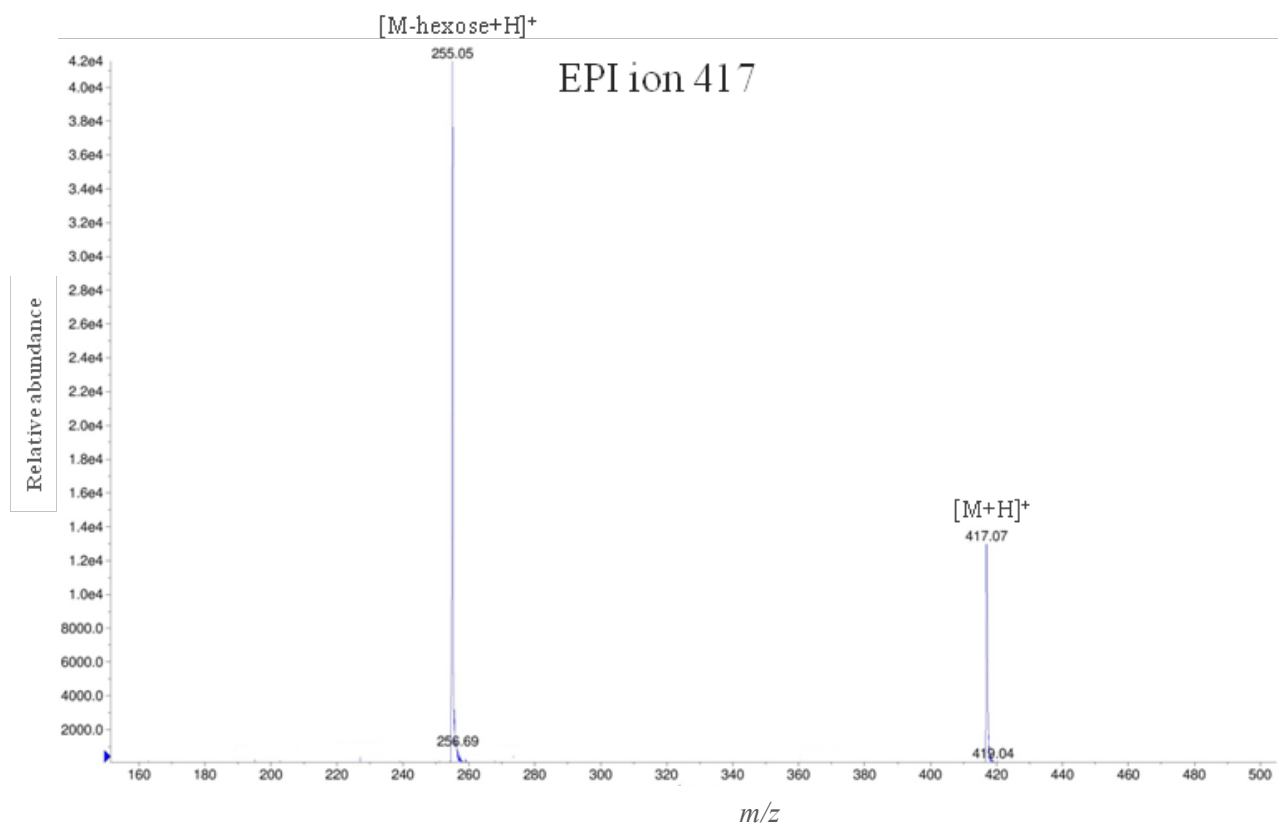


**Appendix 18.** (Continue) EPI mass spectra (CE 10 V) of glycoconjugated flavonoids identified in hydro alcoholic extract of *P. boveana*



**Appendix 18.** (Continue) EPI mass spectra (CE 10 V) of glycoconjugated flavonoids identified in hydro alcoholic extract of *P. boveana*.





**Appendix 18.** (Continue) EPI mass spectra (CE 10 V) of glycoconjugated flavonoids identified in hydro alcoholic extract of *P. boveana*

## ERKLÄRUNG

Ich versichere, dass ich meine Dissertation

**"Phytochemical and Biological Investigation of some Endemic  
Plants of Egypt with Development of a New HPTLC- $\beta$ -  
Glucuronidase Inhibition Assay"**

selbständig ohne unerlaubte Hilfe angefertigt und mich dabei keiner anderen als der von mir ausdrücklich bezeichneten Quellen bedient habe. Alle vollständig oder sinngemäß übernommenen sind Zitate als solche gekennzeichnet.

Die Dissertation wurde in der jetzigen oder einer ähnlichen Form noch bei keiner anderen Hochschule eingereicht und hat noch keinen sonstigen Prüfungszwecken gedient.

---

Ort, Datum

---

Unterschrift

# Curriculum vitae

## Personal Information

**Name:** Ehab Mahran

**Address:** Hansenhäuser Weg 11, 35039 Marburg, Germany

**Telephone:** +49(0) 15773161884

**Date of birth:** 20.01.1984

**Nationality:** Egyptian

**Email:** [mahrane@staff.uni-marburg.de](mailto:mahrane@staff.uni-marburg.de)

## Work Experience

11/2016 – Present **Doctoral researcher**, Institute of Pharmaceutical chemistry Philipps University of Marburg, Marburg, Germany.

01/2015 – 05/2016 **Research Assistant**, Chemistry Department, School of Natural Sciences and Mathematics, Claflin University, SC, USA

12/2013 – 08/2014 **Teaching Assistant**, Phytochemistry Department, Faculty of Pharmacy, Al-Azhar University, Cairo, Egypt

06/2009 – 12/2013 **Research Assistant**, Phytochemistry Department, Faculty of Pharmacy, Al-Azhar University, Cairo, Egypt

01/2007 – 05/2009 **Medical Representative**, Novartis pharmaceutical company (special unit branch, ophthalmic drugs), Egypt

## Education

11/2016 – Present **Ph.D.**, Natural Sciences, Philipps University of Marburg, Germany.

10/2010 – 12/2013 **M.Sc.**, Faculty of Pharmacy, Al-Azhar University, Cairo, Egypt.

09/2010 – 06/2011 **Advanced graduate courses**, Mass and NMR spectroscopic methods. Chemistry of natural products.

09/2009 – 06/2010 **Advanced graduate courses**, Basics of Organic chemistry, Analytical chemistry, Physical chemistry and Mathematics

09/2001 – 05/2006 **B.Sc.**, Pharmaceutical Sciences, Faculty of Pharmacy, Al-Azhar University, Cairo, Egypt. (Grade: Excellent).

## Conferences and workshops

- Poster, June 2019: "67<sup>th</sup> ASMS Conference on Mass Spectrometry and Allied Topics", Atlanta, GA, USA
- Oral presentation, June 2019: "48<sup>th</sup> International Symposium on High-Performance Liquid Phase Separations and Related Techniques", Milan, Italy
- Oral presentation, November 2018: "24<sup>th</sup> International Symposium for High-Performance Thin-Layer Chromatography" Bangkok, Thailand
- Workshop, October 2018: "Scifinder on campus". Philipps University of Marburg, Germany
- Conference attendance, August 2017 "Engineering of Functional Interfaces" Marburg, Germany
- Poster, April 2016: "New Iridoid Glycosides from *Anarrhinum pubescens*". 57<sup>th</sup> Experimental Nuclear Magnetic Resonance Conference (ENC), Pittsburg, PA, USA
- Poster, January 2016: "*In vitro* Propagation, Callus Induction and Genetic Fidelity Assessment of *Anarrhinum pubescens*". SC EPSCoR/IDeA State Conference, Columbia, SC, USA
- Workshop, October 2018 "publishing a world class scientific paper". Justus Liebig University. Giessen, Germany
- A member of the Organizing Committee of Al-Azhar international conference for Pharmaceutical and Biological sciences
- Personal and communication skills Courses at NOVARTIS pharmaceutical company

## Publications

- Abdelsalam A, **Mahran E**, Chowdhury K, Boroujerdi A, El-Bakry A (2017) NMR-based metabolomic analysis of wild, greenhouse, and *in vitro* regenerated shoots of *Cymbopogon schoenanthus*. subsp. *proximus* with GC–MS assessment of proximadiol. ***Physiology and Molecular Biology of Plants*** 23:369-383.
- **Mahran E**, Hosny M, El-hela A, Boroujerdi A (2018) New iridoid glycosides from *Anarrhinum pubescens*. ***Natural Product Research*** 33:3057–3064.
- **Mahran E**, Elgamal I, Keusgen M, Morlock G (2019) Effect-directed analysis by high performance thin layer chromatography for bioactive metabolites tracking in *Primula veris* flower and *Primula boveana* leaf extracts (***Journal of Chromatography A***, Accepted, in print).
- **Mahran E**, Morlock G, Keusgen M (2019) Guided isolation of new iridoid glucosides from *Anarrhinum pubescens* by high performance thin layer chromatography-acetylcholinesterase assay. (***Journal of Chromatography A***, Accepted, in print).
- **Mahran E**, Keusgen M, Morlock G. New planar assay for a streamlined detection and quantification of  $\beta$ -glucuronidase inhibitors and application to botanical extracts. (*In submission*)

## Awards and memberships

- **Marburg International Doctorate award:** The award involves travelling allowance and accommodation expenses for poster presentation at the "67<sup>th</sup> ASMS Conference on Mass Spectrometry and Allied Topics" Atlanta, GA, USA,(2019).
- **Merck group award:** The award involves the registration fees to give an oral presentation at the "48<sup>th</sup> International Symposium on High-Performance Liquid Phase Separations and Related Techniques" Milan, Italy,(2019).
- **Yousef Jameel academic foundation award:** PhD scholarship in Philipps University of Marburg, Germany (2016 - present).
- **Egyptian Pharmacists Syndicate award** for scientific excellence performance during Faculty years (2006).
- **Cairo Pharmacists Syndicate award** for scientific outstanding performance during Faculty years, Egypt, (2006).
- **Sharkia Governorate Teaching Professions Syndicate** for outstanding performance during Faculty years, Egypt,(2006).

## Language Skills

**Arabic:** Native, **English:** Very Good, **German:** Understanding